DEACTIVATION CORRELATIONS OF PD/RH THREE-WAY CATALYSTS DESIGNED FOR EURO IV EMISSION LIMITS

Effect of Ageing Atmosphere, Temperature and Time

ULLA LASSI

Department of Process and Environmental Engineering, University of Oulu

OULU 2003

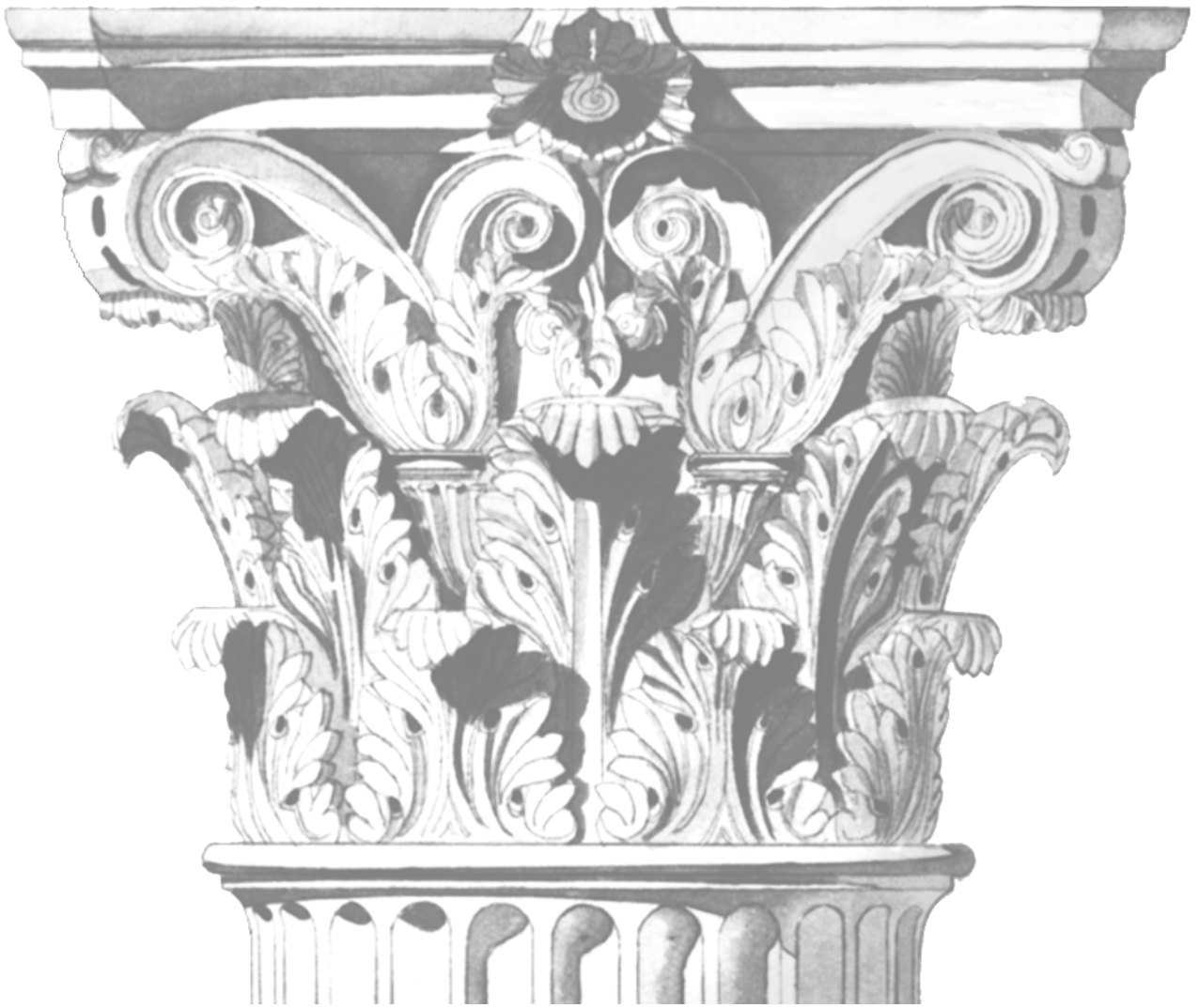

ULLA LASSI

DEACTIVATION CORRELATIONS OF PD/RH THREE-WAY CATALYSTS DESIGNED FOR EURO IV EMISSION LIMITS

Effect of Ageing Atmosphere, Temperature and Time

Academic Dissertation to be presented with the assent of the Faculty of Technology, University of Oulu, for public discussion in Kuusamonsali (Auditorium YB210), Linnanmaa, on February 28th, 2003, at 12 noon.

OULUN YLIOPISTO, OULU 2003

Supervised by
Professor Riitta L. Keiski

Reviewed by
Associate Professor Emilia Björnbom
Professor Zinfer R. Ismagilov

ISBN 951-42-6954-3 (URL: http://herkules.oulu.fi/isbn9514269543/)

ALSO AVAILABLE IN PRINTED FORMAT
Acta Univ. Oul. C 180, 2003
ISBN 951-42-6953-5
ISSN 0355-3213 (URL: http://herkules.oulu.fi/issn03553213/)

OULU UNIVERSITY PRESS
OULU 2003

Lassi, Ulla, Deactivation Correlations of Pd/Rh Three-way Catalysts Designed for Euro IV Emission Limits. Effect of Ageing Atmosphere, Temperature and Time
Department of Process and Environmental Engineering, University of Oulu, P.O.Box 4300, FIN-90014 University of Oulu, Finland
Oulu, Finland
2003

Abstract

The aim of this thesis is the knowledge of the most relevant deactivation mechanisms of Pd/Rh three-way catalysts under different ageing conditions, the deactivation correlation of laboratory scale ageing and engine bench/vehicle ageings, and the evaluation of the deactivation correlation. In the literature review, the phenomena involved in the three-way catalyst operation and its deactivation are considered. In the experimental section, ageing-induced phenomena in the catalyst are studied and deactivation correlations between laboratory scale and engine bench/vehicle ageings are presented, based on the results of several surface characterization techniques. The effects of ageing atmosphere and temperature, and time are considered in particular.

Fresh and aged catalysts used in this study were metallic monoliths designed for Euro IV emission limits. Thermal ageings were carried out in the reductive, oxidative and inert atmospheres in the temperature range of 800°C to 1200°C, and in the presence of water vapour (hydrothermal ageing). The engine ageing was carried out in the exhaust gas stream of a V8 engine during a 40 hour period. The ageing procedure composed of rich and stoichiometric air-to-fuel ratios carried out consecutively. The vehicle ageing was accomplished under real driving conditions (100 000 kilometres).

According to the results, deactivation of a Pd/Rh monolith is a combination of several ageing phenomena. The most important deactivation mechanisms are the sintering of active phase, the collapse in surface area and ageing-induced solid-solid phase transitions in the bulk washcoat. Furthermore, poisoning is a relevant deactivation mechanism of the vehicle-aged catalyst. High ageing temperature, gas phase composition and exposure time are essential variables to the deactivation of a Pd/Rh three-way catalyst.

This thesis presents an approach to discover the deactivation correlation between the laboratory scale ageing and under the vehicle's operation in an engine bench or on-road. Based on the characterization results, the accelerated laboratory scale air ageing does not correspond to the ageing-induced changes in the catalyst under the vehicle's operation. Therefore, there is a need for a modified ageing cycle and according to the results, a deactivation correlation between the laboratory scale ageing and the engine bench ageing can be presented as a function of ageing temperature and atmosphere, and time. Instead, after the vehicle operation, the deactivation correlation cannot be presented based solely on the studied variables because, after 100 000 kilometres of driving, the role of poisoning should be taken into account in the ageing cycle.

The results of this thesis can be utilized and applied in the development of laboratory scale ageing cycles, which corresponds closely to the ageing-induced changes in the catalyst during the vehicle operation. This enables a rather fast testing of the catalyst's performance and reduces the cost during the manufacturing of catalysts.

Keywords: activity, ageing, catalyst, characterization, deactivation, hydrothermal, poisoning, TWC

To my Family

Acknowledgements

The present study has been carried out in the Department of Process and Environmental Engineering at the University of Oulu during the years 1998-2002. During this time I have been a student in the Finnish Graduate School in Chemical Engineering (GSCE). The work of this thesis was also a part of the TEKES project called 'Catalyst Deactivation and Diagnosis'. The aims of the project were the knowledge on the deactivation of exhaust gas catalysts, and the development of methods for diagnosing catalyst's deactivation in the laboratory scale and during real use.

I would like to thank my supervisor, Professor Riitta Keiski, head of the Laboratory of Mass and Heat Transfer Process, for giving me an opportunity to work in the field of exhaust gas catalysis and to write my thesis under her direction. My warmest and deepest gratitude is expressed for her scientific guidance, for her continuous support and encouragement, and for her insistence in pushing me forward with my thesis. Without your support this thesis might not have existed.

I am grateful to people at Kemira Metalkat Oy, especially to Matti Härkönen, Lic. Tech.; Dr. Kauko Kallinen; Auli Savimäki, Lic. Phil., and Marja Louhelainen, M.Sc., for providing me with an opportunity to carry out this work. I owe my sincere thanks to Juha Ahola, Lic. Tech., my research colleague on the project, for his collaboration throughout the past years.

I would also like to thank all of my publications' co-authors, especially Dr. Katariina Rahkamaa-Tolonen and Marko Hietikko, M.Sc. at the University of Oulu as well as Dr. Sami Suhonen and Raija Polvinen, M.Sc., both of the Tampere University of Technology.

I am grateful to Professor Risto Laitinen, Docent Mika Valden and Professor Jouni Pursiainen for the comments and clarifications regarding my thesis, publications and manuscripts. In addition, Professors Tapio Rantala and Vilho Lantto are acknowledged for their support, collaboration and help in understanding phenomena at the molecular level.

I would also like to convey my appreciation to Professor Zinfer R. Ismagilov and Associate Professor Emilia Björnbom for reviewing the manuscript of this thesis and to Ms. Hilary Ladd for linguistic corrections and proofreading. Your suggestions helped greatly to improve the quality of the thesis.

I would like to express my special thanks to Jomppe and Hannele for the encouragement in the course of this thesis and for the excellent work they have done during the laboratory experiments. Without your good spirits, I might have given up and then I might not have made it to the finish-line! Special thanks are also due to Satu, Ritu, Tanja, Mika, Pekka, Liisa, Päivi, and Virpi, and all my friends and colleagues in the laboratories of Mass and Heat Transfer Process, Industrial Environmental Engineering and Chemical Process Engineering.

I owe my warmest thanks to my parents, Anita and Lasse, my brother Kai, and my grandmother for their support and encouragement throughout my everlasting studies. Finally, my heartfelt gratitude is due to my loving husband Janne and to our little son Eetu for giving me a reason to stop working.

The financial support from GSCE (Graduate School in Chemical Engineering) and the Academy of Finland, TEKES (National Technology Agency of Finland), Kemira Foundation, Tauno Tönning Foundation, and Alfred Kordelin and Emil Aaltonen foundations is also gratefully acknowledged.

Kempele, 30th January, 2003 Ulla Lassi (neé Pulkkinen)

List of symbols and abbreviations

Latin letters

d	Distance between two atomic planes in the crystalline phase, m
D	Dispersion of metal particles, %
D_0	Initial dispersion of metal particles, %
D_{eq}	Final dispersion of metal particles, %
g	Gram
h	Hour(s)
k	Kinetic reaction rate constant for sintering, 1/s
m/z	Mass-to-charge ratio, dimensionless
n	Sintering order, dimensionless
n	Order of diffraction, dimensionless
Re	Reynolds number, dimensionless
t	Time, s
T	Temperature, °C
T_{50}	Light-off temperature at which 50% conversion is attained, °C
$T_{Hüttig}$	Hüttig temperature, °C
$T_{melting}$	Melting temperature, °C
T_{Tamman}	Tamman temperature, °C
x	Integer in stoichiometric coefficient
y	Integer in stoichiometric coefficient

Greek letters

β	Heating rate, °C/min
λ	Dimensionless air-to-fuel ratio
λ	Wavelength, 1/m
θ	Diffraction angle, °

Abbreviations

A/F-ratio	Air-to-fuel ratio
BET	Brunauer-Emmett-Teller Method
BJH	Barrett Joyner Hallender Method
CC	Close-coupled catalytic converter
CDD	Catalyst Deactivation and Diagnosis (project name)
CVS	Constant Volume Sampler
DRIFT	Diffuse Reflectance Fourier Transform Infrared Spectroscopy
EDS	Energy Dispersive X-ray Spectrometer
EPA	Environmental Protection Agency
EU	European Union
EUDC	European Extra-Ultra Driving Cycle
FTIR	Fourier Transform Infrared Spectroscopy
FTP	Federal Test Procedure
GHSV	Gas Hourly Space Velocity
HK	Horvath-Kawazoe Method
ICP-AES	Inductively Coupled Plasma-Atomic Emission Spectrometry
IR	Infrared
IUPAC	International Union of Pure and Applied Chemistry
NEDC	New European Driving Cycle
PDF	Power Diffraction Database File
OBD	On-Board Diagnostics
OSC	Oxygen Storage Capacity
SEM	Scanning Electron Microscopy
TEKES	National Technology Agency of Finland (in English)
TEM	Transmission Electron Microscopy
TGA-DTA	Thermogravimetric Analysis-Differential Thermal Analysis
TPD	Temperature-programmed Desorption
TWC	Three-way catalyst, three-way catalytic converter
WGSR	Water-gas Shift Reaction
XPS	X-ray Photoelectron Spectroscopy
XRD	X-ray Diffraction
ZDP	Zinc Dialkyldithiophosphate

List of tables

List of figures

Contents

1 Introduction

1.1 Background

Recently, environmental concern and demand for a catalyst's high performance have increased the research activity focused on the operation of a three-way catalyst (TWC) at the end of its lifetime. Currently-used three-way catalysts are exposed to high operation temperatures due to the use of closed-loop coupled catalysts near the engine. Three-way catalysts have a lifetime requirement of at least 100 000 kilometres or five years (Directive 98/69/EC). Catalytic materials used in TWC applications have also changed, and the new materials have to be thermally stable under the fluctuating exhaust gas conditions. The new emission limits (Euro IV level for 2005) are becoming tighter and new restrictions are set for the fuel consumption and quality, e.g. low sulfur content of gasoline (Directive 98/70/EC). Further demands are being placed on discovering other techniques to minimise emissions during cold start to obtain a fast light-off of a catalyst. In addition, there are new requirements regarding the catalyst's monitoring techniques, e.g. On-Board Diagnostics (OBD), which is used to monitor the degree of the catalyst's deterioration. All these requirements correlate to the catalyst's deactivation phenomenon. The attainment of these requirements demands highly active and thermally stable catalysts as well as an optimised design of the exhaust system and engine control. (Heck & Farrauto 1997, Farrauto & Heck 2000, Shelef & McCabe 2000, Bosteels & Searles 2002)

The requirement for high thermal stability and activity, which the current three-way catalysts have to fulfill, is one of the most crucial demands for a successful commercial application. Therefore, the understanding of deactivation phenomena and deactivation correlations is an important issue in the design and preparation of a catalytic system. Deactivation of a three-way catalyst can be due to many ageing phenomena, such as thermal, chemical and/or mechanical. Thermal or thermo-chemical degradation is reported to be one of the main causes for the deactivation of three-way catalysts (Ihara *et al.* 1987, Funabiki & Yamada 1988, Härkönen *et al.* 1991, Usmen *et al.* 1992, Jobson *et al.* 1993). High temperature and temperature gradients, the presence of poisons and other impurities, as well as the fluctuating gas phase composition and flow rate in the catalytic

converter increase the possibility of deactivation. Furthermore, some other factors, such as the chemical composition of the catalyst and pressure changes in the converter affect the catalytic activity. Thus, it is essential to study the role of different ageing factors in order to understand the relevant physical and chemical mechanisms of deactivation and deactivation correlations of a three-way catalyst.

As indicated in the previous paragraphs, deactivation of a three-way catalyst is a complex phenomenon and it extensively affects the catalyst's preparation and use. When preparing catalysts for the purification of exhaust gases of gasoline engines, catalyst manufacturers have to guarantee the required lifetime for the catalyst. It is, therefore, essential to know which are the most important factors during the deactivation. Furthermore, it is also important to understand these factors's effect *i.e.*, what are the ageing-induced chemical and physical changes in the catalysts in order to arrive at the deactivation correlations. It is reasonable to assume that currently-used laboratory scale ageing cycles are not consistent with the ageing phenomena in an engine bench or on-road. Therefore, there is a need for a novel laboratory scale ageing cycle, which better corresponds to the physical and chemical changes where the catalyst is exposed during real driving conditions.

1.2 Aims of the work

The topic of research presented in this thesis is the evaluation of deactivation and deactivation mechanisms of industrially manufactured Pd/Rh exhaust gas catalysts that are designed for Euro IV emission limits. The ageing-induced changes in the catalyst have been studied by using a number of surface characterization techniques, such as X-ray diffraction and temperature-programmed techniques. The effects of ageing atmosphere, temperature and time are considered. The main aims of the present work arise from two observations. Firstly, catalyst's ageing and testing in an engine bench or on-road are both slow and expensive. Thus, in order to keep catalyst manufacturers competitive in the global market, new, fast and reliable laboratory scale ageing cycles are needed. Secondly, currently-used laboratory scale ageing procedures are not necessarily equivalent to the ageing conditions under the real life operation of a catalyst. Therefore, the first main goal of this thesis is the knowledge of the most relevant deactivation mechanisms of Pd/Rh monoliths under different ageing conditions. Several characterization techniques are utilized in order to reach this goal. The catalyst's properties, especially its performance, cannot be understood solely on the basis of some separate characterization techniques; moreover, the applicability of multiple techniques will provide a larger view of deactivation phenomenon.

The second goal of this research is the deactivation correlation between laboratory scale ageing and engine bench and vehicle ageings. The attainment of this goal implies the integration and comparison of the characterization results of different techniques. A third aim of this work is the utilisation of the results of the first two main goals and the critical evaluation of ageing cycles. The results of this thesis can be used in the development of laboratory scale ageing cycles which correspond to the ageing in an

engine bench or on-road, in particular to the ageing-induced physical and chemical changes in the catalyst. The laboratory scale ageing cycle would allow for the possibility of a rather fast testing of the catalyst's durability (activity and thermal stability) during the research and development stage of the catalyst's manufacturing.

As indicated, some of the driving forces behind this thesis involved environmental, health and legal factors. Furthermore, from the catalyst manufacturer's viewpoint, the economic factors are also essential. Since catalyst research is a multi-disciplinary field of science, involving chemistry, physics and engineering aspects, it gave the author the opportunity for a fruitful collaboration with chemists and physicists.

1.3 Scope and outline of the work

Catalyst deactivation is a complex phenomenon and it is affected by several known, and even unknown, factors and it is also extensively studied. Some limitations and preliminary assumptions had to be made at the beginning of this work. First, the effects of only three affecting variables (ageing temperature, atmosphere and time) were considered in order to keep the matrix of the experimental work reasonable. These three variables were selected on the basis of the knowledge that they are essential factors in the deactivation of a three-way catalyst, as indicated in several published articles on this topic. Furthermore, the role of ageing temperature, atmosphere and time can be studied at the laboratory scale under well-controlled conditions in an ageing furnace. These three variables were under investigation, although the catalytic activity, and thermal and chemical stability of the catalyst during real use is also affected by several other factors, such as the chemical composition of the catalyst.

Secondly, in order to gain a basic understanding of deactivation phenomenon in Pd/Rh monoliths, the structure of catalysts was kept similar. Thus, all the catalysts were identical in their chemical composition and only the changes induced by ageings are considered. For instance, the role of a catalyst's chemical composition, which certainly affects deactivation, has been limited out. It is considered only briefly and most often based on the literature when needed. It is also reasonable to ignore the effect of the chemical composition of a catalyst on deactivation because it is rather difficult to find a series of catalyst samples with different chemical composition, and which have been aged accordingly on-road for 100 000 kilometres, for example. Therefore, the comparison between catalysts with different chemical compositions cannot be carried out. Furthermore, the number of the characterization techniques utilized in this thesis was also limited on the basis of heuristic rules (the applicability, cost, availability and informative aspect of the method).

The present study was also a part of the activities within the TEKES project (1999-2002) "Catalyst deactivation and Diagnostics (CDD)" (Ahola & Lassi 2001, Ahola *et al.* 2002). The work has been carried out in close collaboration with Kemira Metalkat Oy (Finland), which provided the fresh, engine-aged and vehicle-aged catalysts. These catalysts were used as a frame of reference with which to compare the characterization results of thermally aged catalysts. The characterizations of aged catalysts were mostly

done in the Department of Process and Environmental Engineering at the University of Oulu. X-ray Diffraction (XRD) and X-ray Photoelectron Spectroscopy (XPS) measurements were carried out in collaboration with the Department of Chemistry at the University of Oulu and with the Surface Science Laboratory at the Tampere University of Technology respectively. The author of this thesis is largely responsible for carrying out the major parts of the experiments (except XPS measurements) and for the integration of the research results within the final outcome.

This thesis is composed of the following sections: a review of the relevant literature, a description of the experimental methods applied, and the sections of results and their integration and evaluation. In the literature review of this thesis, a general perspective of the theory behind three-way catalysis is given in Chapter 2, whereas in Chapter 3 catalyst deactivation phenomena are considered. In particular, the deactivation mechanisms that are relevant in this thesis are examined. The experimental part of this research aims at providing support to the theses presented at the end of the work. The experimental part is organised as follows: In Chapter 4 the catalysts, ageing procedures and characterization techniques are described. Chapter 5 presents the results of ageing-induced phenomena. In Chapter 6, the integration of results is carried out and the deactivation correlations are considered. In particular, the effects of ageing atmosphere, temperature and time, are taken into account. Furthermore, the evaluation of the applicability of the deactivation correlations is carried out. Key literature in the respective fields is also discussed in these two chapters. Finally, in the last chapter, the conclusions based on the results of earlier chapters are drawn, and suggestions for future work are given.

2 Three-way catalysis

2.1 General

Automotive exhaust gases formed in the gasoline engines contain many environmentally harmful compounds. As a result of incomplete combustion, exhaust gases can include carbon monoxide (CO) and hydrocarbons (HC). A typical composition of exhaust gases is presented in Table 1. Catalytic purification has proven to be an efficient way to reduce emissions from exhaust gases. Due to the increased demand for low-emission vehicles, most automobiles are currently supplied with a three-way catalytic converter (TWC) for the simultaneous removal of major pollutants CO, NO_X and HC from a gasoline engine's exhaust gases (Heck & Farrauto 2001). The current and forthcoming European emission limits for gasoline engines are presented in Table 2.

Table 1. Typical concentrations of the exhaust gas constituents of gasoline-fuelled engines. Air-to-fuel ratio contributes significantly to these concentrations (Taylor 1993).

HC	750 ppm*	CO_2	13.5 vol-%
NO_X	1050 ppm	O_2	0.51 vol-%
CO	0.68 vol-%	H_2O	12.5 vol-%
H_2	0.23 vol-%	N_2	72.5 vol-%

* Based on C_3

Table 2. European emission limits (g/km) for gasoline-fuelled passenger cars and light commercial vehicles (Directive 98/69/EC).

Stage:	In new types:	CO (g/km)	HC (g/km)	NO_X (g/km)
EURO III	1.10.2000	2.3	0.20	0.15
EURO IV	1.10.2005	1.0	0.10	0.08

The currently-used exhaust gas purification system consists of a catalytic converter and an electronically controlled air/fuel management system as shown in Fig. 1. The oxygen sensor measures the net oxygen content that is proportional to stoichiometry in the exhaust gas. The air inlet and fuel injection are controlled to provide a stoichiometric

ratio between oxygen (air) and fuel. The objective is to keep the air-to-fuel ratio (A/F-ratio) within the so-called lambda window (as presented in Fig. 2). In this narrow window, the high conversions (> 80-90%) of CO, HC and NO_X are achieved simultaneously. If the A/F-ratio is below 14.6, the exhaust gas contains more reducing reactants (CO, HC) than oxidizing reactants (O_2, NO_X) and the engine operates under rich conditions. If the A/F-ratio exceeds 14.6, the engine operates under lean conditions. The reduction reactions of NO_X are favoured under rich conditions, whereas the lean conditions favour the catalytic oxidation reactions of CO and hydrocarbons (Lox & Engler 1997). The refinement of the engine management system affects both the performance and the durability of the emission control system. Due to its performance in promoting the main reactions to reach completion and at the same time minimizing the extent of the secondary reactions, the closed-loop-controlled three-way catalyst has become the most widely applied technique for catalytic emission control. (Shelef & McCabe 2000)

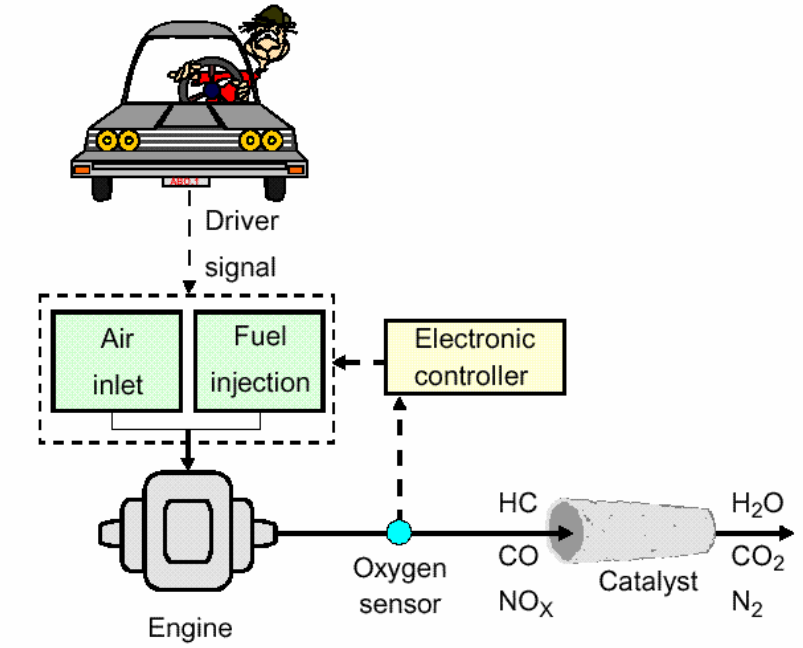

Fig. 1. Purification system of exhaust gases of gasoline engines. Purification system includes an electrically controlled air-to-fuel management system (cf. Holmgren 1998).

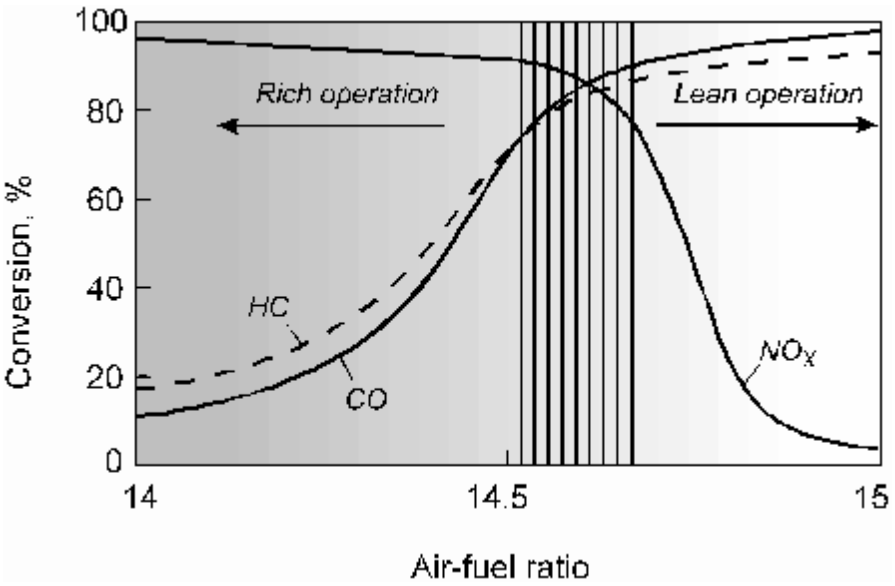

Fig. 2. The conversion efficiency (%) of a three-way catalyst as a function of A/F-ratio. The lambda window, an A/F-ratio of 14.6 corresponds to stoichiometric operation, λ=1 (cf. Holmgren 1998).

2.2 Structure of a three-way catalyst

Three-way catalysts have a honeycomb-like, monolithic structure as shown in Fig. 3. The monolith support is made either from metallic (stainless steel) or ceramic (cordierite) material. The structure of a metallic monolith is presented in Fig. 4. The monolith contains small channels, each about 1 mm in diameter (300-600 channels per square inch). The washcoat, which includes the active catalyst material, is impregnated on these channel walls. The washcoat consists of porous oxides, such as γ-Al_2O_3 and precious metals. The thickness of the washcoat layer is *circa* 20-60 μm and it has a large surface area of approximately 50-200 m^2/g. Thus the diffusional resistance is minimal and gases easily reach the active surface sites, which allows close to 100% conversion with a high catalytic activity. Recently, the use of a layered washcoat has been applied in commercial three-way catalysts. Double-layered washcoats enhance specific reactions and improve the stability of the catalyst by separating the washcoat components. (Cybulski & Moulijn 1994, Heck & Farrauto 1996, Heck & Farrauto 2001, Lox & Engler 1997, Wan 1991)

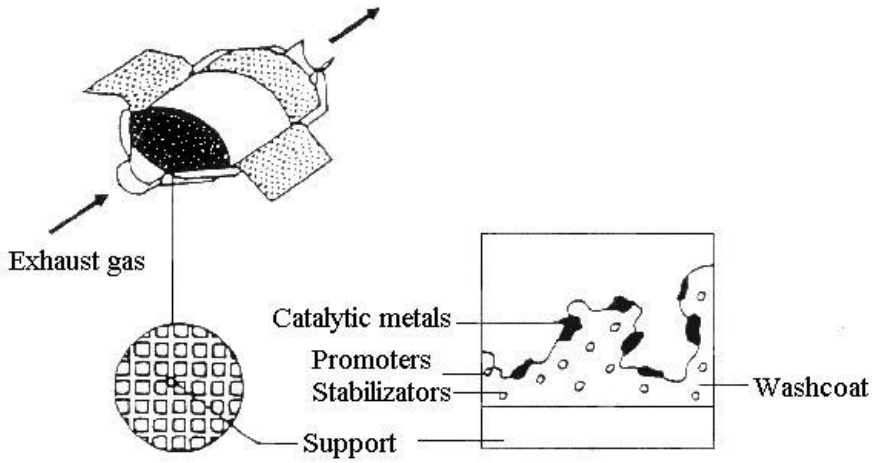

Fig. 3. The structure of a monolithic exhaust gas catalyst.

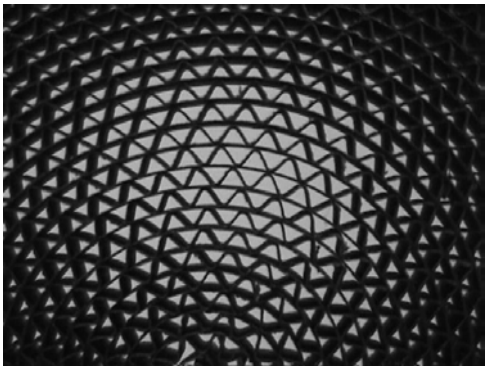

Fig. 4. Close-up view of a metallic monolithic support (cf. Rahkamaa-Tolonen 2001).

The main compounds in the washcoat are base-metal oxides, such as aluminium, cerium and zirconium. In addition to these oxides, minor washcoat compounds are CaO and MgO as well as the oxides of rare earth elements, such as La_2O_3 (lanthana). These compounds are used as promoters or stabilizers (additives) in the washcoat to increase the catalytic activity or to stabilise the structure of the catalyst. Cerium is present in high quantities in the form of CeO_2 (*circa* 20 wt-% of washcoat Al_2O_3). Cerium has multiple functions. It is added to promote the low temperature water-gas shift reaction (WGSR), to store oxygen under lean (fuel deficient) conditions, to stabilize precious metal dispersion against thermal damage and to alter carbon monoxide oxidation kinetics (Lox & Engler 1997, Oh & Eickel 1988). Cerium is also known to minimize the thermally-induced

sintering of an alumina washcoat (González-Velasco *et al.* 1994). The recent use of ceria-zirconia mixed oxides ($Ce_XZr_{1-X}O_2$) as catalytic washcoat materials has been promising due to the better thermal stability in closed-loop coupled applications. (Cuif *et al.* 1997, Fornasiero *et al.* 1996, Narula *et al.* 1996, Ozawa *et al.* 1993, Ozawa 1998)

The precious metals currently used in three-way catalyst applications are platinum, palladium and rhodium. These metals are well-known catalysts with high activities for controlling the exhaust emissions, and they are also preferred because they are less prone to poisoning compared to metal oxide catalysts, such as CuO (Shelef *et al.* 1978). The amount of the active metals in the catalyst is normally *circa* 1-2 wt-% of the washcoat. Precious metals are used to reduce the emissions of exhaust gases in the presence of reducing or oxidizing agents, such as hydrocarbons, CO and hydrogen, and oxygen and NO_X respectively. Rhodium has proven to be an efficient catalyst for NO_X reduction (Taylor 1993), whereas palladium and platinum metals are used in CO and hydrocarbon oxidation reactions (Armor 1992), in particular during cold start. Therefore, commercially-used three-way catalysts for gasoline engines are often a bimetallic combination of the precious metals, such as Pt-Rh or Pd-Rh. (Becker & Watson 1998, Koltsakis & Stamatelos 1997)

2.3 Phenomena in the three-way catalyst operation

The performance of a three-way catalyst depends on numerous factors including, for example, the chemistry (such as the preparation, materials and loadings) and the physics (such as the support and converter design) of the catalyst, and the chemical engineering aspects (such as the gas composition, reaction temperatures and dynamic conditions) (Lox & Engler 1997). Three-way catalysts operate under dynamic and fluctuating conditions and catalytic reactions occur at normal exhaust gas temperatures which, in warmed-up gasoline engines, can vary from 300°C to 400°C during idle, even up to about 1000°–1100°C, depending on the driving conditions (Koltsakis & Stamatelos 1997). High operation temperatures should be avoided in order to prevent sintering of the precious metals and washcoat compounds, as will be discussed later in Chapter 3. There are also temperature and concentration gradients present in the catalytic converter, and the space velocity of the gas flow and the exhaust gas composition fluctuate as well. Therefore, catalysts have to be thermally and mechanically stable against the physical and chemical changes to avoid deactivation. (Koltsakis & Stamatelos 1997, Lox & Engler 1997, van Santen *et al.* 1999, Sideris 1998)

2.3.1 Catalytic reactions and chemical kinetics

Several oxidation and reduction reactions take place in the catalytic converter, which is capable of removing the major pollutants HC, CO and NO_X simultaneously, therefore, it is called ‘a three-way catalyst.’ Table 3 summarizes the overall catalytic reactions in the

converter. In addition to these most general reactions, the water-gas shift and steam reforming reactions may contribute to the removal of CO and HC. Some undesired side reactions can occur producing gases such as ammonia and N_2O, the latter being a so-called greenhouse gas. These reactions depend on the temperature and the composition of the exhaust gas. When the engine is started, the exhaust gas gradually heats up until it is warm enough to initiate the catalytic reactions. Once the 'light-off' temperature is reached, CO oxidation reactions typically start first, followed then by HC oxidation. However, NO requires higher reduction temperatures. (Heck & Farrauto 1996, Lox & Engler 1997)

Table 3. The overall reactions in the catalytic converter (Lox & Engler 1997).

$2\ CO + O_2 \rightarrow 2\ CO_2$
$4\ C_XH_y + (4x+y)O_2 \rightarrow 4x\ CO_2 + 2y\ H_2O$
$2\ NO + 2\ CO \rightarrow N_2 + CO_2$

The presence of many simultaneous reactions is a challenge for engineers involved in the design, modeling and manufacturing of catalytic converters. Converter models require reliable kinetic expressions that take into account the composition and temperature dependence of the reaction rates. Therefore, the kinetic equations in the case of a three-way catalyst are typically empirical, and they include both oxidizing and reducing reactions of the Langmuir-Hinshelwood or Eley-Rideal type. (Froment 2001, Froment & Bischoff 1990, Koltsakis & Stamatelos 1997)

The activity of the catalyst as a function of its temperature is a critical feature of the catalyst's performance and is affected by a number of exothermic reactions. Catalytic activity is connected to the number of active sites on the surface. In heterogeneous catalysis, reactions occur on these active sites and thus, the reaction rate depends on the number of the active sites on the catalyst's surface. All the active sites are not identical. Some of the sites are not able to react with adsorbates, or they can have different reaction rates. At steady-state conditions, the reaction rate is proportional to the number of active sites on the macroscopic scale, and the increase in the catalyst's mass also increases the reaction rate with the same magnitude. In the case of an internal reaction rate, this relationship is often nonlinear. (Koltsakis & Stamatelos 1997, Thomas & Thomas 1997)

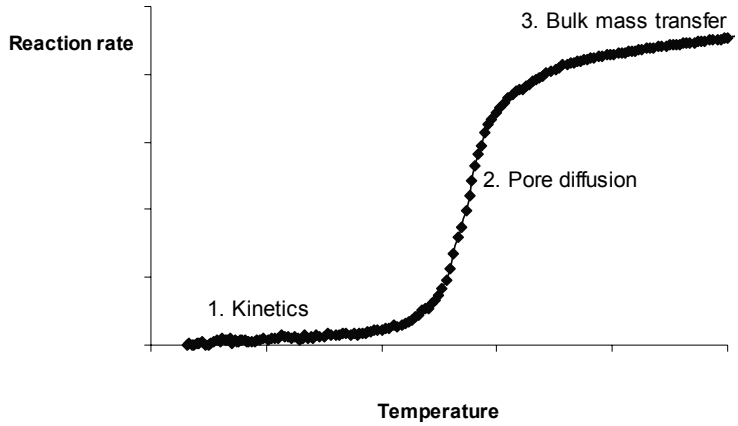

Fig. 5. Conversion as a function of temperature: rate controlling regimes.

Figure 5 presents, as an example, a typical activity plot. In region 1, at low temperatures, the reaction rate is so small that no conversion is reached over the catalyst. In this stage, the reaction kinetics is the controlling factor for the overall reaction rate, whereas in the second stage, the conversion is limited by the pore diffusion in the washcoat. Catalyst light-off typically occurs in this temperature range. The third high temperature region corresponds to bulk mass transfer between the gas phase and washcoat. Catalytic exhaust gas purification reactions are mainly kinetically restricted (corresponding to region 1). Reaction rates are not high enough and the components have not enough time to react on the active surface sites. Instead of this, thermodynamics are not a significant constraint in the exhaust gas purification, not at least in normal operation conditions. (Cybulski & Mouljin 1994, Koltsakis & Stamatelos 1997, Thomas & Thomas 1997)

2.3.2 Heat and mass transfer phenomena

The presence of heat and mass transfer phenomena and several multiphase reactions in the catalytic converter affect the total reaction rate and complicate the catalyst studies. Thus, real catalysts are often studied with simplified models, e.g. with single crystals (Twigg 1989, van Santen *et al.* 1999). The most important heat transfer phenomenon in the converter is the convective heat exchange between the bulk exhaust gas and the substrate. Heat is generated in the exothermic reactions of exhaust gas components on the washcoat. Furthermore, heat radiation from the washcoat to the surrounding walls increases at high operation temperatures. Therefore, the heat losses from the converter to the surroundings occur by convection and/or by radiation. (Koltsakis & Stamatelos 1997, le Page 1987)

The concentration gradients between the flowing exhaust gas and the reactive washcoat induce the convective mass transfer in the monolith channels. Active components are distributed onto a large area, which enables the efficient mass transfer between the bulk gas phase and active catalytic surface to achieve high conversions and activities. Although the flow in the exhaust piping of an engine is normally turbulent, the Reynolds (Re) numbers in the converter channels are in the laminar region ($20<Re<300$). The transition of the flow from turbulent to laminar region occurs after the converter inlet, where the mass transfer phenomena are generally enhanced (Bird *et al.* 1960, Froment & Bischoff 1990, Koltsakis & Stamatelos 1997). According to Cybulski & Mouljin (1994), the length of the transition zone in the converter is typically less than 20% of the monolith length.

When the concentrations of exhaust gases are low, the laws of diffusion are applied in the mass transfer and the analogies between heat and mass transfer are fully applicable. Transient chemical processes, such as changes in the catalytic activity or the accumulation of reactive species in a catalyst can affect the dynamic behaviour of three-way catalysts. Mass transfer processes have an influence on the rate at which these changes occur and thus affect their importance under dynamic conditions. (Herz 1981, Koltsakis & Stamatelos 1997)

Flow and temperature distributions in a catalytic converter are not constant as a function of converter configuration, radial and axial coordinate and time. These non-uniformities may cause poor converter performance, localized high space velocities increased thermal and chemical ageing, due to temperature and concentration gradients and the accumulation of poisons in high mass flow rate areas of the converter. (Koltsakis & Stamatelos 1997, Marin & Hoebink 1997)

Studies of the position-dependent phenomena in the converter have shown significant differences in the catalytic activity as a function of a converter's axial direction. The loss in surface area and catalytic activity were the highest in the front region of the converter, and this was also associated with poison deposition. Only the front part of the converter contained poisons derived from fuel. The low performance at the front part of the converter and the relative high performance at the centre and rear parts of the converter were observed. (Angove & Cant 2000a)

2.3.3 Oxygen storage capacity

Three-way catalysts have an ability to store oxygen. This property is known as Oxygen Storage Capacity (OSC) and enables the simultaneous oxidation and reduction reactions in the catalytic converter, as reported in section 2.3.1. In modern engines, the oscillation cycle of the engine's air-to-fuel ratio fluctuates close to the stoichiometric value. Under these conditions, the high oxygen storage capacity is of crucial importance. High OSC is normally reached by cerium or cerium compounds in the washcoat and, to a much lesser extent, by other washcoat materials. The recent use of large levels of CeO_2-based promoters provides a way to increase the efficiency of TWC's by enlarging the air-to-fuel

operating window. (Fornasiero *et al.* 1996, Koltsakis & Stamatelos 1997, Lox & Engler 1997)

CeO_2 acts as an oxygen buffer by storing excess oxygen under oxidizing (lean) conditions and releasing it in rich (reducing) conditions to oxidize CO and HC according to the reaction:

$$2\,CeO_2 \rightleftharpoons Ce_2O_3 + 0.5\,O_2 \quad (1)$$

This is based on the ability of cerium to form three (Ce^{3+}) or four (Ce^{4+}) valent oxides in rich and lean conditions respectively. Oxygen storage capacity is also closely related to temperature in the catalytic converter where a high OSC is reached at temperatures of 300°–400°C or 600°C for fresh and aged catalysts respectively. (Koltsakis & Stamatelos 1997, Lox & Engler 1997, Sideris 1998)

2.3.4 Cold start and catalyst fast light-off

An important development to increase the performance of the catalytic converter is to minimize emissions during the cold start by decreasing the catalyst light-off temperature. During cold start, the temperature of the catalytic converter is low and the converter is not yet activated. Hence the catalyst light-off temperature (temperature at which the conversion of an exhaust gas component reaches 50%) is not yet reached, hydrocarbons and CO are not converted and they contribute to the majority of the total emissions in the legislated driving cycles (see section 3.4) during the first couple of minutes after the engine is started. Special techniques have been developed in order to minimize emissions during a cold start. These fast light-off techniques either employ changes in the exhaust system design (passive systems), or they rely on the controlled supply of additional energy to raise exhaust gas temperature during the cold start (active systems). (Koltsakis & Stamatelos 1997, Marin & Hoebink 1997, Sideris 1998)

The main techniques to minimize cold start emissions are categorized as follows: the use of close-coupled (CC) catalyst, electric heaters, hydrocarbon traps or fuel burners and afterburners (Koltsakis & Stamatelos 1997). The catalytic converter is traditionally located under a vehicle's floor. The commonly used CC-catalytic converter consists of a pre-catalyst and a main catalyst, as shown in Fig. 6. The location of the pre-catalyst closer to the engine's manifold enables decreasing pollutant concentrations during the warm-up, *i.e*. the first minutes of engine's operation. This allows for a faster light-off since the catalyst is heated by the exhaust gas rather rapidly. On the other hand, the temperature of the pre-catalyst can even rise up to 1100°C, depending on the driving conditions. This accelerates the catalyst's ageing and requires better thermal resistance from the catalytic materials. The common formulation of a pre-catalyst in TWC applications is either Pd-Rh or Pd-only with high precious metal loading, thus favouring exothermic oxidation reactions and producing heat utilized to heat-up the main catalyst. (Becker & Watson 1998, Farrauto & Heck 1999, Farrauto & Heck 2001, Heck & Farrauto 1997, Sideris 1998)

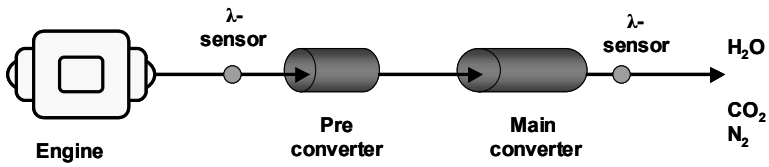

Fig. 6. Automotive emission control system showing the pre- and main catalytic converters.

3 Catalyst deactivation – Ageing

3.1 Overview

Catalyst deactivation, the loss of catalytic activity and/or selectivity over time, is of crucial importance in three-way catalysis where catalytic materials are exposed to high temperatures under fluctuating conditions. In the literature, there are several definitions for deactivation, but none of them, as yet found by the author, is exclusively broad enough as a definition of the deactivation of a three-way catalyst. The precise definition of deactivation is rather difficult to present, because deactivation is a complex phenomenon, as will be indicated in this Chapter, and the type of deactivation changes depending on the application area. In this thesis, catalyst deactivation is defined as a phenomenon in which the structure and state of the catalyst change, leading to the loss of active sites on the catalyst's surface and thus causing a decrease in the catalyst's performance. Furthermore, another important term in this thesis is **ageing**, which is commonly used to describe high temperature-induced deactivation.

Catalyst deactivation is a result of a number of unwanted chemical and physical changes. The causes of deactivation are classically divided to three categories: chemical, thermal and mechanical (Butt & Petersen 1988, Bartholomew 2001). In this thesis, mechanisms of thermal and chemical deactivation are mostly considered. Mechanical deactivation as a result of physical breakage, attrition or crushing is also an important deactivation phenomenon. However, for the current catalytic converters, deactivation during the normal vehicle operation is typically a result of chemical and thermal mechanisms, rather than fouling and mechanical factors (Koltsakis & Stamatelos 1997), one reason why mechanical deactivation has been excluded from this thesis.

Recently, several papers have reviewed the causes of deactivation (Forzatti & Lietti 1999, Bartholomew 2001, Moulijn *et al.* 2001). Deactivation of a catalyst is usually an inevitable and slow phenomenon. Despite its inevitable nature, some immediate consequences of deactivation may at least be partly avoided, or even reversed. Deactivation of a three-way catalyst can result from various processes (deactivation mechanisms) as summarized in Table 4. The three major categories of deactivation mechanisms are sintering, poisoning, and coke formation or fouling (Forzatti & Lietti

1999). They may occur separately or in combination, but the net effect is always the removal of active sites from the catalytic surface. Some other deactivation mechanisms, such as pore blockage, volatilization of active component, destruction of the active surface and incorporation of the active component into the washcoat in an inactive form can also cause decline in the catalyst's activity. (Butt & Petersen 1988, Bartholomew 2001)

Table 4. A summary of the deactivation mechanisms of three-way catalysts (Carol et al. 1989, Koltsakis & Stamatelos 1997, Sideris 1998).

Thermal	Chemical	Fouling	Mechanical
Sintering	Poisoning: irreversible adsorption or reaction on/with the surface	Coke formation (carbon deposits)	Thermal shock
Alloying	Inhibition: competive reversible adsorption of poison precursors		Attrition
Support changes	Poison-induced reconstruction of catalytic surfaces		Physical breakage
Precious metal-base metal interactions	Physical/chemical blockage of support pore structure		
Metal/metal oxide-support interactions			
Oxidation			
Precious metal surface orientation			
Metal volatilization			

Deactivation of a three-way catalyst is a complex phenomenon since the purification performance of a three-way catalytic converter is affected by many factors, such as changes in the exhaust gas velocity and composition, temperature, precious metal loading and the catalyst's age. Three-way catalysts are designed to withstand momentarily high operation temperatures, but the long-lasting exposure to high thermal loading increases the risk of thermal deactivation. (Beck *et al.* 1997a, Beck *et al.* 1997b, Koltsakis & Stamatelos 1997)

Thermal, or thermo-chemical degradation, is probably the main cause for the deactivation of automotive exhaust gas catalysts. Three-way catalysts are known to loose their activity, especially under oxidizing conditions at temperatures higher than 900°C (Ihara *et al.* 1987, Härkönen *et al.* 1991). Exposure to high operation temperatures enhances the reduction of the alumina surface area and sintering of the precious metals, resulting in a loss of effective catalytic area. The thermal degradation of three-way catalysts is caused not only by high temperature but also by sudden temperature changes in the catalytic converter. Catalysts may also be poisoned in the presence of some pollutants, such as sulfur or phosphorus. These components contaminate the washcoat and precious metals and reduce the active catalytic area by blocking the active sites. On the other hand, deactivation by fouling or coke formation is not regarded as a major problem in the current high-temperature catalytic purification systems. (Koltsakis & Stamatelos 1997, Sideris 1998)

3.2 Catalyst deactivation mechanisms

3.2.1 Deactivation by thermal degradation and sintering

Temperature has become an increasingly important factor for deactivation of three-way catalysts due to the fact that the converter is installed near the engine to confirm the efficient purification of hydrocarbons. Most of the emissions are formed during cold start, and during the low temperature operation of the catalyst, as mentioned earlier. Since the pre-converter is installed near the engine, the temperature inside the converter is higher than in the main converter due to higher temperature of exhaust gas. Thus, catalytic materials have to work even at temperatures higher than 1000°C (Koltsakis & Stamatelos 1997, Becker & Watson 1998). Thermal degradation of a three-way catalyst begins in the temperature area of 800°–900°C, or even at lower temperatures, depending on the materials used. It is a physical process leading to a catalyst deactivation at high temperatures because of the loss of catalytic surface area due to crystal growth of the catalytic phase, the loss of washcoat area due to a collapse of pore structure, and/or chemical transformations of catalytic phases to non-catalytic phases. The first two processes are typically referred to as sintering, and the third as the solid-solid phase transition at high temperatures. (Butt & Petersen 1988, Somorjai 1994, Bartholomew 2001, Moulijn *et al.* 2001)

In Fig. 7, the deactivation mechanisms of a three-way catalyst are illustrated. These mechanisms are examined in detail in the following paragraphs and references to Fig. 7 are given concurrently. Sintering, as illustrated in Figures 7C and 7D, is the loss of catalyst's active surface due to crystal growth of either the bulk material or the active phase. In the case of supported metal catalysts, reduction of the active surface area is provoked *via* agglomeration and coalescence of small metal crystallites into larger ones (Gunter *et al.* 1997, Stakheev & Kustov 1999). Two different models have been proposed for sintering *i.e.*, the atomic migration and the crystallite migration models. As such, sintering occurs either due to metal atoms migrating from one crystallite to another *via* the surface or gas phase by diminishing small crystallites in size and increasing the larger ones (atomic migration model). Or sintering can occur *via* migration of the crystallites along the surface, followed by collision and coalescence of two crystallites (crystallite migration model) (Forzatti & Lietti 1999, Bartholomew 2001). Figure 7C presents a schematic representation of atomic migration and crystallite migration models.

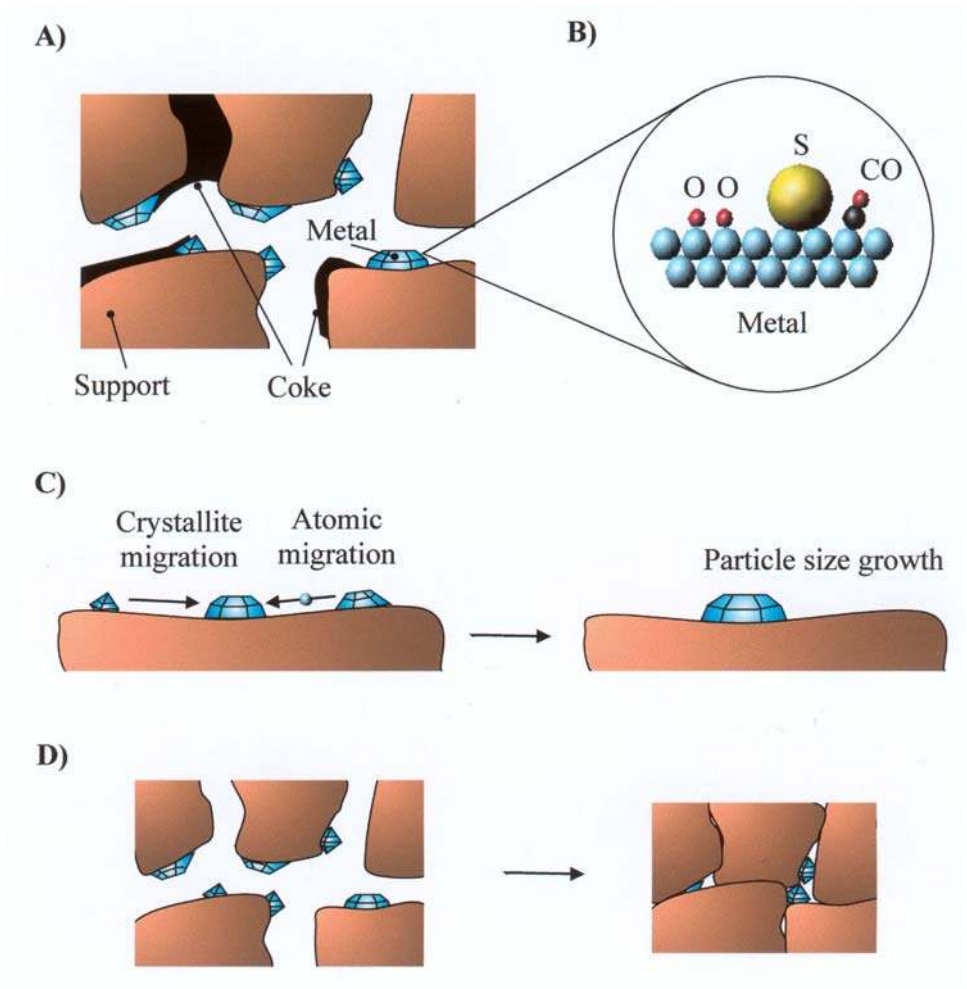

Fig. 7. Deactivation mechanisms: A) Coke formation, B) Poisoning, C) Sintering of the active metal particles, and D) Sintering and solid-solid phase transitions of the washcoat and encapsulation of active metal particles (cf. Suhonen 2002).

As mentioned earlier, sintering on supported metal catalysts involves complex physical and chemical phenomena that make the understanding of the mechanistic aspects of sintering difficult. Experimental observations have shown that sintering is strongly temperature-dependent (Bartholomew 2001, Mouljin *et al.* 2001), but is also affected by the surrounding gas atmosphere (Forzatti & Lietti 1999). The rate of sintering increases exponentially with temperature and, for example, the sintering of precious metals becomes significant above 600°C. The underlying mechanism of sintering of small metal particles is the surface diffusion, or at higher temperatures, the mobility of larger agglomerates. The so-called Hüttig and Tamman temperatures indicate the temperature at which sintering starts. The following semi-empirical relations for Hüttig and Tamman temperatures are more commonly used (Mouljin *et al.* 2001):

$$T_{Hüttig} = 0.3\ T_{melting} \quad (2)$$

$$T_{Tamman} = 0.5\ T_{melting} \quad (3)$$

Temperature at which the solid phase becomes mobile depends on several factors such as texture, size and morphology. For instance, highly porous γ-alumina is much more sensitive to sintering than non-porous α-alumina. (Mouljin *et al.* 2001)

Sintering processes at high temperatures are also affected by atmosphere, as expressed earlier. Supported metal catalysts sinter relatively rapidly under an oxidizing atmosphere, however the process is more slow under reducing and inert atmospheres (Wanke & Flynn 1975). Sintering is also generally accelerated, e.g. in the presence of water vapor (Mowery *et al.* 1999, Bartholomew 2001). In addition to temperature, atmosphere and time, the sintering rate is also dependent on several other factors, such as precious metal loading and washcoat composition. The presence of specific additives is known to reduce the sintering of a catalyst: BaO, CeO_2, La_2O_3 and ZrO_2 improve the stability of γ-Al_2O_3 towards sintering in the presence of high H_2O content in the exhaust gas. (Heck & Farrauto 1997)

Solid-solid phase transitions, as presented in Fig. 7D, can be viewed as an extreme form of sintering occurring at very high temperatures and leading to the transformation of one crystalline phase into another. Phase transformations typically occur in the bulk washcoat, e.g. aluminium oxide has many phases from the porous γ-Al_2O_3 to non-porous α-Al_2O_3, which is the most stable phase of alumina. The phase transformations of Al_2O_3 (boehmite), as shown in Fig. 8, become significant at high temperatures and remarkably decrease the surface area of the catalysts (Hayes & Kolaczkowski 1997, Forzatti & Lietti 1999). On supported metal catalysts, the incorporation of the metal into the washcoat can be observed, *i.e.* the reaction of Rh_2O_3 with alumina to form inactive Rh-aluminate at high-temperatures, especially in lean conditions. (Shelef & Graham 1994)

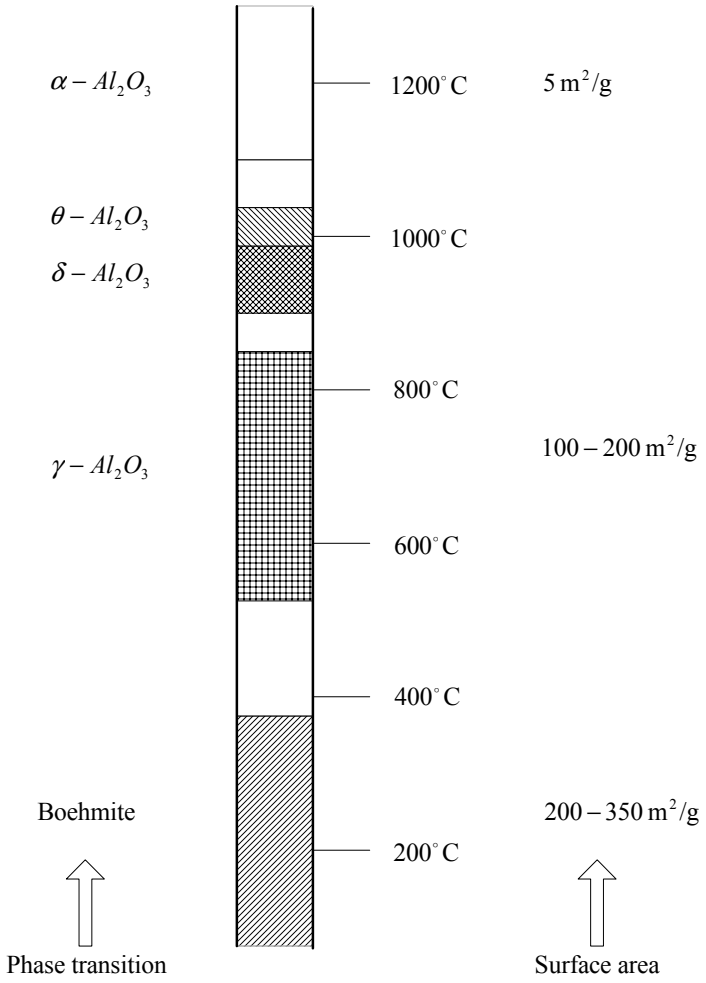

Fig. 8. Phase transitions and surface areas of Al_2O_3 (boehmite) as a function of temperature.

Active precious metals are well-known catalysts for the exhaust gas purification. The sintering behaviour of Pt, Pd and Rh under different ageing atmospheres is considered in Table 5. Among the active metals, rhodium is known to be the most sensitive metal towards sintering at high temperatures under the exhaust gas conditions. This leads to poor activity, especially in the reduction of NO_X (Taylor 1993). The use of a bimetallic catalyst, such as Pd-Rh or Pt-Rh, gives a better catalytic activity at high temperatures. The operation conditions (rich or lean) also affect the sintering of active metals; for example, ageing atmosphere and the oscillation between oxidizing and reducing atmospheres can accelerate deactivation. (Butt & Petersen 1988, Koltsakis & Stamatelos 1997)

Table 5. Effect of ageing atmosphere on the sintering behaviour (particle size) of Pt, Pd and Rh (washcoat La_2O_3-doped Al_2O_3, precious metal content 0.14 wt-%) (Shinjoh et al. 1991).

Particle size (Å)	Pt	Pd	Rh
N_2 / 1100°C	210	970	140
Exhaust gas / 1100°C	780	680	880
Air/ 1100°C	970	n.d.	n.d.

n.d. = not determined

Redispersion is an opposite process to sintering. During redispersion, many complex phenomena take place, the particle sizes decrease and surface areas increase. In particular, the interaction between oxygen and precious metals may lead to the formation of species that are mobile on the surface and reverse the process of agglomeration. Sintering is normally physical rather than chemical in nature and, therefore, the magnitudes of thermal activation are quite different. Typical activation energies for sintering may be twice or even three times lower than those associated with the chemical processes in poisoning or coke formation. Furthermore, ageing time is important because it correlates both with sintering and redispersion. (Flynn *et al.* 1975, Butt & Petersen 1988, Gunter *et al.* 1997)

The kinetics of a catalyst deactivation is a function of temperature, time, pressure and the concentrations of different substances. The change in catalytic activity can be an effect of one or several of the previously mentioned processes. For sintering, the kinetics can be derived from active metal surface area *versus* time measurements at constant temperature. A number of researchers, Wanke & Flynn (1975), Bartholomew (1984) and Fuentes & Gamas (1991), have attempted to correlate sintering kinetics of supported metal catalysts. The following simple correlation of sintering kinetics can be applied:

$$\frac{d(D/D_0)}{dt} = -k(D/D_0)^n \qquad (4)$$

where D is the metal dispersion (or metal surface area),
D_0 is the initial metal dispersion (or initial metal surface area),
k is the kinetic rate constant for sintering, and
n the sintering order.

It has been found that the use of this equation (Eq. 4) leads to values of k varying with sintering time, and hence with dispersion. Recently, a more sophisticated expression for sintering kinetics has been proposed by Bartholomew (1997) and Fuentes & Salinas-Rodriguez (1997), which takes into account the asymptotic approach (by adding the term $-D_{eq}/D_0$) observed in the typical dispersion *vs.* time curves (as will be presented in Fig. 26):

$$\frac{d(D/D_0)}{dt} = -k(D/D_0 - D_{eq}/D_0)^n \quad (5)$$

where D is the metal dispersion (or metal surface area),
D_0 is the initial metal dispersion (or initial metal surface area),
D_{eq} is the final dispersion (when the asympototic approach is achieved),
k is the kinetic rate constant for sintering, and
n the sintering order.

Equation (5) can be applied in a quantitative comparison regarding the effect of temperature, time and atmosphere on the sintering rate of supported metal catalysts. (Bartholomew 2001)

3.2.2 Deactivation by poisoning

The activity of a three-way catalyst reduces gradually when the unwanted, harmful components of fuels and lubricants, or other impurities, are accumulated on the catalyst's surface and slowly poison the catalyst (Koltsakis & Stamatelos 1997). Poisoning is defined as a loss of catalytic activity due to the chemisorption of impurities on the active sites of the catalyst. Usually, a distinction is made between poisons and inhibitors. Poisons are substances that interact very strongly and irreversibly with the active sites, whereas the adsorption of inhibitors on the catalyst surface is weak and reversible. In the latter case, the catalytic activity can be at least partly restored by regeneration. This irreversible/reversible or permanent/temporary nature of deactivation and the regeneration possibility of a catalyst are the main differences between poisoning and inhibition (Butt & Petersen 1988, Forzatti & Lietti 1999). However, the distinction between permanent and temporary poisoning is not always so clear, since strong poisons at low temperatures may be less harmful in high-temperature applications (Moulijn *et al.* 2001). Catalyst poisons can also be classified as selective or non-selective. The description of a poison as selective or non-selective is related to the nature of the surface and the degree of interaction of the poison with the surface. A poison can also be selective in one reaction, but not in another. (Butt & Petersen 1988)

Poisoning of a three-way catalyst as a result of the accumulation of impurities on the active sites (see Fig. 7B) is typically a slow and irreversible phenomenon. The accumulation of poisons on the active sites blocks the access of reactants to these active sites (Butt & Petersen 1988). As a result of poisoning, the catalytic activity may be decreased without affecting the selectivity, but often selectivity is also changed since some of the active sites are deactivated while others are practically unaffected. In some cases, depending on the adsorbed poison, the poisoned catalyst can be regenerated and its activity can be at least partly restored (Angelidis & Sklavounos 1995, Forzatti & Lietti 1999, Rokosz *et al.* 2001). However, the poisoned three-way catalyst can hardly be regenerated and, therefore, the best method to reduce poisoning is to decrease the amount of poisons in the fuel and lubrication oils to more acceptable levels.

Catalytic converters are poisoned by the impurities in fuel and lubrication oil, or by shavings from the exhaust tailpipe. Even the low levels of impurities are enough to cover the active sites and decrease the performance of a catalytic converter. It follows that the analysis of poisoned catalysts may be complicated since the content of poison of a fully deactivated catalyst can be as low as 0.1 wt-% or even less (Forzatti & Lietti 1999). Lead (Pb), sulfur (S), phosphorus (P), zinc (Zn), calcium (Ca), and magnesium (Mg) compounds are typical catalyst poisons (Liu & Park 1993, Culley *et al.* 1996). Earlier, the effects of lead (Pb) had been studied extremely carefully (Williamson *et al.* 1979a, Williamson *et al.* 1979b, Monroe 1980). The catalytic converters were known to loose already their effectiveness after 10 refills with leaded gasoline (Heck & Farrauto 1996). Nowadays, mostly due to the use of unleaded or low Pb concentrations in gasoline, the role of lead as a catalyst poison is far less significant than in the past.

Fuel (gasoline) contains sulfur in small amounts. New requirements for a low sulfur content (<50 ppm) in the gasoline fuel are introduced together with Euro IV (Directive 98/70/EC). Sulfur clearly affects, and often very quickly, the efficiency and oxygen storage capacity (OSC) of the catalyst. Sulfur poisoning can lead to the formation of new inactive compounds on the catalyst's surface and also to the morphological changes in the catalyst. Fast poisoning by sulfur can be to some extent reversible and the poisoned catalyst can be regenerated (Yu & Shaw 1998). Beck & Sommers (1995) have shown that the impact of sulfur on vehicle-aged catalysts was irreversible at temperatures below 650°C, but the original activity could be restored at higher temperatures. However, it should be noted that although the purification efficiency is recovered, the oxygen storage capacity is not (Beck *et al.* 1997b). During the combustion processes in the engine, fuel sulfur oxidizes to SO_2 and SO_3. These compounds adsorb on the precious metal sites on the catalyst's surface at low temperatures (below 300°C) and react with alumina to form aluminium sulfates that reduce the active surface of washcoat and deactivate the catalyst. The air-to-fuel ratio also affects the behaviour of sulfur. In lean conditions, SO_2 is stored on cerium, and in rich conditions both SO_2 and SO_3 are reduced to form hydrogen sulfide (H_2S). Three-way catalysts are known to loose their activity more in oxidizing (lean) than in reducing (rich) conditions in the presence of sulfur compounds. The problem of sulfur poisoning also appears to be more significant at low temperatures, whereas at elevated temperatures (T>1000°C), the adsorption of sulfur species is almost absent. (Butt & Petersen 1988, Heck & Farrauto 1996)

Phosphorus (P), zinc (Zn), calcium (Ca), and magnesium (Mg) compounds are typical impurities in the lubrication oils. These substances and/or their compounds accumulate on the catalyst's surface and they can be regarded as notable as fuel poisons. The considerable amounts of phosphorus, zinc, calcium, and/or magnesium are normally observed on the surface of an aged catalyst after years of driving. Several studies of the deactivation of a three-way catalyst by phosphorus, calcium and zinc compounds have been published. (Williamson *et al.* 1984, Williamson *et al.* 1985, Inoue *et al.* 1992, Liu & Park 1993, Culley *et al.* 1996)

Zinc dialkyldithiophosphate (ZDP), a typical oil additive, is a common source of phosphorus and zinc. Several studies have shown that the individual effects of P and Zn on deactivation are small compared to that of the combined effect of P and Zn. At low exhaust temperatures in particular the formation of zinc pyrophosphate ($Zn_2P_2O_7$) decreases the catalytic activity (Williamson *et al.* 1984, Williamson *et al.* 1985). The

phosphorus contamination is observed either as an overlayer of Zn, Ca and Mg phosphates ($M_3(PO_4)_2$, M= Zn, Ca or Mg), or as aluminium phosphate ($AlPO_4$) within the washcoat (Liu & Park 1993, Ueda *et al.* 1994). Recently, cerium has also been observed to form cerium phosphates, $CePO_4$ and/or $Ce(PO_3)_3$ (Rokosz *et al.* 2001). Phosphates form a film layer on the catalyst surface that covers the precious metals in the porous washcoat and prevents contact between the catalyst and the surrounding gas atmosphere. (Brett *et al.* 1989, Heck & Farrauto 1996)

The poisoning of a catalyst is clearly dependent on the phosphorus level in the lubrication oil (Brett *et al.* 1989, Culley *et al.* 1996). The use of calcium or magnesium containing oil additives can decrease the harmful effects of phosphorus (Culley *et al.* 1996). Calcium and magnesium sulfonates form Ca and Mg phosphates and thus prevent the accumulation of phosphorus on the catalyst's surface (Ueda *et al.* 1994). Similar observations have also been made in the case of zinc compounds (Monroe 1980). The largest contaminant levels are typically observed in the front edge of the catalyst (Culley *et al.* 1996, Beck *et al.* 1997a, Beck *et al.* 1997b). Experimental observations have also shown that even small amounts of these compounds are high enough to decrease the performance of a catalytic converter. (Joy *et al.* 1985)

Active metal catalysts are preferred in the controlling of the exhaust gas emissions, because they are less liable to sulfur poisoning than metal oxide catalysts (Shelef *et al.* 1978), as reported above. Precious metals have different types of resistance against poisoning. Palladium is more sensitive than platinum and rhodium to chemical deactivation, in particular to poisoning by sulfur and lead (Taylor 1993, Lox & Engler 1997). Currently, the use of Pd catalysts is possible because of the rapid decrease in fuel lead content, as discussed previously. The additives used and the chemical composition of the washcoat has an effect on the sulfur behaviour in the catalyst. In particular additives, which play a significant role in Pd-only catalysts. (Heck & Farrauto 1996)

Driving conditions also affect the catalyst's chemical deactivation. Especially in Nordic countries, where the cold weather and urban driving keep the catalyst's temperature low during a long time period. This accelerates the catalyst's chemical ageing, because the unburned soot and particles adsorb on the active material. The stability against thermal and chemical deactivation can be improved by a proper choice of the catalyst material. In addition, the placement of the active material in separate washcoat layers improves the durability. (Laurikko 1994, Laurikko 1995)

3.2.3 Other relevant mechanisms of deactivation

There are other essential forms of the deactivation of three-way catalysts. For example, pore blockage, encapsulation of metal particles, volatilization of active compounds, fouling or coke formation and metal-metal or metal-washcoat interactions, which will be briefly discussed below.

According to Graham *et al.* (1999), high temperature ageing may result in deep encapsulation of sintered precious metal particles (see Fig. 7D) as the surface area of the washcoat decreases. This is a serious type of deactivation because of its permanent

nature. The encapsulated metal particles cannot participate in catalysis since they are inaccessible to gas phase molecules. Furthermore, support can interact with the metal catalyst also by the support-induced changes observed in the metal particle morphology, by the formation of specific active sites on the metal-support interface and by the charging of metal particles. (Hu *et al.* 1998)

Fouling covers all phenomena where the surface is covered with a deposit, e.g. with combustion residues such as soot or with mechanical wear. Coke formation is the most widely known form of fouling (it is even used as a synonym for fouling). Coke formation is not very clearly defined. There are probably as many mechanisms of coke formation as there are reactions and catalysts where this phenomenon is encountered. During the coke formation, carbonaceous residues cover the active surface sites (see Fig. 7A), and decrease the active surface area. First, this blocks out the active compounds to reach the surface sites, and second, the amount of coke might be so large that carbon deposits block the internal pores in the catalyst. In many cases, hydrocarbons and aromatic materials are primarily responsible for coke formation. Among these other deactivation mechanisms, pore blocking is probably one of the most important mechanisms. Pore blocking is often connected to coke formation, and when the amount of coke is high on the catalyst's surface, it may be possible for the coke itself to block off the pore structure. (Butt & Petersen 1988, Mouljin *et al.* 2001)

At high temperatures, catalysts may suffer from the loss of active phase through volatilization**.** Metal loss through direct volatilization is generally an insignificant route of the catalyst deactivation. By contrast, metal loss through the formation of volatile compounds is important over a wide range of conditions (Bartholomew 2001). Large amounts of catalytic materials can be transported to either substrate where they can react, or into the gas phase where they are lost in the effluent gas stream. High volatility limits the selection of otherwise useful catalytic materials, e.g. the oxides of Pt, Pd and Rh formed during the reaction cycles are not as volatile as the other noble metal oxides, such as RuO_2, OsO_4 and Ir_2O_3. (Cotton & Wilkinson 1988)

The thermodynamics of volatilization and thermodynamic equilibrium calculations are useful in the evaluation of the volatility of metals and metal oxides in order to assess which materials are stable over long periods at high temperatures (Forzatti & Lietti 1999). Thermodynamic equilibrium calculations of the oxidation/reduction behaviour of palladium have shown that phase stability in a Pd/PdO system changes as a function of temperature and oxygen partial pressure. The lower the pressure and the higher the temperature are, the more likely is the Pd phase (Ribeiro *et al.* 1994). In Table 6, vapour pressures of Pt, Pd and Rh as metals and metal oxides are given at a temperature of 800°C in air (Shinjoh *et al.* 1991). The vapour pressure increases with temperature, and it is also strongly dependent on the composition of the surrounding atmosphere, *i.e.* Pd is volatile at temperatures around 850°C and above, depending on the surrounding environment. (Bartholomew 2001)

As can be seen in Table 6, the orders of vapour pressures of active metals and their oxides are as follows (Shinjoh *et al.* 1991):

Metals: Pd > > Pt > Rh

Oxides: Pt > Rh >> Pd

Hence the vapour pressure of metallic Pd is clearly several magnitudes higher than the vapour pressures of Pt and Rh, while as oxides, the situation is the reverse.

Table 6. Vapour pressures (torr) of Pt, Pd and Rh at 800°C in air (Shinjoh et al. 1991).

	Pt	Pd	Rh
Metal	9.1×10^{-17}	1.2×10^{-9}	2.9×10^{-17}
Oxide	1.2×10^{-5}	Negligible	5.8×10^{-6}

As an example, in Figures 9A and 9B, thermodynamics equilibrium curves of Pd and Rh are presented respectively. According to the thermodynamics, Pd is easily oxidized at room temperature to PdO and it reduces to metallic Pd in the temperature range of 500°–1200°C. The formation and decomposition of PdO occurs as follows:

$$2\,PdO \rightleftharpoons 2\,Pd + O_2 \tag{6}$$

The most stable oxidation state of Pd is +2 and the formation of PdO is kinetically restricted at low temperatures. As shown in Fig. 9A, the metallic Pd is totally volatilised in a 5% O_2/N_2 atmosphere at a temperature of 1400°C, and the increased amount of oxygen in the gas phase moves the reduction curve of Pd to higher temperatures. According to Farrauto *et al.* (1992), two kinds of palladium oxides, PdO_X-Pd and PdO, and metallic Pd have been observed on the surface supported on γ-alumina. PdO supported on pure alumina is known to decompose in two steps to metallic palladium in air at a temperature above 800°C. Instead, the re-oxidation of metallic Pd to PdO and PdO_X species during the cooling process is very slow at temperatures 550°–650°C, a temperature range at which PdO is the thermodynamically favoured phase. Temperatures above 800°C convert all PdO_X and PdO to metallic Pd and subsequent cooling again leads to redispersed PdO/Al_2O_3 and PdO_X-Pd/Al_2O_3 phases. Therefore, there is a window of a few hundred degrees in which the catalyst could be in the form of Pd metal or PdO. This hysteresis-like behaviour is strongly dependent on the surroundings of Pd/PdO phases, especially the chemistry of washcoat material and stabilisers. (Farrauto *et al.* 1992, Farrauto *et al.* 1995, Datye *et al.* 2000)

A)

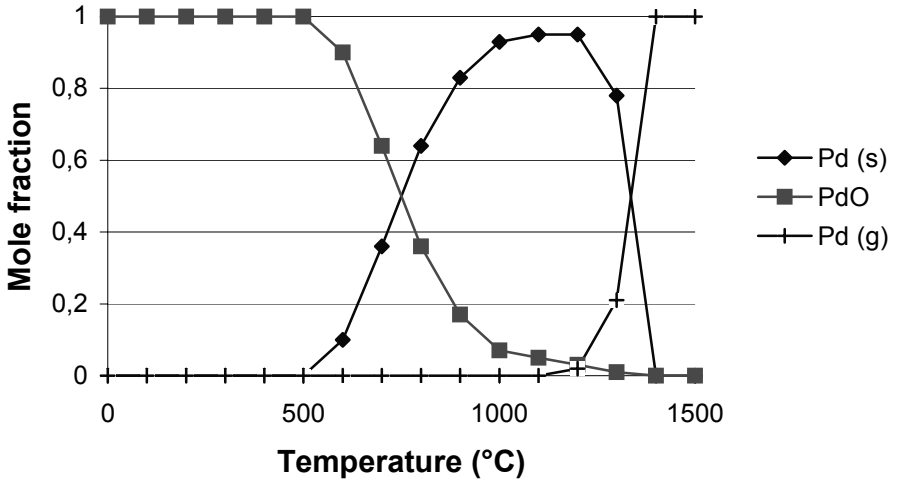

B)

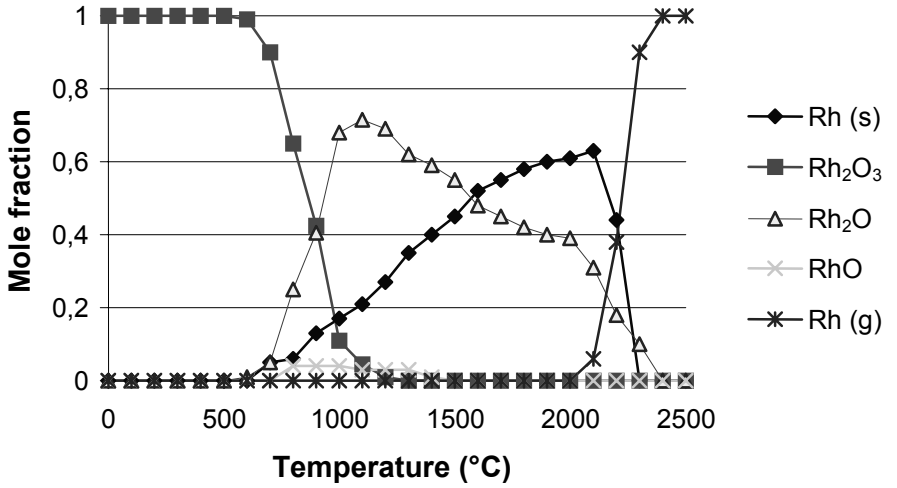

Fig. 9. Thermodynamic equilibrium calculations of volatilization of A) Pd and B) Rh in a 5 % O_2/N_2 atmosphere (lean) (Turpeinen & Maunula 1993).

Studies of the stabilization of rhodium oxide phases supported on γ-alumina have shown several thermodynamically stable bulk rhodium oxide phases within the ageing temperatures of 500°–1050°C. According to Weng-Sieh *et al.* (1998), ageing in air below 650°C results in the formation of highly dispersed rhodium oxide – RhO_2, and above 650°C large particles of Rh_2O_3 are observed together with smaller particles of RhO_2. The

observed low thermal stability and catalytic activity of rhodium under oxidizing conditions has been attributed to the interaction of Rh with the alumina support and the diffusion of rhodium into the bulk of alumina at high temperatures (Yao *et al.* 1977, Hu *et al.* 1998). However, the nature of rhodium oxides formed during the ageings in air is still unclear and it does not necessarily coincide with that expected on the basis of bulk-phase thermodynamics (Weng-Sieh *et al.* 1998). In Fig. 9B, the thermodynamical equilibrium curves of Rh are presented in a 5 % O_2/N_2 atmosphere. At room temperature, the most stable oxidation state of Rh is +3, and Rh has many oxidation states, as can be seen in Fig. 9B. The oxidation/reduction of Rh occurs as follows:

$$2\,Rh_2O_3 \rightleftharpoons 2\,Rh_2O + 2\,O_2 \rightleftharpoons 4\,Rh + 3\,O_2 \qquad (7)$$

At normal operation temperatures of the catalytic converter, Rh is in the form of Rh_2O_3, if the oxidation of Rh is kinetically favoured. The oxygen content in the exhaust gas strongly affects the formation of Rh oxides; the higher the amount of oxygen, the higher the transition temperature is.

3.3 Accelerated catalyst ageing

Deactivation of a three-way catalyst is typically a very slow phenomenon, a reason why a large number of catalyst ageing cycles have been developed for the relative fast testing of catalyst thermal stability. A number of non-vehicle test methods have been developed to achieve the accelerated catalyst ageing under laboratory-controlled conditions. These ageing methods typically involve the use of test engines, atmosphere controlled ageing furnaces and pulse-flame reactors. The ageing procedures can be divided into the following three categories: vehicle ageing cycles, engine bench ageing and laboratory ageing in furnace (Summers *et al.* 1990, Hannington 1991, Bartley *et al.* 1993, Kumar *et al.* 1994, Koltsakis & Stamatelos 1997). These ageing procedures are briefly described in the next paragraphs.

A vehicle ageing cycle represents, in the best possible way, the real driving conditions to which a given vehicle could be subjected to during a required catalyst lifetime. Automotive manufacturers use vehicle ageing test procedures to test the stability and durability of catalytic converters under real driving conditions. However, the use of such test procedures is normally limited due to the high operation costs. (Koltsakis & Stamatelos 1997)

The aim of engine bench ageing is to test the thermal and chemical stability of a catalyst. An engine bench cycle contains the subjection of the catalyst to thermal loading, high temperature oxidation and the presence of catalyst poisons. As mentioned earlier, the major damage to a catalyst results from the exposure to oxidizing atmosphere at high temperatures (Koltsakis & Stamatelos 1997). Such conditions are normally encountered during vehicle braking with fuel cut after running at moderate or high power. These conditions can be simulated in an engine bench. All the catalyst manufacturers have their own ageing cycles for engine ageing that can include the measurements of activity,

oxygen storage capacity and emissions, as well as redox scanning with varying air-to fuel ratios. (Kumar *et al.* 1994, Heck & Farrauto 1997, Koltsakis & Stamatelos 1997)

The high temperature laboratory ageing procedures simulate the oxidation and the sintering of washcoat and precious metals in artificial atmospheres, temperatures and flow conditions. In order to simulate severe ageing conditions within the minimum time, the laboratory scale furnace ageing is usually performed at very high temperatures and under gas atmospheres (typically in air) that are far removed from real driving conditions. Laboratory scale ageing procedures may also involve cycled feedstreams or pulses. (Koltsakis & Stamatelos 1997)

3.4 Vehicle test cycles

The new emission standards of the EU and the U.S.A. demand more sophisticated optimisation of all the compounds that contribute to the performance of the emission control system. In order to control the vehicle's emissions, several test procedures have been developed and standardized. The most common test procedures are the European Driving Cycle (EC2000) and FTP (Federal Test Procedure) established by the EU and the U.S. Environmental Protection Agency (EPA) respectively. The test procedure is always a compromise between real driving conditions and the repeated measurements in the laboratory scale, and it has to, in a given accuracy, represent real driving style and conditions. (Heck & Farrauto 1996, Sideris 1998)

Test cycles are performed on a dynamometer. The emissions are sampled during the cycle by a constant volume sampler (CVS) and they are expressed in g/km. The test methods and conditions are standardized. The European test driving cycle is based on Euro III and it is presented in Fig. 10. The driving cycle consists of two parts, ECE15 and EUDC, that correspond to urban and highway (extra-urban) driving conditions in that order. ECE15 test cycle simulates a 4.052 km urban trip at an average speed of 18.7 km/h and at a maximum speed of 50 km/h. Its duration is 780 seconds. The same part of the ECE15 driving cycle is repeated four times to obtain an adequate driving distance and temperature. The EUDC cycle instead illustrates the aggressive, high speed driving at a maximum speed of 120 km/h. Its duration is 400 seconds and 6.955 km at an average speed of 62.6 km/h. Since the year 2000, the 40 seconds idle period at the beginning of the European driving cycle (EC2000) was omitted. Thus, the emissions during the cold start are included in the driving cycle and this makes EC2000 a more realistic test procedure. (Heck & Farrauto 1997, Koltsakis & Stamatelos 1997)

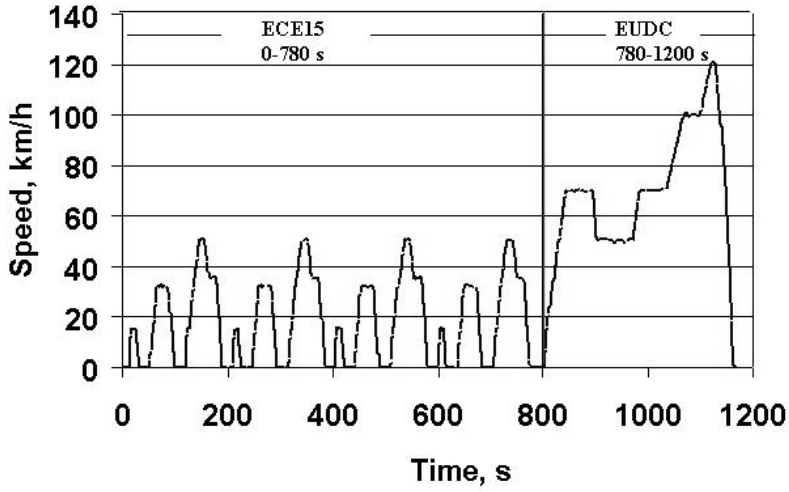

Fig. 10. The European Driving Cycle (EC2000): The speed of a vehicle as a function of time.

FTP test cycle, as shown in Fig. 11, corresponds to the European test driving cycle. It illustrates real driving time and conditions by measuring the speed of a vehicle as a function of time. FTP test cycle simulates the 17.7 kilometres (11.4 miles) of driving cycle through Los Angeles at an average speed of 34.1 km/h (corresponding to 21.2 miles per hour). The test measures the emissions of CO, HC and NO_x, and involves a cold start after the engine's idle period for eight hours, a hot start, and a combination of urban and highway conditions (Heck & Farrauto 1996, Sideris 1998). A change that is being assessed is to expand the FTP to include the conditions that involve aggressive driving behaviour at high speed and acceleration, and rapid fluctuation in speed and start-up after the engine is turned off for intermediate periods. This will result in higher concentrations of pollutants and greater demand on the catalyst. (Heck & Farrauto 1996, Sideris 1998)

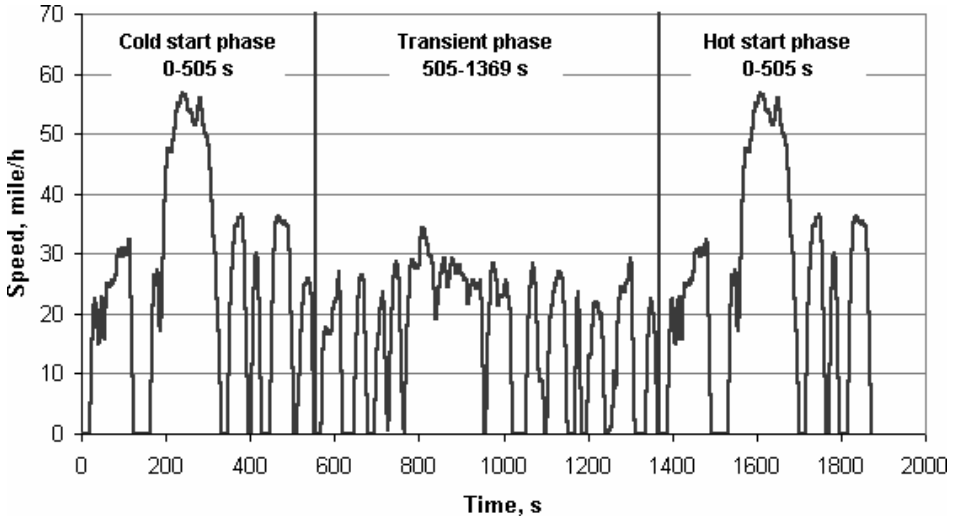

Fig. 11. FTP-75 test driving cycle established by the EPA.

The comparison of these two test cycles, EC2000 and FTP, is rather difficult because both the speed and time profiles of the cycles are quite different. At the beginning of the ECE15 cycle, the driving speed is slow and the load of an engine is lower compared to the FTP cycle. Thus, in the European test cycle, both the engine and catalytic converter warm up slowly. This is also observed by looking at the emissions of CO and HC and catalyst light-off values that are much smaller in the case of the FTP cycle. In this case, the European test cycle is more reliable, because the emissions formed during the cold start are taken into account. On the other hand, the FTP test cycle is a transient test cycle with a highly dynamic nature, whereas the European test cycle is a more static one. Therefore, the FTP test cycle corresponds better to emissions during real driving, where the temperature of exhaust gases increases gradually. (Laurikko 1994, Lox & Engler 1997, Sideris 1998, Laurikko 2001)

4 Experimental

4.1 Catalysts

The catalysts used in this study were metallic Pd/Rh monoliths, as shown in Fig. 12, designed for Euro IV emission limits and, therefore, catalysts have close to commercial structure. The model catalysts consisted of a thin Fe-Cr-Al foil coated with a layered washcoat (see Fig. 13), mainly containing γ-Al_2O_3. The washcoat material content of the catalyst was 62.8 g/m^2 and the amounts of the active metals in the catalyst were Pd 0.29 wt-% and Rh 0.03 wt-%. The active metals, being palladium and rhodium, were added on the different washcoats of the catalyst. In addition to palladium and γ-Al_2O_3, the other washcoat (washcoat 2) also contained La_2O_3 and minor amounts of OSC material as stabilizers and promoters (additives). Another washcoat (washcoat 1) included rhodium, γ-Al_2O_3 and OSC compounds. CeO_2 and $Ce_XZr_{1-X}O_2$ mixed oxides were used as OSC material in the catalyst.

The catalysts were prepared by mixing the washcoat materials with precursor salts in a water slurry and by coating to a layered structure as mentioned above. Finally, the catalysts were dried at 100°–150°C and then calcined in air at 300°–550°C. The dried and calcined catalysts are referred to as 'fresh' in the following text. Due to the complex structure of the catalyst, separate samples were prepared from the washcoats of the catalyst to help with the interpretation of the results. Furthermore, some of the experiments, in particular NO-TPD experiments, were also carried out with simplified model catalysts (γ-Al_2O_3, modified γ-Al_2O_3, Pd/modified γ-Al_2O_3 and Rh/γ-Al_2O_3) with the active metal loadings of 1 wt-% and 3 wt-% in the washcoat.

A) B)

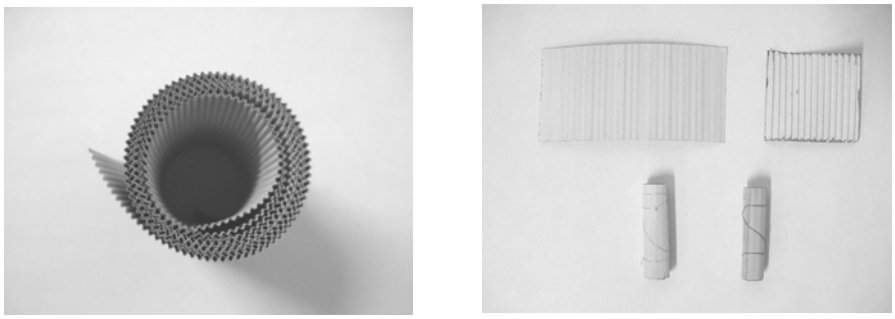

Fig. 12. A) A metallic monolith and B) the fresh catalyst on the left and the engine-aged catalyst on the right.

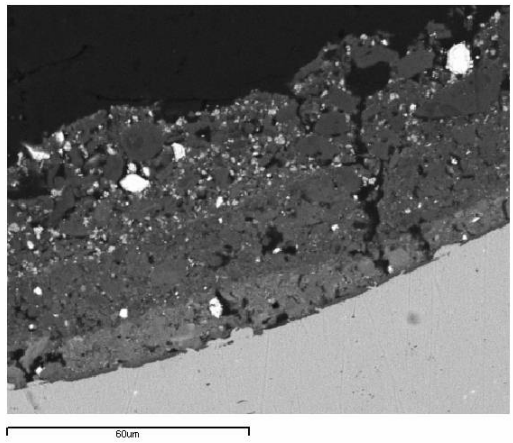

Fig. 13. A SEM image of an engine-aged catalyst.

4.2 Ageing procedures

Catalysts were aged to simulate the high temperature conditions in the exhaust gas streams. The aged catalysts were prepared from the fresh catalyst by using different thermal ageing procedures, as described in Table 7. In addition to those presented in Table 7, the effect of some other ageing atmospheres, such as 5 % O_2/N_2 were also tested. Thermal and hydrothermal ageings were accomplished in a tubular furnace (inlet diameter 40 mm and length 1500 mm) in the temperature range of 800° to 1200°C, and varying the ageing times (3, 24, or 42 hours). Figure 14 presents the experimental set-up

for the ageing furnace. The temperature of the ageing furnace was monitored by a thermocouple that was in close contact with the catalysts, and several catalysts were aged simultaneously. The total gas volumetric flow rate during the ageing was 1 dm^3/min (25°C, 1 atm). The standard size of the cylindrical catalyst in the laboratory tests was 1.4 cm^3 by volume (length 28 mm and diameter 8 mm). Therefore, GHSV was approximately 43 000 h^{-1} during the ageing procedure.

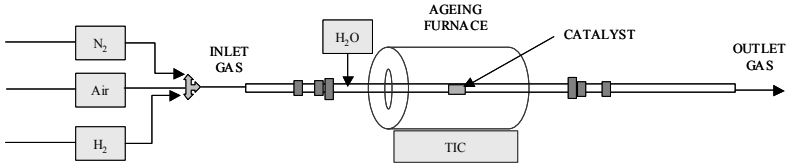

Fig. 14. The experimental set-up of the ageing furnace.

Table 7. Ageing procedures.

Gas feed	Temperatures	Duration
1. Oxidative ageing (air)	800°–1200°C	3, 24 or 42 hours
2. Reductive ageing (5 vol-% H_2 and N_2 balance)	800°–1200°C	3, 24 or 42 hours
3. Inert ageing (nitrogen)	800°–1200°C	3 or 24 hours
4. Hydrothermal oxidative ageing (air and 10 vol-% H_2O)	800°–1200°C	3 hours
5. Hydrothermal reductive ageing (5 vol-% H_2, 10 vol-% H_2O and N_2 balance)	800°–1200°C	3 hours
6. Engine ageing (exhaust gas)	1030°–1060°C	40 hours
7. Vehicle ageing (exhaust gas)		100 000 km

In the thermal ageing procedure, catalysts were treated in oxidative (air), inert (nitrogen), and reductive (5% H_2/N_2) ageing atmospheres. Hydrothermal ageings were accomplished in oxidative (H_2O/air) and reductive (H_2O/H_2) ageing atmospheres in the presence of 10 vol-% water vapour, which corresponded to the water flow of 0.1 cm^3/min into the furnace. Ageing temperatures higher than 1200°C were not used in this study because those temperatures are not present in normal operating conditions. Engine ageing was carried out in the exhaust gas stream of a V8 engine for 40 hours. The ageing procedure was composed of rich (50 min, 1030°C, λ=0.98-0.99) and stoichiometric (10 min, 1050°–1060°C, λ=1.00) air-to-fuel ratios carried out consecutively. The vehicle ageing was accomplished under European driving conditions (100 000 kilometres). Kemira Metalkat Oy (Finland) provided the industrial reference catalysts (fresh, engine-aged and vehicle-aged). All the catalysts were identical in chemical composition and thus only the changes induced by ageings were considered. The engine-aged and vehicle-aged catalysts were also divided into different test zones (as presented in Fig. 15) in order to evaluate the effect of the position-dependent phenomena. In particular, the characterization results of different test zones were used when evaluating the role of poisons on the catalytic activity.

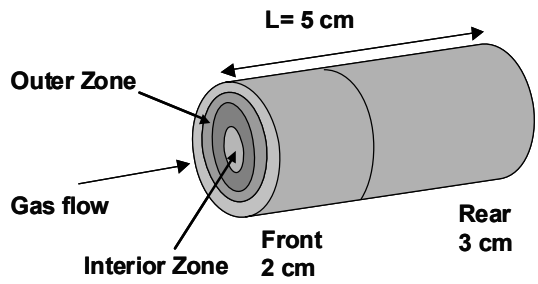

Fig. 15. Test samples from the different zones of the pre-catalyst.

4.3 Catalyst characterization techniques

Experimental surface characterization methods were used to study ageing-induced changes in the active metals and washcoat oxides. The characterization techniques included both microscopic and spectroscopic methods, such as Scanning Electron Microscopy (SEM) and X-ray Diffraction (XRD). Several characterization techniques are available to study solid surfaces and the properties of catalysts, and no single characterization method can be used to explain the basis for the catalyst deactivation phenomena of three-way catalysts (Wachs 1992, Niemantsverdriet 2000). In the proceeding sections, the characterization techniques utilized in this thesis are presented in detail.

4.3.1 Scanning Electron Microscopy

Scanning Electron Microscopy (SEM) was used in this thesis for high magnification imaging and elemental analysis. A Jeol JSM-6400 scanning electron microscope equipped with an energy dispersive spectrometer (EDS) was used for the analysis. In the pretreatment stage, flat pieces of fresh and aged catalysts were cut, and either potted in epoxy or fastened with a carbon tape in order to obtain side or top views of the catalyst respectively. Catalysts were polished down to 1 μm using diamond paste and coaled prior the analysis to avoid the accumulation of charge. The accelerating voltage and current in the measurements were 15 kV and 12 nA, respectively, and the resolution of the instrument was 3.5 nm (35 kV). SEM-EDS resources were used in the Institute of Electron Optics at the University of Oulu.

4.3.2 Physisorption analyses

Measurements of gas adsorption isotherms are widely used for determining the surface area and pore size distribution of solids. The use of nitrogen as the adsorptive gas is recommended if the surface areas are higher than 5 m^2/g (Serwicka 2000). The first step in the interpretation of a physisorption isotherm is to identify the isotherm type. This in turn allows for the possibility to choose an appropriate procedure for evaluation of the textural properties. Non-specific Brunauer-Emmett-Teller (BET) method is the most commonly used standard procedure to measure surface areas, in spite of the oversimplification of the model on which the theory is based. The BET equation is applicable at low p/p_0 range and it is written in the linear form (Wachs 1992):

$$\frac{p}{n^a(p_0 - p)} = \frac{1}{n^a{}_m C} + \left(\frac{C-1}{n^a{}_m C}\right)\frac{p}{p_0} \tag{8}$$

where p is the sample pressure,
p_0 is the saturation vapour pressure,
n^a is the amount of gas adsorbed at the relative pressure p/p_0,
$n^a{}_m$ is the monolayer capacity, and
C the so-called BET constant.

Equation (8) can be applied for determining the surface areas and pore volumes from adsorption isotherms, if the adsorption isotherms are of type IV according to IUPAC classification. The pore size distributions can be calculated from desorption isotherms. The pores are usually classified according to their widths as micropores (diameter less than 2 nm), mesopores (diameter between 2 and 50 nm) and macropores (diameter exceeding 50 nm) (Hayes & Kolaczkowski 1997). Several approaches have been developed to assess the micro- and mesoporosity, and to compute pore size distribution from the adsorption-desorption data. All of these involve a number of assumptions, e.g. relating to pore shape and mechanism of pore filling. (Serwicka 2000)

In this thesis, physisorption measurements were carried out to characterize catalysts before and after the ageings. Specific surface areas (m^2/g) and pore volumes were measured according to the standard BET method, as described above, by using a Coulter Omnisorp 360CX. The specific surface areas and pore volumes were obtained from N_2 adsorption isotherms at -196°C by assuming the cylindrical shape of pores. Catalysts were outgassed in a vacuum at 140°C overnight before the measurements. All the BET values in this study were measured within a precision of ± 5%. Pore size distributions for micropores as well as meso- and macropores were calculated from N_2 -desorption isotherms by differential HK (Horvath-Kawazoe) and BJH (Barrett-Joyner-Hallender) methods respectively (see Anon 1992). Since the monoliths showed systematically lower BET values than the crushed samples after similar ageing procedures, all the BET values presented in this thesis have been determined for the metallic monoliths with a standard shape and mass.

4.3.3 Chemisorption analyses

Chemisorption measurements were carried out in order to determine the dispersions of Pd and Rh metal particles, monolayer capacities and the amount of active metal in the catalysts. Hydrogen and carbon monoxide were used as the adsorbate gases. H_2-chemisorption and CO-chemisorption experiments were carried out close to room temperature (30°C) by volumetric adsorption method by using a Coulter Omnisorp 360CX (at the University of Oulu) and a Sorptomatic 1900 (at Kemira Metalkat Oy), respectively. The accuracy of the measurements was estimated to be better than ± 5%. The experimental procedure for the H_2-chemisorption measurements is presented in Table 8. In the chemisorption procedure, the temperature ramping rate of the furnace was 10°C/min. As shown in Table 8, the adsorption of H_2 was measured twice. The difference between these two measurements was assumed to be the amount of irreversibly adsorbed H_2, which is further used to calculate the dispersion values.

Table 8. The experimental procedure for the H_2-chemisorption measurements at the University of Oulu (Anon 1992).

1. Flow of He at 150°C for 5 minutes followed by 10 minutes at 375°C
2. Evacuation at 375°C for 10 minutes
3. Reduction in flowing H_2 at 375°C for 10 minutes followed by 5 minutes at 400°C
4. Evacuation at 400°C for 20 minutes followed by 10 minutes at 30 °C
5. Leak test at 30 °C
6. First analysis with H_2 at 30 °C
7. Evacuation at 30 °C for 30 minutes
8. Second analysis with H_2 at 30 °C

Chemisorption has long been employed as a valuable technique for rapid evaluation of the active metal dispersions and hence the particle sizes of supported metals (Gasser 1985). This method has, however, undergone severe criticism, since the underlying assumptions of the stoichiometry between adsorbate gas and precious metal and the particle geometry may not be true, in particular in the case of small particles (Di Monte *et al.* 2000). Furthermore, in the case of metal oxides (such as CeO_2 and Ce-Zr-mixed oxides) in contact with active metals, adsorbed H_2-molecules can also diffuse from the active metal particles to the washcoat. This spillover effect can be reduced by lowering the adsorption temperature, as has been reported by Bernal *et al.* (1993) and Fornasiero *et al.* (1995).

Active metal dispersions and particle sizes are calculated by assuming the stoichiometry factor between chemisorbed gas molecules and surface metal atoms. In this thesis, chemisorption measurements are based on the assumption of the stoichiometry of 2:1 for H_2 and the stoichiometry 1:1 for CO adsorption, respectively, and regardless of the particle size. The stoichiometric ratio may depend on the precious metal particle size, a reason why caution should be exercised when comparing the dispersion values of different catalysts. However, it is assumed that all the aged catalysts as well as the fresh catalyst exhibit rather large metal particle sizes due the low dispersion values (below 30%). Therefore, the changes in dispersion values presented in this thesis reflect the

structural changes induced by ageings, such as the sintering of the precious metals. As well, the chemical correctness behind the stoichiometry assumptions is not relevant because, in this case, the relative dispersion values are more interesting than the absolute ones.

4.3.4 Temperature-programmed techniques

Transient techniques are powerful in the investigation of catalytic surface phenomena. Temperature-programmed methods can provide useful information on solid surfaces, their interactions with adsorbed gas molecules, and thermal stability of surface desorption states (Falconer & Schwarz 1983, Malet 1990, Salvador & Merchán 1998). In this research, temperature-programmed desorption (TPD) of NO is used to obtain information on the ageing-induced changes in the adsorption-desorption behaviour of NO, and to evaluate how these changes are associated with the deactivation of catalysts. NO was chosen as the adsorbate gas molecule because it is the key compound in the purification process of exhaust gases of gasoline engines. (Armor 1992, Taylor 1993)

NO-TPD measurements were carried out in a vacuum or under the carrier gas flow by using NO as the adsorbate gas. NO/Ar (5%) gas mixture and carrier gas Ar (99.998%) were supplied by AGA Ab, Sweden. The gas flows were regulated with mass flow controllers (Bronkhorst High-Tech B.V., The Netherlands). In the pretreatment stage, catalysts were evacuated at two hours and then reduced under hydrogen flow for 10 minutes at 500°C, followed by 15 minutes at 550°C. The catalysts were then cooled down by evacuation before the measurements. NO/Ar (5%) was adsorbed on the catalyst surface at room temperature for 10 minutes. The NO-TPD measurements were carried out in a quartz chamber at temperatures 30°–800°C. The volume of the catalyst monolith was 1.4 cm^3 and the mass of the washcoat about 250 milligrams. Pressure in the reactor chamber was below 10^{-4} mbar (down to 10^{-7} mbar) during the vacuum measurements, whereas the carrier gas measurements were performed at atmospheric pressure. A small portion of the product flow was taken through a capillary into a quadrupole mass spectrometer (Carlo Erba Instruments Q.T.M.D., Italy) (see Anon 1988). The mass numbers of interest molecules were monitored and the results were stored in a PC. The sensitivity factors of the corresponding molecules were determined by using appropriate gas mixtures. A scheme of the reactor system for TPD measurements is presented in Fig. 16.

The TPD profiles were measured as a function of temperature at a linear heating rate (30°C/min). Prior to every TPD run, the excess of gas was removed by evacuation until no residual gases were detected. A West TP190 temperature controller was used to control the heating rate. The heating rate was found to affect the position of the peak maximum. A higher temperature of maximum desorption was observed by increasing the heating rate (Acke 1998, Niemantsverdriet 2000). Therefore, the heating rate was kept constant during the experiments. Furthermore, blank tests were carried out with the uncoated metal foil and no desorption or reactions were detected.

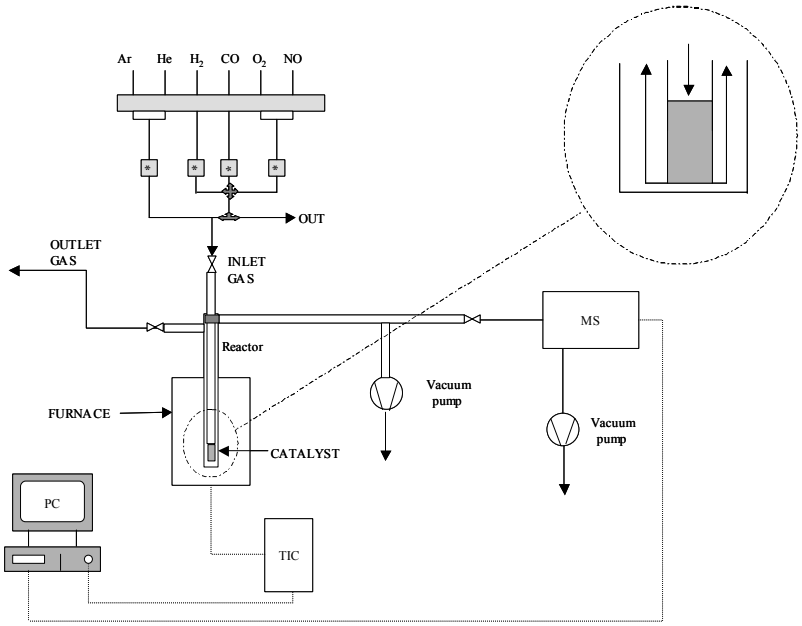

Fig. 16. Experimental set-up for NO-TPD measurements in a vacuum.

4.3.5 X-ray diffraction

X-Ray diffraction (XRD) was used to investigate the bulk phases present in the sample and to determine the ageing-induced solid-solid phase transformations. X-rays are energetic enough to penetrate into the material and their wavelengths are of the same order of magnitude as interatomic distances in solids. Thus, a collimated beam of X-rays is diffracted by the crystalline phases in the sample according to Bragg's Law (Atkins 1995):

$$n\lambda = 2d \sin \theta \qquad (9)$$

where λ is the wavelength of the X-rays,
d is the distance between two atomic planes in the crystalline phase,
n is the order of the diffraction, and
θ the incoming diffraction angle.

The XRD diffractograms presented in this study were recorded on a Siemens D5000 diffractometer employing nickel-filtered Cu Kα radiation (λ = 1.5406 Å, 40 kV, 30 mA) at 0.020° intervals in the range $20° \leq 2\theta \leq 75°$ with 1s count accumulation per step directly from the catalyst foils. The aged catalysts were prepared as mentioned above (see section 4.2). Diffraction patterns were assigned using the PDF database supplied by the

International Centre for Diffraction Data (PDF2- Diffraction Database File). XRD resources of the Institute of Electron Optics at the University of Oulu were used.

4.3.6 X-ray Photoelectron Spectroscopy

While XRD gives information on the bulk phases present in the sample, X-ray Photoelectron Spectroscopy (XPS) can be used to study the sample surface. In this thesis, XPS was mainly utilized to study the ageing-induced changes in the chemical states of active metals. The XPS measurements were carried out at Tampere University of Technology, Finland, by using a Kratos XSAM 800 electron spectrometer with a base pressure less than 1×10^{-8} Torr (1.33×10^{-6} Pa). An analytical chamber was connected to a preparation chamber in which the catalysts could be heated up to 300°C in H_2 atmosphere (99.9999%, AGA Ltd.). Non-monochromatic Mg Kα X-rays were used as a primary excitation. No severe charging of the catalysts was observed. The hemispherical energy analyzer was run in a fixed analyzer transmission (FAT) mode with the pass energy of 38 eV. Due to the known difficulties in referencing the binding energies to the C 1s line (Bhattacharya *et al.* 1997), the Al 2p line at 74.2 eV was used as a reference together with the C 1s line at 284.6 eV. All binding energies quoted in this study were measured within a precision of ±0.2 eV. The reducibility of the Rh oxide phases formed in the different ageing procedures was investigated by annealing the catalysts *in situ* in 400 mbar of static H_2 at 300°C for 30 minutes followed by the XPS measurement. The adequacy of the reduction treatment time was verified by repeating reduction-measurement cycles several times. No remarkable additional changes in the XPS spectra were found after the first reduction treatment. The intention was to discover the relative amount of easily reducible Rh oxide species, and not to try to reduce all oxide species to metallic. A detailed description of the theory behind the XPS and the measurement system can be found in Suhonen (2002).

4.3.7 Activity measurements

Catalytic activities were determined by laboratory scale light-off experiments to compare the catalysts after the ageings. Catalyst light-off is determined as the temperature of 50% conversion, which is used to indicate the efficiency of an automotive exhaust gas catalyst (the lower the light-off temperature, the more active the catalyst is). In addition to light-off temperatures, the conversions of CO and NO at 400°C were also determined.

The experimental set-up for the activity measurements is presented in Figures 17 and 18. Catalytic activities were determined by using a simple model reaction: the reduction of NO by CO in lean and rich conditions. The composition of test gas mixture is presented in Table 9. Before the measurements, the catalysts were reduced in a hydrogen flow (99.98%, AGA Ltd.) at 500°C for 10 minutes, followed by 15 minutes at 550°C. Activity measurements were carried out at atmospheric pressure by using a cylindrical

catalyst with a volume of 1.4 cm^3 (length 28 mm and diameter 8 mm). In the measurements, the gas-solid reactor system equipped with mass flow controllers (Brooks 5850TR), magnetic valves for flow selection, tubular furnace with a quartz reactor and analysis instruments were used. The total gas flow during the experiments was 1 dm^3/min corresponding to the feed gas hourly space velocity (GHSV) of 43 000 h^{-1}. The temperature of a catalyst was increased from room temperature up to 400°C, with a linear heating rate of 20°C/min. The concentrations of CO, NO, CO_2, N_2O and NO_2 as a function of temperature were measured every 5 seconds by an FTIR gas analyser (Gasmet^{TM} CR2000) and the gas flow was controlled by mass flow controllers (Brooks 5850TR). Furthermore, the effect of poisoning on the catalytic activity was evaluated by changing the flow direction in the catalyst. Blank tests were carried out with the uncoated metal foil to ensure the inactivity of metal foil in the thermal treatments. In the following discussion, differences larger than ± 5°C in the light-off temperatures and ± 1% in the conversions of CO and NO can be regarded as statistically significant.

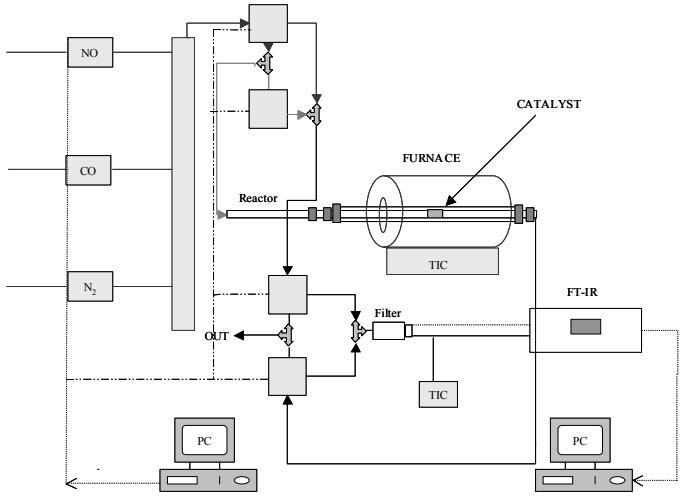

Fig. 17. Experimental set-up for the activity measurements at the University of Oulu.

Table 9. Composition of the test gas mixture for the activity measurements.

Component	Lean	Rich
CO	800 ppm	1200 ppm
NO	1000 ppm	1000 ppm
N_2	Balance	Balance

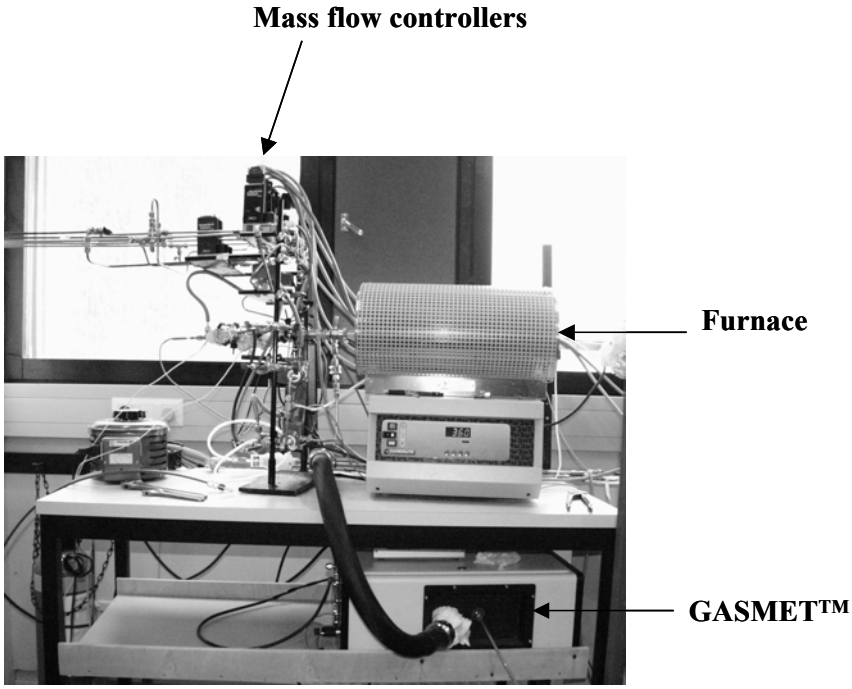

Fig. 18. Activity measurement system equipped with the GASMET™ gas analyzer (University of Oulu).

The activity of some aged pre-catalysts and main catalysts was also tested at Kemira Metalkat Oy, Finland. In these measurements, the conversions of CO, HC and NO_X were measured as a function of catalyst's temperature using a test gas mixture simulating the real exhaust gas composition. Catalyst light-off temperatures (T_{50} values) as well as conversions at 400°C were determined. Furthermore, OSC was measured for fresh and aged monoliths by CO-O_2 exchange experiments at constant adsorption temperatures of 450°C, 600°C and 750°C. The consumption and the adsorption of O_2 and CO were determined by mass spectrometer. (Härkönen *et al.* 2001)

4.3.8 Chemical analyses

Chemical analysis provides the information on elemental composition of the catalyst. The 'wet' and 'dry' analyses were performed due to low quantities of poisons present in the catalysts. The dry analysis was carried out beyond the SEM-EDS sensitivity, as described in section 4.3.1. In a wet analysis, the fresh and aged catalysts were dissolved in an acidic solution in order to determine the quantities of the most important catalytic poisons (Ca, P, S, Pb, Mg and Zn) and the amounts of active metals (Pd and Rh). These elements were typically present in small quantities, and unevenly distributed in the catalyst. Therefore,

separated samples were prepared from the inlet and outlet parts of the engine-aged and vehicle-aged catalysts. For the chemical analysis, 0.010 to 0.050 g of the washcoat (scraped from the monolith) was dissolved in an acidic solution (HNO_3, HCl, HF and H_3BO_3) and subjected to the digestion of the sample in the microwave oven (Milestone MLS 1200). This resulted partly in an incomplete dissolution of the analysed solids. The decomposed sample was analysed quantitatively by plasma atomic emission spectrometry (Pye Unicam 7000 ICP-AES) in the Trace Element Laboratory at the University of Oulu.

5 Ageing-induced changes in the catalyst

The effect of ageing atmosphere, temperature and time on the catalyst's activity was evaluated on the basis of several characterization techniques. This Chapter presents the main findings of the high temperature, engine bench and vehicle ageings-induced changes in the catalyst.

5.1 Collapse in surface area and pore structure

The evaluation of the effects of ageings on the surface areas and pore size distributions of the catalysts was carried out according to the standard BET method. The physisorption data was obtained from N_2 adsorption-desorption isotherms at -196°C. Aged catalysts were compared to each other on the basis of this method, and similarities and/or differences after different ageing temperatures, atmospheres and times are reported. The results of the BET method indicate the ageings-induced structural changes in the pore structure and the increase in the pore size of the catalyst. The BET method does not, however, give any clear evidence of the reasons for deactivation. A summary of the BET results (specific surface areas and pore volumes) after oxidative and reductive thermal treatments with dry gases is presented in Tables 10 and 11, respectively.

Table 10. Catalyst characterization results for thermally aged catalysts. Thermal ageing was carried out in the oxidative ageing atmosphere (air) for 3 and 24 hours.

Ageing temperature (°C)	Oxidative ageing 3 hours		Oxidative ageing 24 hours	
	BET surface area (m^2/g)	Volume adsorbed (cm^3/g support)	BET surface area (m^2/g)	Volume adsorbed (cm^3/g support)
800	70	17.0	65	15.0
900	39	8.9	31	7.1
1000	25	5.7	21	5.0
1100	9.1	2.4	6.6	1.5
1200	1.5	0.4	0.1	<0.1

Table 11. Catalyst characterization results for thermally aged catalysts. Thermal ageing was carried out in the reductive ageing atmosphere (5% H_2 and N_2 balance) for 3 and 24 hours.

Ageing temperature (°C)	Reductive ageing 3 hours		Reductive ageing 24 hours	
	BET surface area (m^2/g)	Volume adsorbed (cm^3/g support)	BET surface area (m^2/g)	Volume adsorbed (cm^3/g support)
800	65	15.0	67	15.5
900	60	13.7	59	13.5
1000	49	11.0	42	9.6
1100	30	7.0	27	6.3
1200	18	4.0	7.0	1.7

Figure 19 presents the surface areas of the catalysts after reductive, inert and oxidative ageings as a function of ageing temperature. In order to compare the results, the BET surface areas of fresh, engine-aged and vehicle-aged catalysts are also presented. The surface area of a fresh catalyst (69 m^2/g) was found to be about three times larger than that of the engine-aged (22 m^2/g) or vehicle-aged (16 m^2/g) catalysts. As indicated in Fig. 19, structural changes take place upon thermal, engine, and vehicle ageings of the catalyst. The catalyst's specific surface areas and pore volumes decreased strongly as a function of ageing temperature in all ageing atmospheres. (Pulkkinen *et al.* 2001)

Specific surface area of a catalyst after the ageings was not a linear function of temperature. As can be seen in Fig. 19, thermally aged catalysts prevailed high specific surface areas up to the ageing temperature of 800°C. A significant temperature region for ageing in the oxidative ageing atmosphere was around 850°–900°C, where the significant loss in surface area was observed indicating a close correlation with the catalyst's deactivation. As reported by Angove *et al.* (2000b), the surface area loss in air becomes pronounced above 1000°C with the growth of the oxide particles and the formation of low surface area α-Al_2O_3. As can be seen in Fig. 19, the surface areas of air-aged catalysts decreased to half of the original by the ageing temperature of 950°C. This collapse in surface area was associated with a significant decrease in the pore volume and an increase in the pore size, which will be discussed below. After the oxidative ageings at 1200°C, catalysts were almost non-porous. This was associated with the formation of α-Al_2O_3 in air ageing at around 1200°C, as observed by XRD measurements. This will be discussed later in section 5.4.

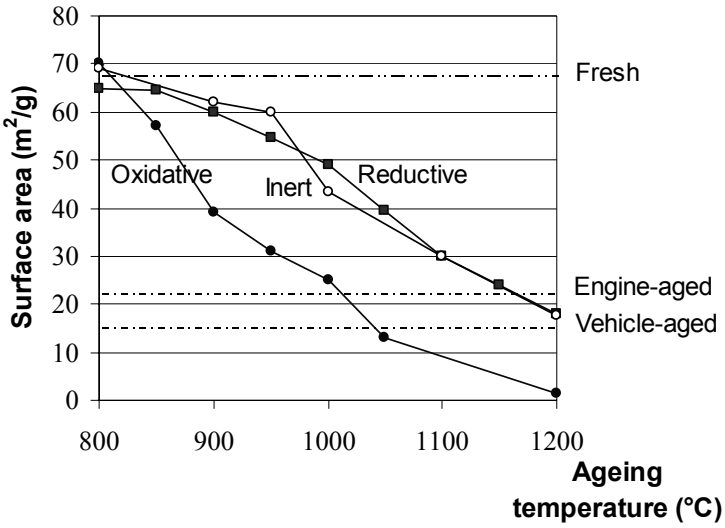

Fig. 19. Effect of ageing temperature on the BET surface areas of catalysts. The comparison after 3 hours of ageing in the reductive (■), inert (O), and oxidative (●) atmospheres.

The effect of ageing on the BET surface areas in reductive and inert atmospheres is rather different. After the reductive (5% H_2/N_2) and inert (N_2) ageings, the surface areas started to decrease, again, at ageing temperatures around 850°–900°C, but this decrease in surface area was not as extensive as in the oxidative atmosphere (air and/or 5% O_2/N_2). The BET surface areas after reductive and inert ageings remained, except the lowest ageing temperatures of 800-850°C, approximately 20 m^2/g higher than after oxidative ageings with the same ageing temperatures and times (Pulkkinen *et al.* 2001). This is consistent with the measurements of Piras *et al*. (2000), who found that the surface areas remained higher in reductive or redox conditions over Al_2O_3 and ceria-supported Al_2O_3 catalysts. They also found that under oxidative conditions at around 1200°C, cerium oxide (ceria) was almost totally ineffective as a stabilizing agent for aluminium oxide, whereas under the reductive conditions, its stabilizing effects were remarkably enhanced. The stabilizing effects of CeO_2 are also associated with its reactions with γ-alumina, as will be discussed later in this thesis when the ageing-induced solid-solid phase transitions in the bulk material are considered. Furthermore, it is rather difficult to determine differences between inert and reductive ageing atmospheres solely on the basis of the BET results within the measurement accuracy, as can be seen in Fig. 19. Therefore, it can be expected that the physical and chemical changes caused by the ageings in these atmospheres may be fairly similar (e.g. the formation of Ce-aluminates) as will be summarized later in this thesis.

The effect of water vapour (hydrothermal ageing) on the collapse of surface area was also evaluated in rich and lean conditions. It is important to establish the role of hydrothermal ageing in deactivation since there is always water vapour (approximately 10-vol-%) present in the exhaust gas mixture (Taylor 1993). The detailed results of

specific surface areas and pore volumes after 3 hours of reductive and oxidative hydrothermal ageings are collected in Table 12.

Table 12. Catalyst characterization results for hydrothermally aged catalysts. Hydrothermal ageing was carried out either in the reductive (5 vol-% H_2, 10 vol-% H_2O and N_2 balance) or in the oxidative (air and 10 vol-% H_2O) atmospheres for 3 hours.

Ageing temperature (°C)	Oxidative hydrothermal ageing 3 hours		Reductive hydrothermal ageing 3 hours	
	BET surface area (m^2/g)	Volume adsorbed (cm^3/g support)	BET surface area (m^2/g)	Volume adsorbed (cm^3/g support)
800	54	12.5	54	12.4
900	38	8.7	36	8.2
1000	28	6.5	30	6.9
1100	20	4.7	22	5.1
1200	1.4	0.3	6.4	1.5

Water vapour is known to be a sintering agent for many metal oxides (Johnson 1990, Bartholomew 2001). Here, the effect of hydrothermal ageing on the BET surface areas of catalysts is rather different compared to air-aged and H_2-aged catalysts. Water vapour has an active accelerating effect in the deactivation process, as can be seen in Figure 20. Hydrothermally aged (H_2O-H_2 and H_2O-air) catalysts had lost approximately one fifth (20%) of the initial surface area at the lowest ageing temperature of 800°C. Thus, the presence of water vapour seems to accelerate the surface area loss already at temperatures below 800°C. This is also consistent with H_2-chemisorption results, where the dispersion values of hydrothermally aged catalysts after ageings at 800°C were small, as will be presented in section 5.2. At higher ageing temperatures, on the contrary, the accelerating effect of water vapour on the deactivation process is evidently less compared to air ageing (see Fig. 20). Therefore, at an ageing temperature of 900°C and above, the loss in surface area after hydrothermal ageings is more dependent on the high ageing temperature rather than on atmosphere. (Lassi *et al.* 2002a)

In Fig. 20, the comparison of the surface areas in different ageing atmospheres after 3 hours of ageing is presented. As indicated, catalysts prevailed with high surface areas up to 800°C, except the hydrothermally aged catalysts, as reported above. According to the BET results, ageing in the oxidative atmosphere was the most demanding treatment for the catalysts, whereas after the reductive and inert ageings, catalysts prevailed with clearly higher specific surface areas. The surface areas of hydrothermally aged catalysts lay between these two limits, except the lowest ageing temperatures. Furthermore, on the basis of the BET results, it is rather difficult to find significant differences between the reductive and oxidative hydrothermal ageing atmospheres.

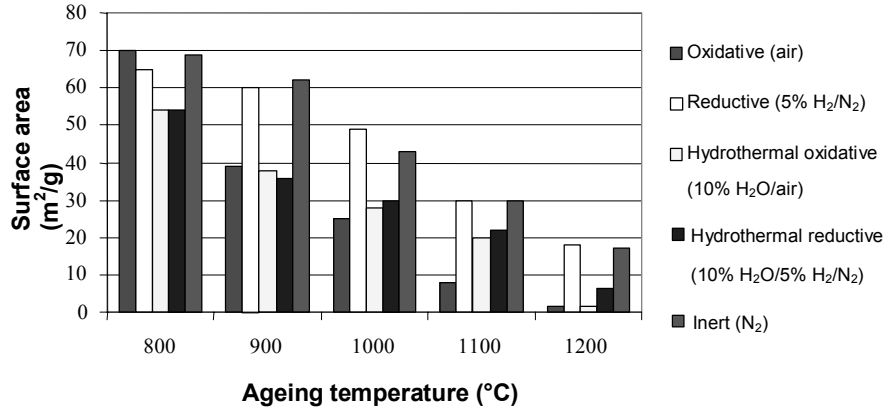

Fig. 20. The comparison of surface areas in different ageing atmospheres after 3 hours of ageing.

As indicated, the effect of ageing temperature and atmosphere are crucial for the surface area loss of the catalyst in the ageings. The role of ageing time can be evaluated on the basis of Fig. 21, where the specific surface areas of catalysts after 3, 24 and 42 hours of reductive ageing are presented. Furthermore, considering the results presented in Table 11, it can be said that significant differences between 3 and 24 hours of ageing in reductive atmosphere were not observed. At the maximum, this difference was about 11 m^2/g and at average 4.8 m^2/g. Thus ageing time was not a very critical variable in the reductive ageing atmosphere. According to BET results, the role of ageing time was only slightly pronounced in the oxidative atmosphere. The differences between 3 and 24 hours of ageing were at maximum 12 m^2/g, the average being 6.0 m^2/g, as can be seen in Table 10. However, the BET surface areas were clearly smaller compared to the fresh catalyst after the oxidative and reductive ageings at temperatures above 800°C. Therefore, it can be concluded that ageing induced the collapse in pore structure, which is most probably caused by high ageing temperature and atmosphere rather than time. The major collapse in surface areas occurred during the first ageing hours and, therefore, the effect of ageing time on the loss of surface area is clearly of secondary importance compared to high ageing temperature and ageing atmosphere.

The loss in surface area of catalysts is associated with the changes in the pore structure and with the crystallite growth that can be considered as a pre-sintering phenomenon, followed by sintering between the crystallites. In this thesis, the sintering of washcoat oxides was mostly promoted after the oxidative ageings. Some earlier observations have shown that high-temperature ageings strongly favour sintering of this kind of oxide materials with high surface areas. It has also been reported that pure CeO_2 easily sinters under the reductive conditions (Perrichon *et al.* 1995, Vidal *et al.* 2000), but when ceria is stabilized on Al_2O_3 or La_2O_3 (Kubsh *et al.* 1991), it is known to prevent sintering under these conditions.

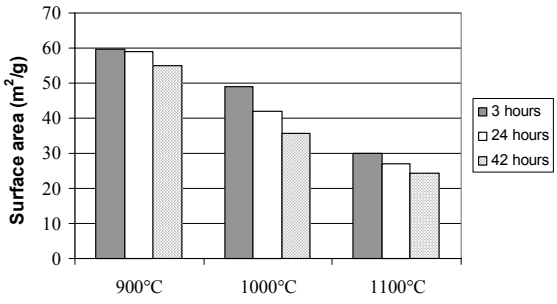

Fig. 21. Effect of ageing time on the BET surface areas of catalysts at ageing temperatures of 900°C, 1000°C and 1100°C. The comparison after 3, 24 and 42 hours of ageing in the reductive ageing atmosphere (%5 H_2/N_2).

The high temperature region of 850°–900°C is critical for the thermal deactivation of the catalyst, but deactivation is also strongly dependent on the surrounding gas atmosphere, as shown earlier. The decrease in surface areas was linked to the ageing- induced changes in the structure of bulk oxides, and catalytic properties after the ageings are strongly dependent on the washcoat properties. However, it is rather difficult to conclude which of the washcoat materials are mostly responsible for the surface area loss after the ageings, because the composition of the catalyst is complicated. Nor do the BET studies for separate washcoats of the catalyst give any further explanation for this. Therefore, some publications are referred to in this respect.

Surface area can be lost by migration of material from smaller particles to larger ones (Johnson 1990, Perrichon *et al.* 1995). The loss in the surface area after the high-temperature ageings on this type of catalyst is generally associated with the reduction of γ-Al_2O_3 washcoat, which typically has a high specific surface area. The rate of surface area loss can be lowered by the use of additives, such as Ba and La (Johnson 1990). A number of studies have indicated a growth in the crystallite size of CeO_2 upon high-temperature calcinations (Bunluesin *et al.* 1997), which has lead to a conclusion that deactivation phenomena on these catalysts probably depend on the surface area loss of CeO_2 at elevated temperatures (Härkönen *et al.* 1991, Perrichon *et al.* 1995, Trovarelli 1996), or on poor contact between the precious metals and ceria in aged catalysts, or on the decreased reducibility of large ceria crystallites (Bunluesin *et al.* 1998). However, the increased loading of ceria does not solve the problem and other factors must be relevant. Recently, Jen *et al.* (1999) and Fernández-García *et al.* (2001) have reported that pure or nearly pure CeO_2 washcoats showed poor surface area stability compared to ceria-zirconia mixed oxides, especially under reducing conditions, and the increased Zr content of the mixed oxide leads to higher surface areas (Cuif *et al.* 1997, 1998). Furthermore, as shown by González-Velasco *et al.* (1999, 2000a & 2000b), the activity of Ce-Zr mixed oxides in TWCs in a given Ce/Zr molar ratio is associated with the specific surface areas of the catalysts.

In this thesis, the surface area loss was clearly larger after the oxidative ageing than after the reductive and inert ageings with the same ageing temperature and time, which

proved that the air-aged catalysts were the most sintered. In this respect, the results are consistent with the observations of Ihara *et al.* (1987) and González-Velasco *et al.* (2000c). Furthermore, after the reductive hydrothermal ageings, the collapse in surface area was systematically larger than after the ageings in the corresponding dry atmospheres. This supports the hypothesis based on the literature that sintering of washcoat materials is further promoted in the presence of water vapour. The loss of surface area after the ageings can be associated with the sintering of bulk oxides, in particular CeO_2 and γ-Al_2O_3, which have a high surface area. Instead, also based on the literature, it seems that Ce-Zr mixed oxides in the washcoat suffer less deactivation by sintering than pure Ce- and Zr- oxides at high ageing temperatures. (González-Velasco *et al.* 1999)

Ageing time was not as critical a variable as ageing temperature and atmosphere, as indicated in earlier paragraphs. Therefore, even after short ageing times, especially at high ageing temperatures of 1100°C and 1200°C, the collapse in pore structure as a result of ageing was observed, and this led to a growth in the average pore size, which has also been observed by Johnson (1990). The rate of sintering was also strongly dependent on the level of the surface area of the fresh catalyst. It was observed that the rate of sintering was higher in the oxidative atmosphere, which was also observed by González-Velasco *et al.* (2000c). Furthermore, as can be seen in Fig. 22, the loss in surface area was further promoted after the first few hours of ageing, but it became quite constant after 10 hours of ageing.

The ageing procedures also induced structural transformations in the catalyst, such as the increased pore size of the catalyst. Both the fresh and aged catalysts gave similar types of adsorption isotherms corresponding to type IV of the IUPAC classification (Fig. 23). A comparison of adsorption-desorption isotherms showed that in all cases characteristic hysteresis loops in the range of p/p_0 from 0.80 to 0.95 were observed, but the porosity of catalysts decreased during the ageing treatment. Thus, the pore size distribution for thermally aged, engine-aged and vehicle-aged catalysts differed from that of the fresh catalyst. The change in the adsorption isotherm was associated with the shift in the pore size distribution to larger pore diameters when the surface area of the catalyst decreased. (Johnson 1990)

A)

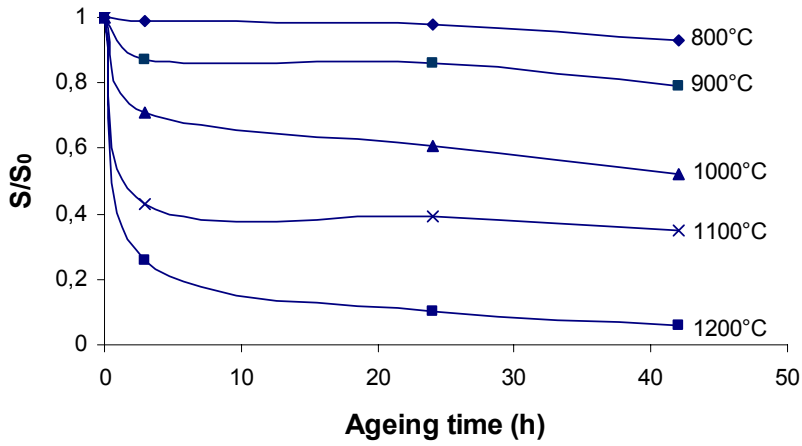

B)

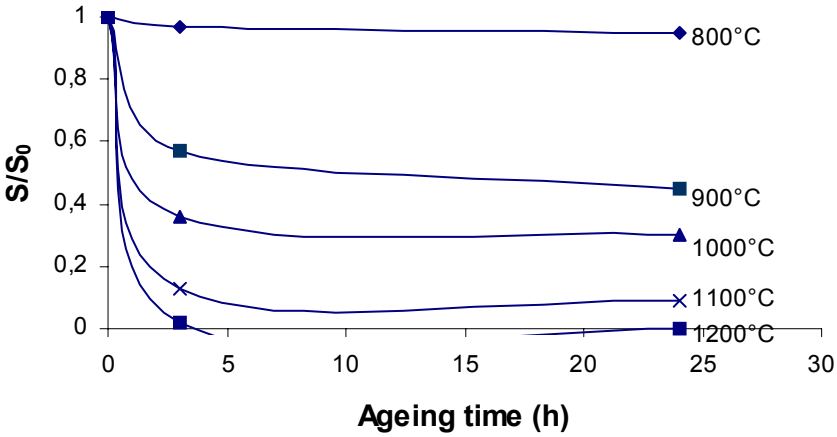

Fig. 22. The effect of ageing temperature on the sintering rate at 800°C, 900°C, 1000°C, 1100°C and 1200°C; A) after the reductive ageing and B) after the oxidative ageing.

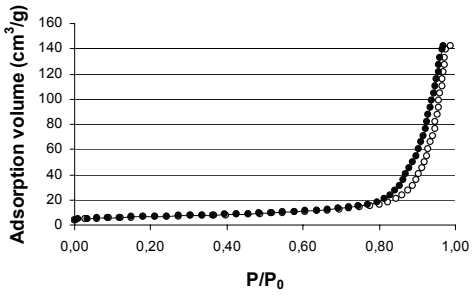

Fig. 23. Adsorption (O) and desorption (●) isotherms measured for the engine-aged catalyst.

In Fig. 24, the pore size distributions of fresh, engine-aged and vehicle-aged catalysts are presented. In Figures 24A and 24B micropore and mesopore distributions are presented respectively. As indicated, the fresh catalyst had many small pores under 20 nm, whereas in the case of aged catalysts, the pore sizes had grown and mesopores (≈ 40-50 nm) were observed. Small pores disappeared during thermal ageing procedures in oxidative, inert, and reductive ageing atmospheres. It was observed that pore sizes were clearly larger after the oxidative ageing than after reductive and inert ageings with the same ageing temperature and time, which proved that the air-aged catalysts were the most sintered. The corresponding mean pore diameters for the fresh, engine-aged and vehicle-aged catalysts were 13.7 nm, 39.9 nm and 45.5 nm respectively. Thus, all the catalysts were essentially mesoporous, according to the classification presented by Hayes & Kolazckowski (1997).

As a conclusion of the results of surface area and pore size distribution analysis of aged catalysts, it can be stated that the loss of the catalyst's surface area was more affected by ageing atmosphere and temperature rather than ageing time. Surface areas after the ageings started to decrease at around 850°– 900°C depending on the surrounding gas atmosphere. The air-aged catalysts showed the lowest surface areas at ageing temperatures of 850°–1200°C, but at lower temperatures the effect of water vapour on surface areas was more pronounced. The loss in surface area after the ageings was associated with the sintering of metal oxides, in particular γ-Al_2O_3 and CeO_2, in the washcoat. Sintering leads to a lower surface area, a reduction in porosity, which is observed as a decrease in the percentage of small pores up to 20 nm. Furthermore, sintering induces a crystallite growth of the oxide particles in the washcoat, which was observed as an increased pore diameter and as a decreased pore volume. As shown, BET results indicate the structural changes induced by ageings, but they give no explanation for the reasons of the collapse of pore structure. Therefore, the BET results should be integrated to other characterization techniques, as will be done in this thesis.

A)

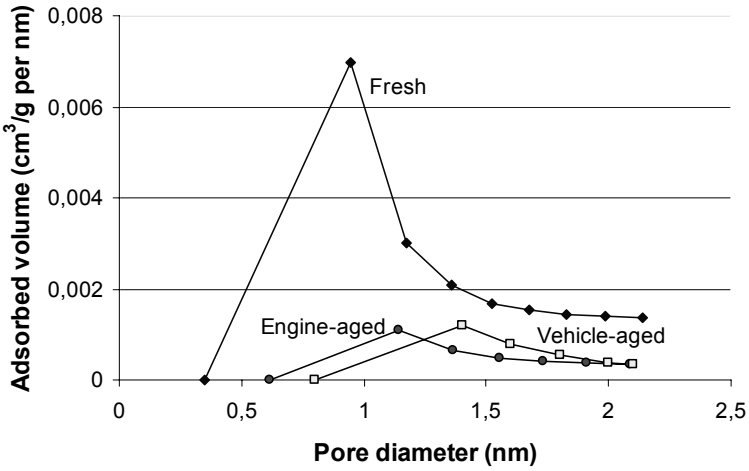

B)

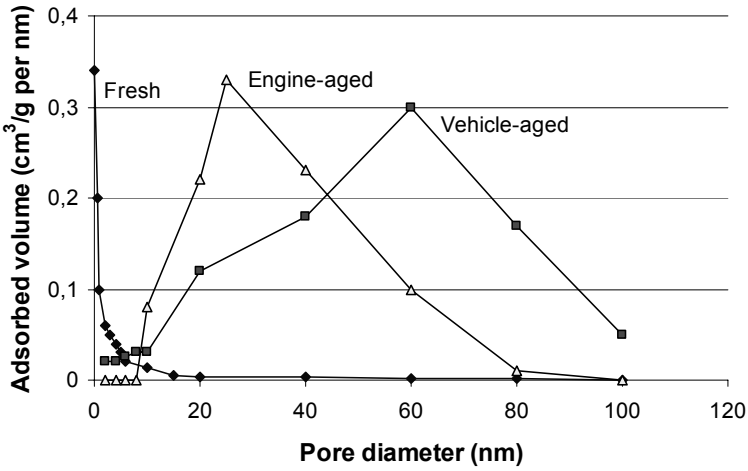

Fig. 24. Pore size distributions for fresh, engine-aged and vehicle-aged catalysts; A) micropores up to 2 nm (differential HK volume) and B) mesopores from 2 nm up to 100 nm (differential BJH volume).

5.2 Loss in active surface area and sintering of metal particles

The effects of ageings on the changes in precious metal dispersions and active metal surface areas of catalysts were studied by chemisorption. Figure 25 presents the metal dispersions of the catalysts as a function of ageing temperature. The corresponding active metal surface areas are presented in Table 13. As can be seen in Fig. 25 and Table 13, precious metal dispersions and metal surface areas decreased as a function of ageing temperature and time. This was observed in all ageing atmospheres. Similar behaviour in precious metal dispersion values was observed after oxidative and reductive ageings, within the limits of the measurement accuracy. The similar behaviour between these two ageing atmospheres is not self-evident because there were significant differences in the surface areas of corresponding catalysts, *i.e.* total surface areas remained high after the reductive ageing, as reported in section 5.1. In this respect, the chemisorption results (the loss of active metal area) do not correlate with the BET surface areas of catalysts.

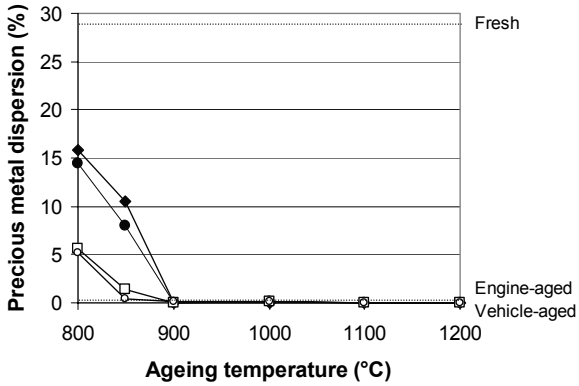

Fig. 25. The effect of ageing atmosphere, temperature and time on the precious metal dispersions of catalysts (based on H_2-chemisorption). Comparison between reductive (3 hours (●) or 24 hours (○)) and oxidative (3 hours (■) or 24 hours (□)) ageing atmospheres.

The precious metal dispersion and the active metal surface area measured by H_2-chemisorption for the fresh catalyst were 28% and 125 m^2/g, respectively. Table 13 presents a summary of the chemisorption data. As indicated, the loss of metal surface area rose with the increasing ageing temperature. The H_2/800°C/3h-aged and air/800°C/3h-aged catalysts showed approximately 50% reduction in the metal surface area compared to the fresh catalyst. After reductive and oxidative ageings at 850°C for 3 hours, approximately two thirds of the original active surface area was lost. At higher temperatures (T>900°C) and after engine and vehicle ageings, the dispersion values were so small (<1%), that it is difficult to draw any reliable conclusions. It can only be stated that ageings clearly affected the changes in the active phase of the catalyst.

Table 13. Catalyst characterization by H_2-chemisorption for fresh, engine-aged, vehicle-aged and thermally aged catalysts.

Catalyst/ Ageing conditions		Dispersion (%)	Active metal surface area (m^2/g metal)	Monolayer capacity (cm^3/g)
Fresh		28	125	0.09
Engine-aged		< 1	<1	< 0.01
Vehicle-aged		< 1	<1	< 0.01
800°C/3 h	Air	16	70	0.05
	H_2	14.5	65	0.05
	H_2O-air	< 1	<1	< 0.01
	H_2O-H_2	< 1	<1	< 0.01
800°C/24 h	Air	5.7	25	0.02
	H_2	5.2	23	0.02
850°C/3 h	Air	10.5	47	0.03
	H_2	9.1	41	0.03
850°C/24 h	Air	1.4	6.4	0.01
	H_2	0.4	1.7	< 0.01
900°C/3 h	Air	< 1	<1	< 0.01
	H_2	< 1	<1	< 0.01

The effect of ageing time was also important in this case, as seen in Fig. 25. The results of this study indicated the rapid growth of metal particles during the first few hours of ageing, which is convergent with the observations after BET measurements. The significant differences between H_2/800°C/3h- and H_2/800°C/24h-aged catalysts as well as between H_2/850°C/3h- and H_2/850°C/24h-aged catalysts were observed. The same is true also for the air-aged catalysts (see Fig. 25). That is, the increase of ageing time from 3 hours to 24 hours led to an approximately 35% decrease in the dispersion value at an ageing temperature of 800°C.

The effect of hydrothermal ageing is rather different compared to thermal ageings with dry gases because the H_2O-air/800°C/3h-aged and H_2O-H_2/800°C/3h-aged catalysts already showed small dispersion values (<1%). Thus, the role of water vapour is essential and it was clearly indicated that the sintering of metal particles is promoted in the presence of water vapour. This is consistent with the results of Bartholomew (2001), who concluded that the presence of water vapour increases the mobility of metal atoms or particles on the washcoat and hence accelerates the sintering of these particles. This mobility of metal particles is also related to the vapour pressures of metals or metal oxides (Barbier & Duprez 1994). This is further discussed in section 5.8, where the volatilization of Pd as a possible deactivation mechanism is considered.

The clearly lower dispersion values compared to the fresh catalyst at an ageing temperature of 800°C and above, gave evidence for the mechanism of catalyst's deactivation during the ageing treatments. The loss in active metal surface area and low dispersion values are closely associated with the sintering of active metal particles in the washcoat. As the dispersions had already decreased after the ageings at 800°C in all ageing atmospheres, sintering of metal particles is an essential cause of deactivation, and it had already started at temperatures below 800°C. As reported by Usmen *et al.* (1992) and Teixeira & Giudici (1999), high temperatures favour the sintering of the active phase. Particle growth and changes in the size distribution of metal particles were thermally

activated and resulted in a loss of the catalyst's activity, and often in changes in the selectivity as well. Washcoat materials, especially thermal stabilizers such as La, enhance the catalyst's performance by inhibiting the surface diffusion of metallic particles, which reduces the sintering of precious metals upon high temperatures. (Oudet *et al.* 1989, Teixeira & Giudici 1999)

Figure 26 presents the normalised active metal area as a function of ageing time. It can be noted that the rate of sintering of active metal particles on the surface was most dominant after the first few hours of ageing. On the other hand, as also shown in Fig. 26, the asymptotic approach has not yet been achieved after 42 hours of ageing below 850°C. According to the H_2-chemisorption results, no differences were found on sintering rates between the reductive and oxidative ageing atmospheres with dry or wet gases. One possible explanation for this may be the low dispersion value of the fresh catalyst, which led to dispersion values below 1% at ageing temperatures of 900°C and above. Therefore, a full comparison of dispersion values cannot be carried out in the ageing temperature range of 800°–1200°C.

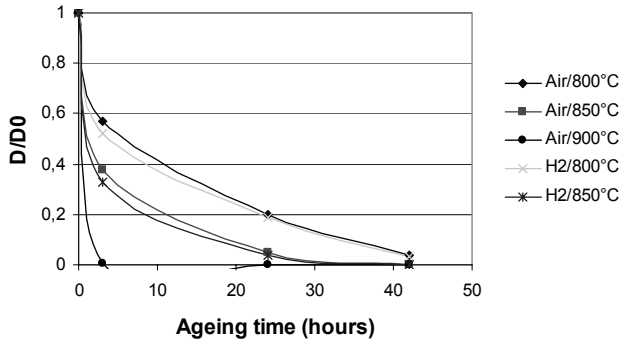

Fig. 26. Effect of ageing atmosphere, temperature and time on the sintering behaviour of the aged catalysts. The normalised active metal surface area D/D_0 as a function of ageing time (hours).

Additionally, on the basis of chemisorption results, conclusions cannot be drawn about which of the two metal particles (rhodium or palladium) were sintered. It is most likely that both Pd and Rh metal particles sintered at high ageing temperatures. Since chemisorption measurements are based on the assumption of monolayer adsorption, it can only be concluded that precious metal particles on the surface are sintered, which is observed as a decrease in dispersion values. Sintering of active metal particles will be discussed later in this thesis, in section 5.5, where the ageing-induced changes in the chemical states of the active metals are determined by the XPS measurements. There, it will be reported that rhodium metal particles in the washcoat were sintered and caused a decrease in catalytic activity. Furthermore, based only on chemisorption results, it is rather difficult to conclude that the sintering of the precious metal particles is a cause of the loss of active metal area. It is also possible that the loss of active metal area is caused by the encapsulation of metal particles in the sintered washcoat pores. In order to

discriminate between these two causes of deactivation, TEM micrographs would have been necessary.

The H_2-chemisorption results are considered in this thesis only qualitatively by comparing the dispersion values of the catalysts after the ageings. This is reasonable, because several assumptions have to be made considering the adsorption stoichiometry between the metal and adsorbate gas, as reported earlier in section 4.3.3. The stoichiometry ratio is also dependent on the particle size. Furthermore, in the case of catalysts containing CeO_2, the extensive adsorption of H_2 on CeO_2 has been duly reported (Bernal *et al.* 1999). This spillover effect of hydrogen makes the quantitative interpretation of chemisorption results difficult. However, the amount of H_2 spilled over the washcoat can be minimised by lowering the adsorption temperature (Fornasiero *et al.* 1997, Fornasiero *et al.* 1999). Recently, Graham *et al.* (1999) and Di Monte *et al.* (2000) have also shown that metal particles may be encapsulated in high temperature reduction. Therefore, the choice of an appropriate metal particle size may be an important factor to avoid deactivation.

In this work, the aged catalysts were also studied by CO-chemisorption in order to obtain results without the possible spillover effect of hydrogen. The results of CO-chemisorption are consistent with the H_2-chemisorption measurements, (Lassi *et al.* 2002a) and no significant differences were observed between these two adsorbing gases. The precious metal dispersions for the fresh catalysts were 28% and 30% measured by H_2- and CO-chemisorption respectively. In addition, no significant differences were found in the resolution (detection limits), and in both cases the precious metal dispersions were under 1% after the ageings at temperatures above 900°C. For these reasons, CO-chemisorption results will not be further discussed in this thesis.

In summary, low dispersion values of the aged catalysts proved that active metal particles were sintered. The rate of sintering of metal particles increased as a result of combined action of water vapour and high ageing temperature. Based on the chemisorption results, it is impossible to state which of the two metal particles (Rh or Pd) was most sintered. It can be concluded, however, that sintering of Pd and/or Rh particles was affected by ageing temperature, atmosphere and time. In particular, the presence of water vapour during the ageing increased the sintering rate. In contrast to the BET results, no differences were found between reductive and oxidative ageing atmospheres with dry gases. Rather, hydrothermally aged catalysts showed low dispersion values already at an ageing temperature of 800°C, which is consistent with the BET results. In order to understand the behaviour of active metals during the ageings, XPS was also used as a characterization technique in this research.

5.3 Ageing-induced changes in the desorption behaviour of NO

Temperature-programmed desorption (TPD) was utilised in this research to evaluate ageing-induced changes in the adsorption-desorption behaviour of NO. In this section, first the interpretation of NO-TPD spectrum of a fresh catalyst is presented and then the effect of ageings is considered. The interpretation of the NO-TPD spectrum is based on

our earlier studies on the simplified model catalysts, Rh/Al_2O_3 and Pd/Al_2O_3, as reported in Rahkamaa *et al.* (2000) and Rahkamaa-Tolonen *et al.* (2002).

5.3.1 Interpretation of NO-TPD spectra

The changes induced by thermal, engine and vehicle ageings were examined with TPD measurements by using NO as an adsorbate. These experiments were carried out both in a vacuum and under carrier gas flow. Based on these experiments, it was found that there was no significant difference between the measurements carried out in a vacuum or under the carrier gas flow (see Fig. 27). The shape of the TPD curve as well as the number and position of desorption peaks of NO were the same in both cases. The other desorption products (N_2, N_2O and O_2) also showed similar desorption behaviour during the vacuum measurements and under the carrier gas flow. Thus it was concluded that the pressure gap is not significant in the measurements. Therefore, in this thesis only the vacuum measurements are considered in detail. Consequently, the possible readsorption effects, which are observed often during the TPD measurements done under a carrier gas flow (Falconer & Schwarz 1983, Malet 1990, Ciuparu *et al.* 2000) and caused by the carrier gas flow rate, can also be at least partially omitted.

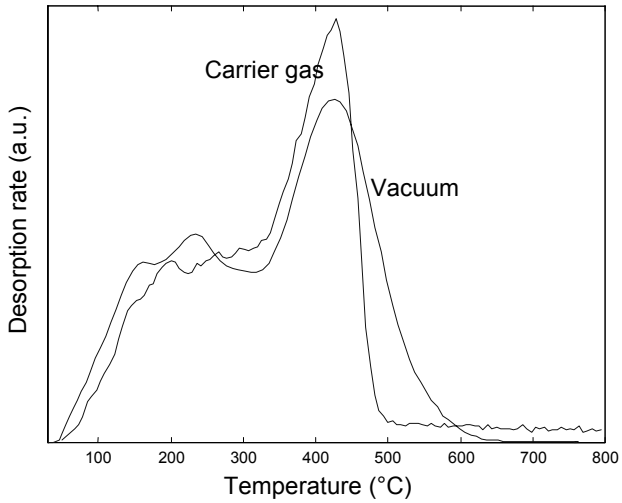

Fig. 27. NO-TPD curve for a fresh catalyst measured under the carrier gas flow at 1 atm and in a vacuum at 10^{-7} atm.

Adsorption-desorption kinetics of NO have been extensively studied, in particular on single crystal surfaces of palladium and rhodium, such as Pd (110) and Rh (111) surfaces. In this work, due to the complex structure of the catalyst, the adsorption-desorption behaviour of NO is a more complicated phenomenon since adsorption can take place on different active sites on the surface, on precious metal sites, on the oxide sites in the bulk

and also on metal-washcoat interfaces. NO may easily adsorb on the washcoat reduced by hydrogen as in the case of La_2O_3 (Fuentes *et al.* 2000) or CeO_2 (Monteiro *et al.* 1995). Furthermore, a part of the adsorbed NO can react catalytically to N_2 and N_2O depending on the adsorption temperature. On the basis of the literature, it can also be expected that on Rh catalysts, at least a part of NO is adsorbed on the active sites of the washcoat as nitrate or nitrite species in the presence of oxides, especially at low temperatures (Shelef & Graham 1994). The adsorption phenomenon can also be connected to the self-decomposition of NO that is known to be remarkable on these types of catalyst surfaces. The decomposition of NO is considered to be a key step preceding any further reactions of NO with the reducing agents. (Altman & Gorte 1988, Taylor 1993, Sellmer *et al.* 1995, Huang *et al.* 2000)

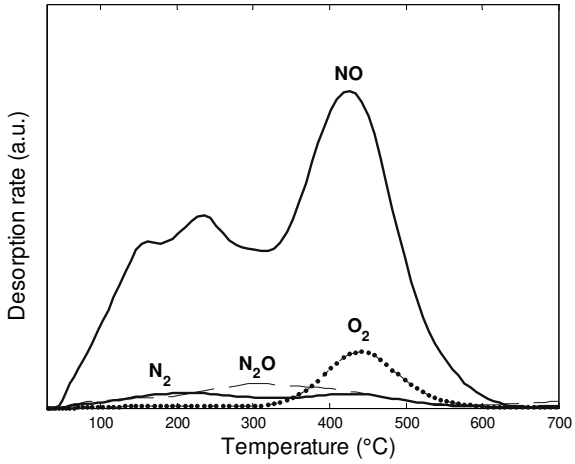

Fig. 28. NO-TPD curves for the fresh catalyst, measured in a vacuum at a linear heating rate of 30°C/min; following the adsorption of 5% NO/Ar at room temperature for 10 minutes.

The NO-TPD profiles for a fresh catalyst (Pd/Rh monolith) are presented in Fig. 28. For all the catalysts investigated, NO (at *m/z*=30), N_2 (at *m/z*=28), N_2O (at *m/z*=44) and O_2 (at *m/z*=32) were the four species detected to desorb from the surface as the temperature of the catalyst was increased. This was observed independently of the ageing procedure. The formation of NO_2 (at *m/z*=46) was not detected in the measurements. This is consistent with the results of Huang *et al.* (2000) and Valden *et al.* (1996), who have conducted NO-TPD experiments on the same type of catalyst surfaces. It is, however, difficult to draw conclusions between peak maxima and positions due to the different pre-treatment procedures and heating rates used in these studies.

In all NO-TPD spectra, NO was the main desorption product. NO can adsorb on a supported metal catalyst both molecularly and dissociatively (Altman & Gorte 1988). Dissociated NO can further be converted to N_2 and N_2O. Chin and Bell (1983) have reported that at room temperature, the adsorption of NO on rhodium supported on Al_2O_3 occurs preferentially molecularly. In this study, the adsorption of NO on the fresh catalyst occurred mainly molecularly, as indicated by the large amounts of NO desorbed and small amounts of N_2O and N_2 formed as a result of partial dissociation of NO during

heating (Pulkkinen *et al.* 2000). In this regard, the results presented here are consistent with the measurements of Taylor (1993) and Valden *et al.* (1996), who concluded that the formation of N_2, N_2O and O_2 during the NO-TPD gave evidence for partial decomposition of NO upon heating.

As can be seen in Figures 28 and 29, three prominent desorption peaks of NO were observed for the fresh catalyst at around 152°C (LT peak), 282°C (MT peak) and 425°C (HT peak), and the highest temperature desorption peak was the dominant one. In the following discussion, the notation of LT, MT or HT peak will be used to represent the desorption peaks of NO in the low (152°C), middle (282°C) and high temperature (425°C) ranges respectively. Furthermore, in the middle temperature range at about 200°–300°C, there are two strongly overlapping desorption peaks of NO, as will be shown later when the normal distributions are fitted to NO-TPD curves (see Fig. 34A). These MT desorption peaks of NO are referred to as MT1 (224°C) and MT2 (282°C) in the following discussion.

The observed desorption peaks correspond to the interactions of NO with washcoat oxides and precious metals. NO adsorption can also occur on the interface of the active metal and washcoat oxide, as mentioned earlier. In order to clarify the origin of desorption peaks, NO-TPD experiments were carried out separately for the different washcoats of the fresh catalyst, as shown in Fig. 29.

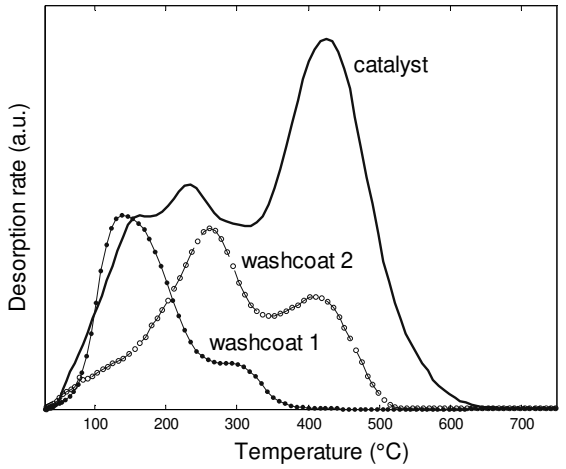

Fig. 29. NO-TPD curves for the fresh catalyst, and for separate washcoats of the catalyst; measured in a vacuum at a linear heating rate of 30°C/min, following the adsorption of 5% NO/Ar at room temperature for 10 minutes.

The desorption behaviour of NO on the Pd/Rh monolith is consistent with our earlier studies on simplified Pd/alumina catalysts, where three desorption peaks of NO were observed at temperatures around 250°C, 310°C and 440°C (Rahkamaa-Tolonen *et al.* 2002). The observed shift in the position of desorption peaks to higher temperatures may be due to the slightly different chemical composition of the catalyst and also due to small differences in pre-treatment procedures involved. The middle temperature desorption peaks of NO at 224°C (MT1) and 282°C (MT2) were most probably caused by the

adsorption of NO on the active sites of washcoat oxides, because they also appeared with samples containing no palladium or rhodium, as indicated in our earlier studies over γ-Al_2O_3 and modified alumina catalysts (Rahkamaa *et al.* 2000, Rahkamaa-Tolonen *et al.* 2002). It can be concluded that the interaction of NO with the washcoat oxides is significant, which has also been proved by other researchers: Falconer & Schwartz (1983), Valden *et al.* (1996) and Huang *et al.* (2000). Thus, the washcoat itself is active, and a strong adsorption of NO onto the washcoat was observed.

In the literature, there has been a great deal of discussion on the number and the origin of NO-TPD peaks on alumina-based catalyst surfaces. Huang *et al.* (2000) have reported three dominant desorption peaks of NO at 100°C, 410°C and 530°C; in contrast, Kijlstra *et al.* (1997) observed only two peaks at 180°C and 375°C, in that order. In this thesis, the HT desorption peak of NO in the area of 425°C is interpreted to have been caused by NO-Al_2O_3 as well as NO-precious metal (Pd/Rh) interaction. Several investigations of the adsorption of NO over well-defined Rh (111) (Root *et al.* 1983, Borg *et al.* 1994) and Pd (111) (Wickam *et al.* 1991) single crystal surfaces have shown that NO adsorbs more strongly on rhodium than on palladium. However, the amount of palladium in the catalyst is about tenfold compared to the rhodium loading. Palladium was also added on the washcoat 2 of the catalyst and the HT desorption peak of NO was detected in this case, as is shown in Fig. 29. Thus, it can be stated that the HT peak is a contribution of NO-Pd interaction rather than NO-Rh interaction. The adsorption of NO on this HT site is also assumed to take place to some extent at the metal-oxide interface and at acid sites of Al_2O_3, because the height of this HT peak is clearly larger compared to the LT and MT peaks of NO, although the active metal loading in the washcoat is small.

The MT2 desorption peak of NO at approximately 282°C (see Fig. 29) is thought to be a contribution of NO interaction with La_2O_3, which was mainly added onto washcoat 2 of the catalyst. The DRIFT and TPD measurements of Huang *et al.* (2000) support the interpretation of the origin of this MT2 desorption peak. The small differences might be due to different heating rates and pre-treatment procedures used. Peak maxima are shifted to higher temperatures when the heating rate is increased (Falconer & Schwarz 1983). The MT1 desorption peak of NO is interpreted to have originated from NO-Al_2O_3 interaction, whereas the LT peak at around 152°C includes the interaction between CeO_2 and NO. It is mainly a contribution from washcoat 1 of the catalyst. All desorption peaks of NO also included Al_2O_3-NO interactions, and to a large extent, this was due to high content of γ-Al_2O_3 in the washcoat.

The NO-TPD curves presented are quite different from those observed on Rh or Pd single crystals (Root *et al.* 1983, Altman & Gorte 1988, Wickam *et al.* 1991, Borg *et al.* 1994, Sellmer *et al.* 1995), which exhibit lower activation energies and higher specific rates. NO-TPD results depend also on particle size, and thus the desorption behaviour of NO on real catalyst surfaces cannot be explained exclusively by simple crystal planes of Rh and Pd.

5.3.2 Effect of ageings on the desorption of NO

Figure 30 shows the comparative NO-TPD curves for the fresh catalyst (A); H_2/900°C/3h-aged (B); H_2/900°C/24h-aged (C); H_2/1100°C/24h-aged (D); air/900°C/3h-aged (E); and air/1100°C/24h-aged (F) catalysts; following the adsorption of 5% NO/Ar at room temperature for 10 minutes. The effect of thermal ageing on the adsorption-desorption behaviour of NO was significant. It was observed that after 3 or 24 hours of ageing in air at 550°C, which corresponds the calcination temperature of the catalyst, the same desorption peaks of NO were observed as in the case of a fresh catalyst, the HT desorption peak being dominant. As indicated, the number of adsorption sites on the surface decreased significantly as a function of ageing temperature. In particular, a significant change in HT desorption peak of NO is observed between temperatures 550°…800°C. After the ageings at 800°C or above, the number of adsorption states on the surface decreased remarkably. At thermal ageings at temperatures above 800°C, engine and vehicle ageings totally destroyed the HT peak of NO, which led to a dominance of the LT and MT desorption states, as will be shown later in Fig. 32. The adsorption capacity was also observed to decrease after the ageings, notably the capacity of the HT desorption peak decreased after oxidative and reductive ageings (see Fig. 30), and no significant differences were observed between these two ageing atmospheres in the HT desorption peak for NO (Pulkkinen *et al.* 2000). This is consistent with H_2-chemisorption measurements where the precious metal dispersions started to decrease in the same temperature range, where the HT desorption peak of NO was observed to be destroyed.

As can be seen in Fig. 30, the LT desorption state of NO at about 152°C was dominant after reductive and oxidative ageings, if ageing was carried out at temperatures higher than 800°C. The LT desorption peak prevailed as dominant after the reductive ageing at all ageing temperatures, and the intensity of LT desorption peak decreased as a function of ageing temperature. Alternatively, after oxidative ageings the relative differences between the LT and MT1 desorption peaks of NO changed as a function of ageing temperature and both peaks became equally dominant after ageing at temperatures 900°…1000°C. Furthermore, desorption amounts of NO were smaller than after the reductive ageing, which correlates well with the BET results. Desorption of NO was no longer detected in the TPD spectra after the reductive and oxidative ageings at temperatures above 1150°C.

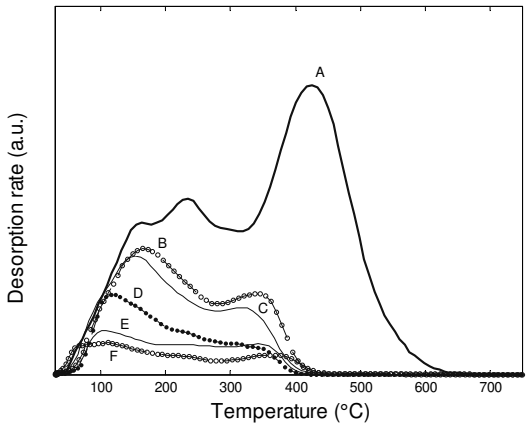

Fig. 30. NO-TPD curves for fresh and thermally aged catalysts; following the adsorption of 5% NO/Ar at room temperature for 10 minutes; Fresh catalyst (A); H_2/900°C/3h-aged (B); H_2/900°C/24h-aged (C); H_2/1100°C/24h-aged (D); air/900°C/3h-aged (E), and air/1100°C/24h-aged (F) catalysts.

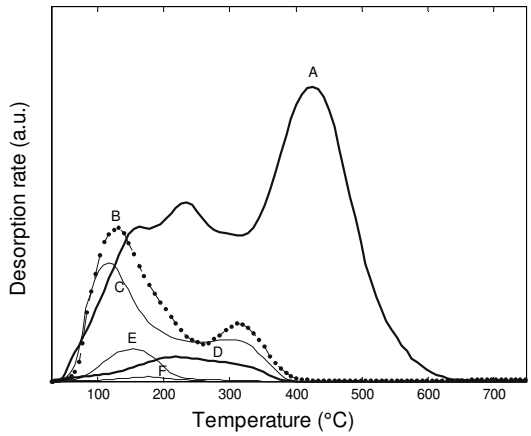

Fig. 31. NO-TPD curves for fresh and hydrothermally aged catalysts; following the adsorption of 5% NO/Ar at room temperature for 10 minutes; Fresh catalyst (A); H_2O-H_2/800°C/3h-aged (B); H_2O-H_2/1000°C/3h-aged (C); H_2O-H_2/1200°C/3h-aged (D); H_2O-air/800°C/3h-aged (E), and H_2O-air/1200°C/3h-aged (F) catalysts.

The effect of hydrothermal ageing on the desorption behaviour of NO was also evaluated. Figure 31 shows the comparative NO-TPD curves for the fresh catalyst (A); H_2O-H_2/800°C/3h-aged (B); H_2O-H_2/1000°C/3h-aged (C); H_2O-H_2/1200°C/3h-aged (D); H_2O-air/800°C/3h-aged (E), and H_2O-air/1200°C/3h-aged (F) catalysts. As can be seen, the shape of desorption curves of NO was similar after the reductive and oxidative hydrothermal ageing treatments, but the amount of desorbed NO is smaller in the presence of the oxidative gas phase. Therefore, there are less active surface sites available

after the hydrothermal oxidative ageing compared to hydrothermal reductive ageing. Furthermore, as a result of hydrothermal ageing at a temperature of 800°C or above, the HT desorption peak of NO at 425°C completely disappeared. This is due to sintering of active metals, in particular Rh metal particles in the washcoat, as will be reported in section 5.5, and a reason why NO molecules do not access the catalytically active sites on the surface.

On the basis of NO-TPD measurements, the most dominant desorption peak of NO after hydrothermal ageings (reductive and oxidative) was the lowest temperature state at around 152°C. This peak, as previously mentioned, originates from the interaction between NO and the washcoat oxides, mainly CeO_2 and Al_2O_3. Reductive hydrothermal ageing showed higher adsorption capacities compared to the oxidative ageing with the same ageing temperatures and times. This is also consistent with the activity measurements presented in this thesis (see section 5.6).

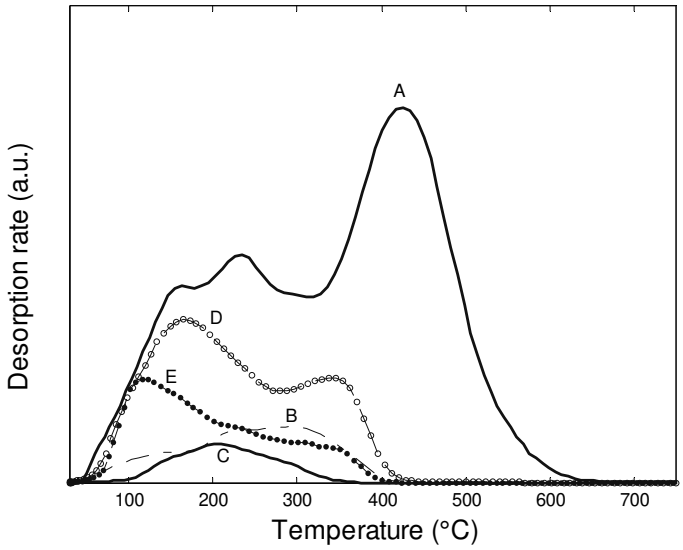

Fig. 32. NO-TPD curves for fresh catalyst (A); engine-aged (B); vehicle-aged (C); H_2/900°C/3h-aged (D), and air/900°C/3h-aged (E) catalysts; following the adsorption of 5%NO/Ar at room temperature for 10 minutes.

Figure 32 shows NO-TPD curves for the fresh catalyst (A); engine-aged (B); vehicle-aged (C); H_2/900°C/3h-aged (D), and air/900°C/3h-aged (E) catalysts. In the case of engine ageing, the highest temperature desorption peak of NO entirely disappeared, and the most dominant desorption peak of NO was observed at around 300°C, near to MT2 desorption peak of NO, as shown in Figures 32 and 34B. This peak also correlates well with desorption of N_2, which was observed at 313°C. The same desorption peak was observable also after the reductive ageing at low ageing temperatures of 800°–900°C, but only slightly after the oxidative ageing at these temperatures. This is consistent with the results presented in this thesis, where it will be concluded that engine bench ageing correlates better to the reductive ageing than to the oxidative one. The height of the

desorption peak at around 300°C decreased as a function of ageing temperature. This peak is also observable for the fresh catalyst in the fitted TPD curve (as will be shown later in Fig. 34A), and the origin of this peak was linked to NO-La_2O_3 interaction, as has been discussed earlier. After the engine bench ageing, the second and third dominant desorption peaks of NO were observed at around 220°C and 140°C respectively. After the vehicle ageing, the most dominant desorption peak of NO was at 202°C (as shown in Fig. 34C). This is linked to NO-Al_2O_3 interaction and corresponds to the MT1 desorption peak of a fresh catalyst. After the engine bench and vehicle ageings, the adsorption capacities were clearly lower than in the fresh catalyst. One possible explanation is that Ce-oxides and La-oxides in the different washcoats of the catalyst, respectively, have reacted with γ-Al_2O_3 and, therefore, there is not so much CeO_2 or La_2O_3 available in the catalyst. This will be further discussed in the XRD section. The low adsorption capacities, in the case of the vehicle-aged catalyst, may also be explained by the poisoning, which covers the active surface sites as will be considered later. Furthermore, the NO desorption peaks at around 86°C and 360°C (shown in Fig. 34 B) are not the real desorption states, but they are caused by the fitting, as will be explained further.

The effect of ageings is also observed in the desorption behaviour of O_2, N_2O and N_2. In Fig. 33, O_2-TPD curves for the fresh catalyst (A); H_2/900°C/3h-aged (B); H_2O-H_2/900°C/3h-aged (C); air/1100°C/3h-aged (D); air/900°C/3h-aged (E), and engine-aged (F) catalysts are presented. Oxygen desorption was observed in all the cases as a single sharp peak, close to the NO main peak (HT peak) in the area of 440°C (see Fig. 33). This is consistent with the results of Huang *et al.* (2000) and our earlier studies (Rahkamaa *et al.* 2000, Rahkamaa-Tolonen *et al.* 2002), where oxygen desorption from Rh/Al_2O_3 and Pd/modified Al_2O_3 surfaces occurred in the same temperature range as the highest temperature desorption state of NO was observed, at around 395°C and 440°C respectively. In the literature, the highest temperature NO-TPD peak is accompanied by oxygen desorption, as in this case, and it has been suggested that this corresponds to the decomposition of nitrate and nitrite species. (Kijlstra *et al.* 1997)

Again, after the air treatment at 550°C, corresponding to calcination temperature of catalysts, desorption behaviour of oxygen was similar to that of the fresh catalyst. On the other hand, thermal and hydrothermal ageings at 800°C result in an extensive decrease in the height of the oxygen peak. As a result of high-temperature thermal ageing, the height of the oxygen desorption peak decreased rapidly and this peak was partly destroyed at ageing temperatures of 800°C. Desorption of oxygen was no longer detected after 3 hours of oxidative and reductive ageings at a temperature of 1000°C. Instead, after the hydrothermal ageings, desorption of oxygen was not observed after the ageings at a temperature of 800°C. This is consistent with the BET and chemisorption results, where hydrothermally-aged catalysts showed low surface areas and dispersion values, respectively, even below the ageing temperature of 800°C. After the engine bench ageing, oxygen desorbed close to 440°C, but the height of this desorption peak was only approximately 2% compared to the fresh catalyst. After the vehicle ageing, no desorption of oxygen was further observed. It was also observed, as shown in Fig. 33, that high temperature ageings did not cause any significant shift to the position of the peak maximum (peak temperature).

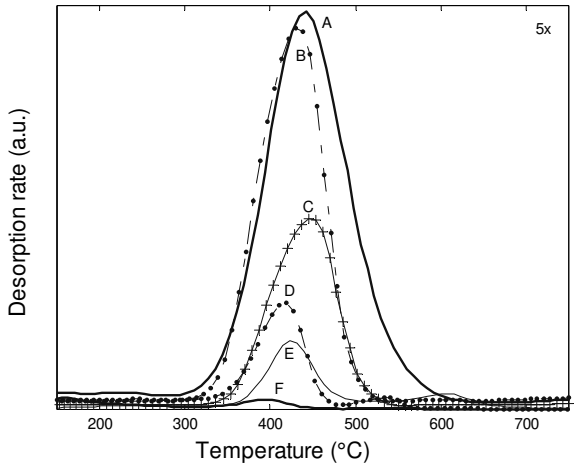

Fig. 33. O_2-TPD curves for the fresh catalyst (A); air/550°C/3h-aged (B); H_2/800°C/3h-aged (C); H_2/900°C/24h-aged (D); air/900°C/3h-aged (E), and engine-aged (F) catalysts; following the adsorption of 5%NO/Ar at room temperature. O_2-TPD multiplied by 5 compared to the desorption rate of NO presented earlier in Fig. 28.

In the case of a fresh catalyst, the formation of decomposition products, N_2O and N_2, was observed in the same temperature range where desorption of NO occurred (desorption curves not shown). Desorption of N_2 was found to occur in two stages, at desorption temperatures of 223°C and 423°C for the fresh catalyst, as shown in Tables 14 and 15. These two desorption peaks correlate well with the MT1 and HT peaks of NO. This is consistent with our NO-TPD studies over Pd/modified Al_2O_3 surfaces (Rahkamaa-Tolonen *et al.* 2002), where we concluded that palladium metal particles are mostly responsible for the decomposition of NO, because the formation of N_2 was higher and the formation of N_2O smaller in the case of 1% and 3% Pd catalysts than in the case of the modified γ-Al_2O_3 washcoat. As a result of thermal ageing, the highest temperature desorption peak of N_2 at 423°C was partly destroyed after oxidative and reductive ageings at around 900°C, and totally after ageings at around 1100°C. After the oxidative ageing at temperatures higher than 800°C, desorption of N_2 occurred in the temperature range of 100°–400°C and desorption peaks were strongly overlapping, whereas after the reductive ageings, two desorption peaks for N_2 could clearly be seen at temperatures around 140°C and 310°C, the lowest temperature state being the dominant one. As can be seen in Tables 14 and 15, N_2O showed quite similar desorption behaviour than N_2.

5.3.3 Modelling of desorption curves

Temperature-programmed desorption (TPD) experiments are often solely interpreted in a qualitative way, as in this case, although TPD profiles include kinetic information of

desorption, or the type and distribution of adsorption. However, in this instance, the quantitative analysis does not essentially provide any new information on the deactivation and deactivation mechanisms. Thus, the comparison of ageing atmospheres, temperatures and times has been carried out in a so-called semi-quantitative manner, which will be described in more detail in the following paragraphs.

Modelling of desorption is based on the proposed shape of a desorption rate curve. A symmetrical desorption curve, which is associated with the second order desorption kinetics (Falconer & Schwarz 1983), is supposed for each desorption state. The second order desorption kinetics is known to be reasonable for the formation of nitrogen and nitrous oxide, but the first order kinetics is more reliable in the case of NO desorption. However, even in fitting two overlapping curves with regression analysis, it is difficult to distinguish different reaction orders (Falconer & Schwarz 1983). Hence, the speculation between the first and the second order desorption kinetics is of minor importance, and normal distributions were selected as a shape of symmetrical desorption curves. (Lassi *et al.* 2002d)

The normal distributions represent the obtained NO-TPD curves semi-quantitatively with the confidence discussed above. The adjustable parameters, variance, maximum desorption rate, and temperature of maximum desorption rate, are obtained by non-linear regression analysis using a Levenberg-Marquardt algorithm. The aim of the fitting was to more reliably predict the real number of desorption states that is normally higher than the visually-observed number. Modelling of desorption curves also helps to evaluate desorption temperatures, peak half-widths and the heights of the desorption peaks and to thus compare a large amount of data. The fitted curves for the fresh, engine-aged and vehicle-aged catalysts are shown in Fig. 34, and the corresponding values of peak temperatures and relative peak heights are presented in Tables 14 and 15, respectively. In Table 15, the values of relative peak heights of 1.00 correspond to the highest desorption peak observed. (Lassi *et al.* 2002d)

A)

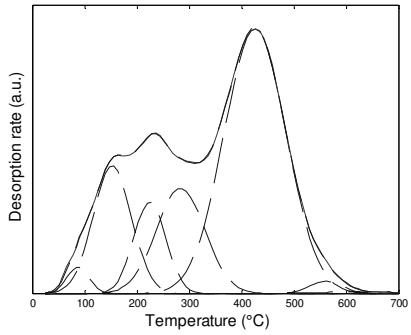

B)

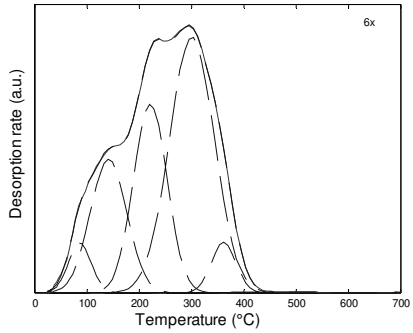

C)

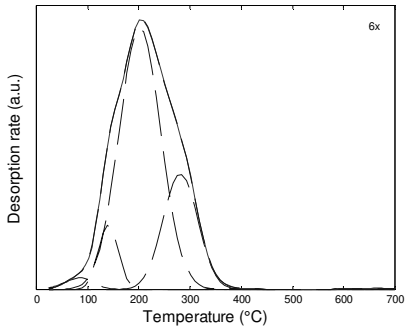

Fig. 34. Fitted NO-TPD curves for A) fresh, B) engine-aged and C) vehicle-aged catalysts (Lassi *et al.* 2002d).

Table 14. Peak temperatures for fresh, engine-aged and vehicle-aged catalysts.

Fresh	Desorption temperatures (°C)					
NO	87	152	224	282	425	560
N_2	85	155	223	294	423	570
N_2O	81	133	256	304	386	572
Engine-aged						
NO	86	141	221	301	361	----
N_2	94	143	224	313	387	----
N_2O	83	135	228	318	379	----
Vehicle-aged						
NO	84	140	202	281	----	----
N_2	85	147	192	272	----	----
N_2O	80	170	224	279	----	----

Table 15. Relative peak heights for fresh, engine-aged and vehicle-aged catalysts.

Fresh	Relative peak heights					
NO	0.101	0.482	0.348	0.398	1.00	0.047
N_2	0.225	0.733	0.814	0.571	1.00	0.123
N_2O	0.235	0.380	0.860	0.176	1.00	0.136
Engine-aged						
NO	0.196	0.522	0.737	1.00	0.200	----
N_2	0.169	0.501	0.550	1.00	0.112	----
N_2O	0.101	0.219	0.466	1.00	0.132	----
Vehicle-aged						
NO	0.044	0.247	1.00	0.442	----	----
N_2	0.045	0.462	1.00	0.594	----	----
N_2O	0.334	0.970	1.00	0.788	----	----

Desorption curves were de-convoluted with six Gaussian bands, from which four for the fresh catalyst or three for the engine-aged and vehicle-aged catalysts can be considered as real desorption states. The lowest temperature (at 87°C) and the highest temperature (at 560°C) Gaussian bands for the fresh catalyst, as shown in Fig. 34A, are a result of the small difference between the shapes of proposed (fitted) and measured desorption curves. Similarly, the lowest temperature (at 86°C) and the highest temperature (at 361°C) states for the engine-aged catalyst, as shown in Fig. 34B, and the lowest state (at 84°C) for the vehicle-aged catalyst (Fig. 34C) are due to fitting, and they are not considered as real desorption states. The positions of temperature maxima shifted only slightly because of the impact of ageing. However, the decrease in adsorption capacities and the shape of desorption curves depend on the ageing procedures, as can be seen in Figures 34A, 34B and 34C. (Lassi *et al.* 2002d)

5.4 Solid-solid phase transitions in the bulk material

Several additives promote and stabilize commercial catalysts or facilitate catalyst's manufacturing. Catalysts are not in a stable form during their use and can undergo several undesired structural changes. These changes mainly comprise the crystallization and solid-solid phase transitions of non-amorphous phases and are normally detectable by XRD measurements. The phase transformations in the bulk material used in exhaust gas catalysts have increasingly attracted attention during recent years (Bogdanchikova *et al.* 1998, Piras *et al.* 2000, Vidal *et al.* 2000). In particular, the chemistry of aluminium oxide and its many phase transformations has been studied extensively, since Al_2O_3 provides a high surface area carrier for the supported precious metal catalysts. In this thesis, XRD is used to study the ageing-induced solid-solid phase transitions in the bulk material and to evaluate their role on catalytic activity.

X-ray powder diffraction data showed that the washcoat of the catalysts is mainly composed of three oxides, *i.e.* Al_2O_3 (alumina), CeO_2 (ceria) and La_2O_3 (lanthana). In addition to these pure oxides, the presence of Ce- and Zr-rich $Ce_xZr_{1-x}O_2$ mixed oxides was observed. These mixed oxides had a Ce content of ~0.8 mol-% and ~0.2 mol-% respectively. The washcoat of a fresh catalyst contained amorphous material and the crystal sizes were small. The crystallization of the catalyst occurs at high temperatures. Therefore, the crystalline phases of the fresh catalyst were not detected by XRD. The XRD diffractograms due to pure cerium oxides and Zr-rich mixed oxides were first observed after ageings at around 800°C-900°C (see Fig. 35). These oxides have characteristic main peaks at $2\theta = 28.7°$ and 29.8° respectively. Furthermore, the presence of the Ce-rich mixed oxide can be observed as a shoulder in the lower XRD peak at $2\theta = 28.7°$ after reductive ageings at 800°–900°C, whereas after oxidative ageings at these temperatures, the presence of Ce-rich mixed oxide was not observed. Instead, at higher ageing temperatures, the Ce-rich mixed oxide can be easily detected, whereas the pure Ce oxide is observed as a shoulder on the peak corresponding to the Ce-rich mixed oxide, as presented in Fig. 36. (Lassi *et al.* 2002c)

Recently, the behaviour of CeO_2-ZrO_2 mixed oxides at high temperatures has been extensively studied by those such as Fornasiero *et al.* 1996; Colón *et al.* 1998; Colón *et al.* 1999; Bozo *et al.* 2000, and Bozo *et al.* 2001. The addition of zirconium to the catalyst has been found to prevent the grain growth of CeO_2 crystallites at high temperatures, and to improve activity and thermal stability of γ-alumina washcoat and supported active metal phases. $Ce_xZr_{1-x}O_2$ mixed oxides are also effective oxygen storage components in a three-way catalyst. They are known to inhibit sintering and the formation of low surface area α-Al_2O_3. (Fornasiero *et al.* 1996, Ozawa 1998)

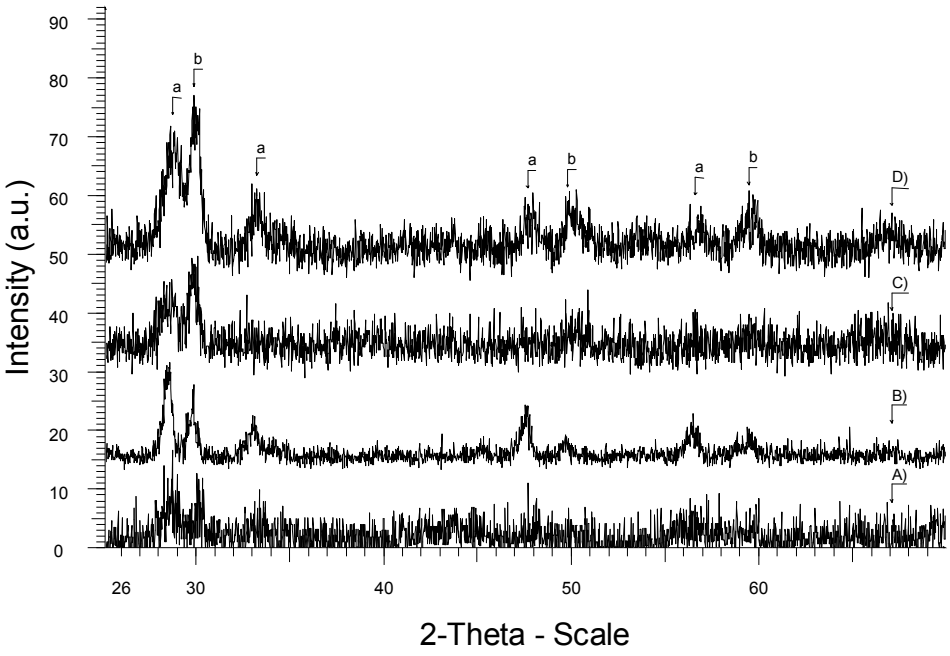

Fig. 35. Crystallization of the catalysts after reductive and oxidative ageings; XRD diffractograms for A) air/800°C/24h-aged; B) air/950°C/3h-aged; C) H_2/800°C/3h-aged, and D) H_2/900°C/3h-aged catalysts. a = CeO_2, b = Zr-rich mixed oxide.

Depending on the cerium content and on the temperature, $Ce_xZr_{1-x}O_2$ mixed oxides exist in three different crystalline phases, namely monoclinic, tetragonal, and cubic phases (Kašpar *et al.* 1999) in the composition range of 0 mol-%<Ce<100 mol-%. Below 1000°–1050°C (*i.e.* at temperatures where solids are used as catalysts), the monoclinic (Zr-rich composition) and cubic (Ce-rich composition) phases appear to be thermodynamically stable, as reported by Fornasiero *et al.* (1996) and Vlaic *et al.* (1999). According to the results presented in this thesis, $Ce_xZr_{1-x}O_2$ mixed oxides maintained high thermal stability up to an ageing temperature of 1000°C. At higher ageing temperatures, these mixed oxides decomposed, as is reported in the next paragraph. Furthermore, the Ce-rich mixed oxide seems to be more stable in thermal treatments than the Zr-rich mixed oxide, which has decomposed in air after 24 hours of ageing at 1200°C (see Fig. 36). This is consistent with the observations of Bozo *et al.* (2000), who studied $Ce_xZr_{1-x}O_2$ solid solutions (x = 0–0.84). They concluded that the $Ce_{0.67}Zr_{0.33}O_2$ solid exhibited the highest thermal stability after hydrothermal ageing (5 vol-% O_2 and 10 vol-% H_2O) at 1000°C.

In addition to the pure Ce-oxide and Ce- and Zr-rich mixed oxides, the presence of new mixed oxides was detected after 24 hours of reductive ageing at 1000°C, inert ageing at 1050°C and after oxidative ageing at 1200°C (Fig. 36). These mixed oxides were formed as a result of high-temperature ageing from the Ce- and Zr-rich mixed oxides, because ageing induced the decomposition of these mixed oxides and the formation of new mixed oxides within the molar composition range of 30 mol-% < Ce < 70 mol-%.

The interpretation of XRD diffractograms, in this respect, was difficult based on the PDF database used and, therefore, it was rather difficult to conclude the exact compositions of mixed oxides formed as a result of ageing. However, the exact composition of these mixed oxides is of secondary importance in this thesis and so the mixed oxides formed in the ageing procedure are marked with the molar composition of 30 mol-% < Ce < 70 mol-%, indicating that the composition clearly differed from those mixed oxides (Ce ~ 20 mol-% and Ce ~ 80 mol-%), which were observed at lower ageing temperatures. (Lassi *et al.* 2002c)

The decomposition and formation of mixed oxides as a result of ageing is consistent with the studies of Bozo *et al.* (2001), who showed that in the composition range of 16 mol-% < Ce < 83 mol-%, the sintering is accompanied by the phase separation of mixed oxides. This phase de-mixing of Ce- and Zr-rich mixed oxides was initiated after hydrothermal ageing at around 1000°C, and became total after ageing at 1200°C. Recently, it has been reported that Ce-Zr solid solutions with Ce molar compositions of 65% and 50% present a phase de-mixing into two other molar compositions under the oxidative conditions at around 950°C (Keveney *et al.* 2001), and after hydrothermal ageings (10 vol-% H_2O and 90 vol-% He) at 1000°C (Yao *et al.* 1997), and (10 vol-% H_2O and air) at 900°C (Colón *et al.* 1998). As reported by Colón *et al.* (1998 & 1999), the decomposition of Ce-Zr mixed oxides is associated with the crystal growth of cerium. Crystal growth takes place until the critical mean crystal size is reached, at which point the favoured process becomes the segregation into more thermodynamically stable molar compositions. In this thesis, the observed decomposition of $Ce_xZr_{1-x}O_2$ -mixed oxides was more pronounced after reductive and inert ageings compared to the oxidative ageing, as reported, which is inconsistent with the results presented on pure mixed oxides (Colón *et al.* 1998, Bozo *et al.* 2001, Keveney *et al.* 2001). Furthermore, the Ce-Zr mixed oxides, which were formed as a result of ageing do not correspond with those presented in the literature for pure mixed oxides. There are, at least, two possible interpretations for this. Firstly, the catalyst's composition is rather far from the pure mixed oxides and as such, pure CeO_2 present in the catalyst may interact with Ce-Zr mixed oxides. Secondly, the interpretation of XRD diffractograms on the basis of available PDF databases in this case may be misleading and ageing in particular could lead to separation of several Ce-Zr mixed oxides in the composition range of 30 mol-%< Ce < 70 mol-%, as reported in the previous paragraph.

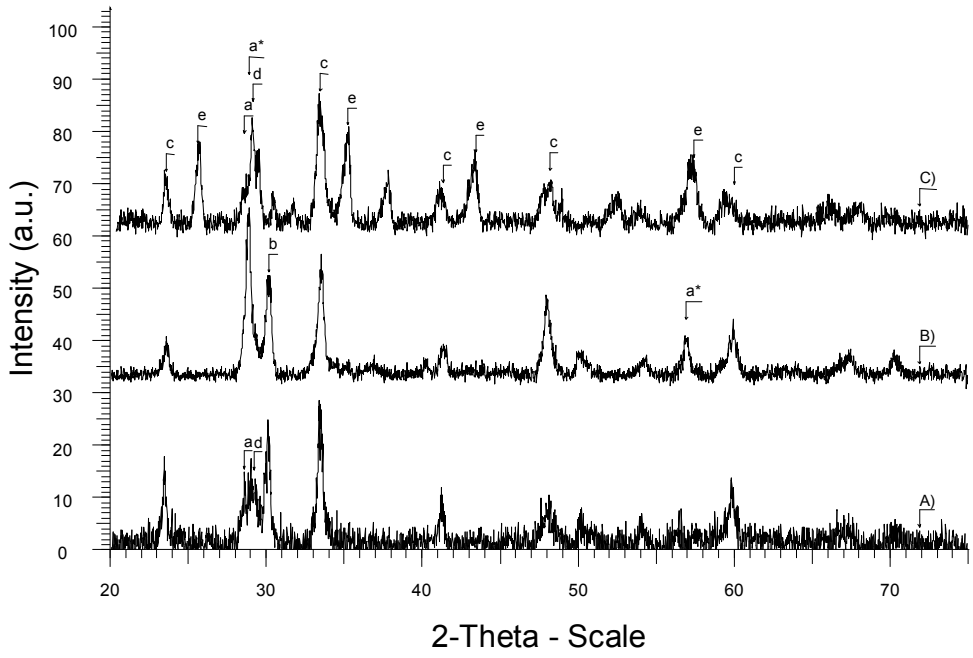

Fig. 36. Formation of $CeAlO_3$ in different ageing atmospheres; XRD diffractograms for A) H_2/1000°C/24h-aged; B) inert/1050°C/24h-aged, and C) air/1200°C/24h-aged catalysts. a = CeO_2, a* = Ce-rich mixed oxide , b = Zr-rich mixed oxide, c = $CeAlO_3$, d = Ce-Zr mixed oxides (30 mol-% < Ce < 70 mol-%) formed in the ageings, e = α-Al_2O_3.

As indicated, high ageing temperature induced phase transformations in the bulk of the catalyst. Furthermore, significant differences were observed between reductive, inert and oxidative ageing atmospheres indicating that the crystalline structure of the catalyst was strongly dependent on the surrounding environment. In addition to the ageing-induced decomposition and formation of mixed oxides, the formation of perovskite structures (XYO_3, where X is either Ce or La and Y is Al) was observed as a result of the high temperature ageing. As can be seen in Fig. 36, the main difference between reductive and inert atmospheres compared to the oxidative atmosphere, was the temperature in which the formation of $CeAlO_3$ started at around 1000°C in reductive and inert atmospheres after 24 hours of ageing. At higher ageing temperatures, $CeAlO_3$ was also observed after shorter ageing times. For the oxidative atmosphere, $CeAlO_3$ was observed only at higher temperatures, after 24 hours of ageing at 1200°C (Lassi *et al.* 2002c). Yao *et al.* (1997) reported that the $CeAlO_3$ phase is formed in reactions of γ-alumina with the surface CeO_2. Furthermore, the formation of $CeAlO_3$ is thermodynamically favoured in the reductive atmosphere (Angove *et al.* 2000b). This is consistent with the result in this thesis, because the formation of $CeAlO_3$ is concluded to be a result of ageing *via* reactions of γ-alumina with the pure cerium oxide in the catalyst's washcoat.

$CeAlO_3$ was identified from the characteristic diffraction peaks at 2θ=23.6°, 33.5°, and 41.4°. The formation of a $CeAlO_3$ phase prevents sintering and hinders the formation of low surface area aluminium oxide (α-alumina) at high temperatures, explaining why the surface areas remained higher after the reductive and inert ageings compared to the oxidative ageing. In an oxidative atmosphere, α-alumina was detected after three hours of ageing at 1200°C, but $CeAlO_3$ was detected only after 24 hours of ageing. This explains the collapse of the surface area after oxidative ageing at high temperatures: α-alumina was formed before $CeAlO_3$ and, therefore, the formation of $CeAlO_3$ could not prevent the formation of α-alumina (Lassi *et al.* 2001, Lassi *et al.* 2002c). It has been reported (Yao *et al.* 1997) that a large amount of ceria on γ-alumina is in a +3 state and that these Ce^{+3} ions can be converted to $CeAlO_3$ upon reduction. This observation is consistent with the results presented in this thesis. Furthermore, according to Yao *et al.* (1997), the formation of $CeAlO_3$ was found only in the reduced samples, which did not include ZrO_2. This also supports the interpretation that $CeAlO_3$ is formed in the reactions of γ-Al_2O_3 with the pure cerium oxide.

Tas & Akinc (1994) have reported the formation of $CeAlO_3$ in a Ce_2O_3-Al_2O_3 system in both inert (Ar) and reductive atmospheres (10% H_2/Ar) at elevated temperatures. In a flowing hydrogen atmosphere, $CeAlO_3$ was formed at 1000°C. Tas & Akinc (1994) also reported that $CeAlO_3$ completely decomposed to CeO_2 and Al_2O_3 in air at 800°C in one hour. The first phase transformation, observed in our measurements, in the reductive atmosphere was the formation of CeAlO3, as mentioned earlier. However, a second phase transformation took place at higher ageing temperatures. The formation of the second compound of Ce and Al, CeAl11O18, started at temperatures 1150°–1200°C in the reductive atmosphere. At these temperatures, the formation of small amounts of low area α-alumina was also observed. This new phase formed upon the consumption of α-alumina and $CeAlO_3$, and it has also been detected on the three-way catalysts after the operation in rich conditions (Angove *et al.* 2000b). In the measurements, the $CeAl_{11}O_{18}$ phase was identified from its characteristic peaks at 2θ=34.1° and 36.3° after 24 hours of reductive ageing at a temperature of 1200°C, as can be seen in Fig. 37. It can also be seen that, under these conditions, $CeAlO_3$ has disappeared almost completely. (Lassi *et al.* 2002c)

The formation of $CeAlO_3$ was also observed after the engine bench and vehicle ageings as shown in Fig. 37. The formation of $CeAlO_3$ is inversely proportional to the loss of surface area, which remained higher in the reductive and inert ageing atmospheres than in the oxidative atmosphere. According to Angove *et al.* (2000b), the surface area loss becomes pronounced at around 1000°C as the starting γ-Al_2O_3 form is converted to the θ-form and finally to the α-form. Furthermore, the loss in surface area between 1000°–1100°C is less under reducing conditions. This is consistent with the results presented in this thesis.

The cerium oxide phases, CeO_2 for the oxidized and $CeAlO_3$ for the reduced catalyst, were also observed by Haneda *et al.* (1993), who concluded that, on this basis, reduced catalysts had higher oxygen storage capacities compared to the oxidized ones. They suggested two possibilities for the structure around Ce ions in the reduced catalyst; Ce ions either remained dispersed in the bulk alumina, or they coagulated to form several non-stoichiometric cerium oxides, CeO_{2-X}.

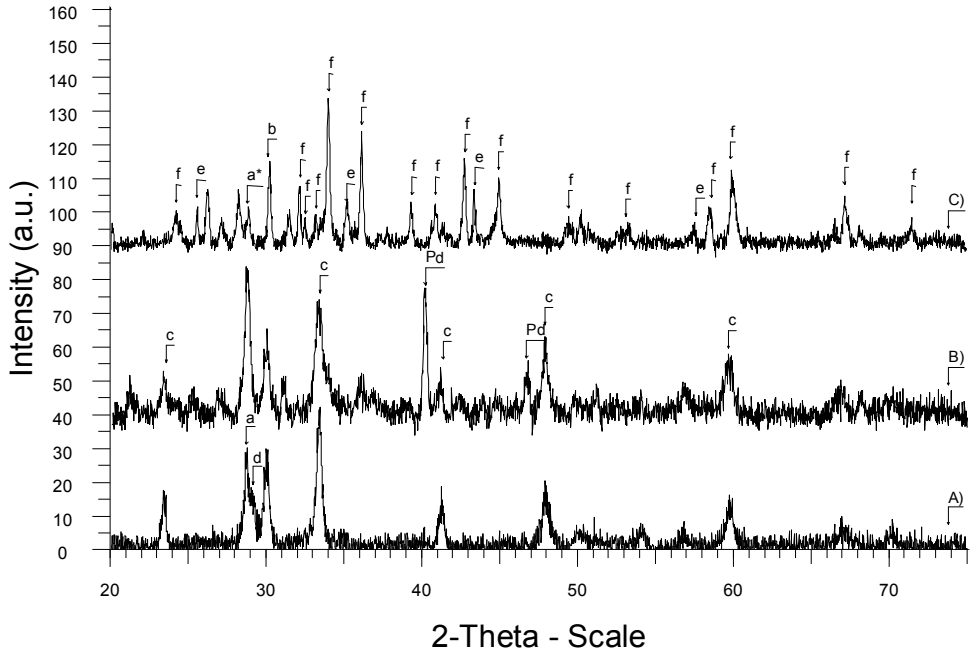

Fig. 37. XRD diffractograms for A) engine-aged; B) vehicle-aged, and C) H_2/1200°C/24h-aged catalysts. a = CeO_2, a* = Ce-rich mixed oxide, b = Zr-rich mixed oxide, c = $CeAlO_3$, d = Ce-Zr mixed oxides (30 mol-% < Ce < 70 mol-%) formed in the ageings, e = α-Al_2O_3, f = $CeAl_{11}O_{18}$.

Figure 38 presents the comparison of XRD diffractograms in different ageing atmospheres after 3 hours of ageing at 1000°C. As indicated, at this ageing temperature, the XRD diffractograms are well defined due to the increased degree of crystallization of compounds at high temperatures. The presence of water vapour does not cause any differences in the solid-solid phase transformations observed in XRD diffractograms. Therefore, the role of water vapour cannot be evaluated solely on the basis of XRD measurements. The increased loss in surface area and pore volume and the loss in active metal area after hydrothermal ageings may probably be due to the increased metal particle size. (Lassi *et al.* 2002c)

An interesting observation of these types of La_2O_3-containing Al_2O_3-based catalysts is the formation of $LaAlO_3$, which has been reported by many researchers: Oudet *et al.* (1989), Bogdanchikova *et al.* (1998) and Piras *et al.* (2000). The formation of an $LaAlO_3$ phase was observed from the lanthana-rich washcoat as a result of ageing. $LaAlO_3$ has been observed to have a main characteristic peak at $2\theta = 31.9°$ and another characteristic peak at $2\theta = 39.5°$. These peaks were typical for samples containing γ-alumina. The presence of the $LaAlO_3$ phase increases the stability of γ-alumina phase at high temperatures and prevents deactivation processes between alumina and the catalytically active precious metal components (Lassi *et al.* 2002c). According to Bogdanchikova *et al.* (1998), the formation of an $LaAlO_3$ phase was observed in the oxidative ageing at

around 1000°C, and it is stable in hydrogen, nitrogen and air at relatively high temperatures.

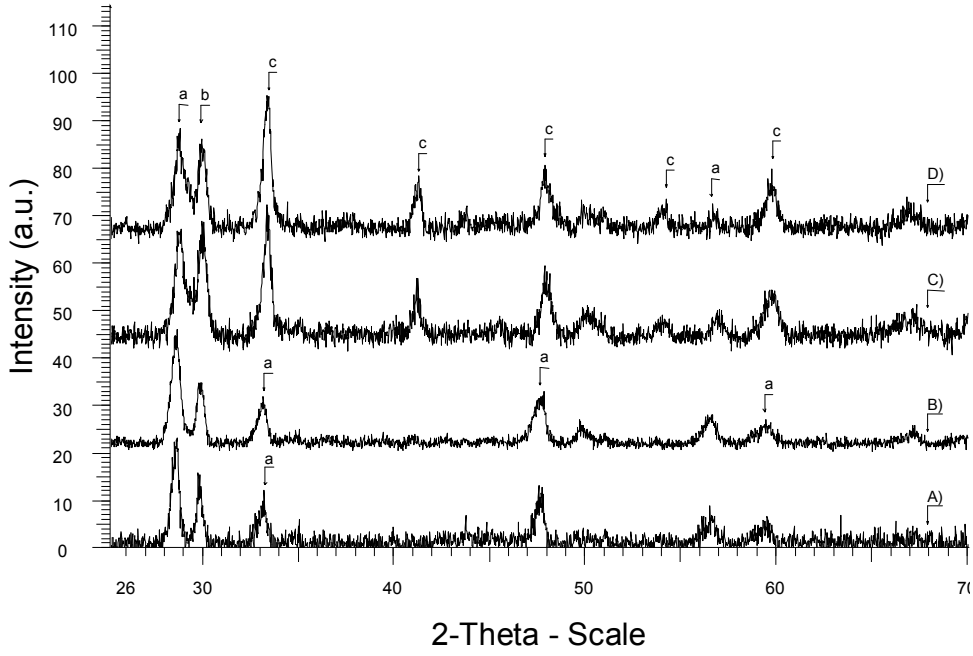

Fig. 38. Effect of water vapour on the phase transitions after the ageings. XRD diffractograms for A) air/1000°C/3h-aged; B) H_2O-air/1000°C/3h-aged; C) H_2/1000°C/3h-aged, and D) H_2O-H_2/1000°C/3h-aged catalysts. a = CeO_2, b = Zr-rich mixed oxide, c = $CeAlO_3$.

In this study, the formation of $LaAlO_3$ was detected from a lanthana-rich washcoat after 24 hours of reductive and oxidative ageings at 900°C and 1050°C, respectively. In the $LaAlO_3$ structure, both La and Al have the oxidation state of 3+. Under oxidizing conditions, La^{3+} can at least partially be oxidized to La^{4+} and, therefore, the formation of $LaAlO_3$ is not favoured. Under reducing conditions, La^{3+} is not oxidized to La^{4+}, and this explains why the formation of $LaAlO_3$ is more facile. The $LaAlO_3$ phase was formed as a result of ageing mainly in the reactions of pure La-oxides with γ-alumina. This is consistent with the results of Piras *et al.* (2000). They showed that Ce-oxide confers remarkable stability to the alumina surface under reducing conditions with a hydrogen-containing atmosphere. This stability is connected to the formation of $CeAlO_3$, which inhibits the sintering in a similar manner such as that observed for La_2O_3 on Al_2O_3 under oxidizing conditions. In the literature, it has also been reported that CeO_2 forms a mixed oxide phase with La_2O_3, which enhanced oxygen storage capacity (Ferrandon *et al.* 2001). The formation of mixed (Ce-La)AlO_3 phase is reasonable due to the similarity of the Ce^{3+} and La^{3+} ionic radii. However, in this case the likely formation of (Ce-La)AlO_3 as a result of ageing was not observed in the lanthana-rich washcoat because this washcoat does not contain pure Ce-oxides. (Lassi *et al.* 2002d)

As indicated in this section, ageing-induced solid-solid phase transitions were of crucial importance to catalyst's activity and thermal stability. The formation of perovskite structures, $CeAlO_3$ and $LaAlO_3$, in the reactions of γ-Al_2O_3 with CeO_2 and La_2O_3 as a result of ageing was observed. The formation of $CeAlO_3$ and $LaAlO_3$ was more pronounced after reductive and inert ageings. It prevents the formation of low surface area α- Al_2O_3 and, therefore, the surface areas remained higher after reductive and inert ageings. Based on the XRD results, after hydrothermal ageings no differences were found in the XRD diffractograms compared to the 'dry' ageing atmospheres. Furthermore, high temperature ageings induced the decomposition of Ce-Zr mixed oxides, which led to the formation of new mixed oxides with molar compositions in the range of 30 wt-% < Ce < 70 wt-%.

5.5 Changes in the chemical states of active metals

In ageing, the changes in chemical states and the stabilization of active metal phases are of crucial importance. Several studies of the effect of ageing on the interaction of oxygen and active metals (Pd and Rh) have been published: see Farrauto *et al.* (1992); Farrauto *et al.* (1995); Weng-Sieh *et al.* (1997); Hu *et al.* (1998), and Weng-Sieh *et al.* (1998). The interactions of oxygen and precious metals are complicated, and the mechanisms of these interactions are not well known, as reported in Chapter 3. It is, however, known that changes in the chemical states of palladium and rhodium remarkably affect the activity and thermal stability of a catalyst.

The changes in the chemical states of Rh and Pd after the ageings were studied by XPS. In Fig. 39, the Rh 3d XPS peaks of fresh (A); H_2/900°C/3h-aged (B); H_2/1000°C/3h-aged (C); H_2/1100°C/3h-aged (D); air/1000°C/3h-aged (E); engine-aged (F), and vehicle-aged (G) catalysts are shown both before (solid line) and after (dashed line) the samples reduction *in situ* in 400 mbar of static H_2 at 300°C for 30 minutes. In Fig. 39, changes both in the Rh $3d_{5/2}$ binding energy and intensity can be observed as a function of the ageing conditions. The intensity of the Rh 3d photoelectron peaks reflects the particle size so that the Rh/Al ratio is higher for small particles compared to larger ones (Jen *et al.* 1999, Niemantsverdriet 2000). On the other hand, the ageing-induced loss of pore volume (see Tables 10 and 11) and the subsequent occlusion of Rh particles can also affect the measured Rh 3d intensity. (Lassi *et al.* 2002b)

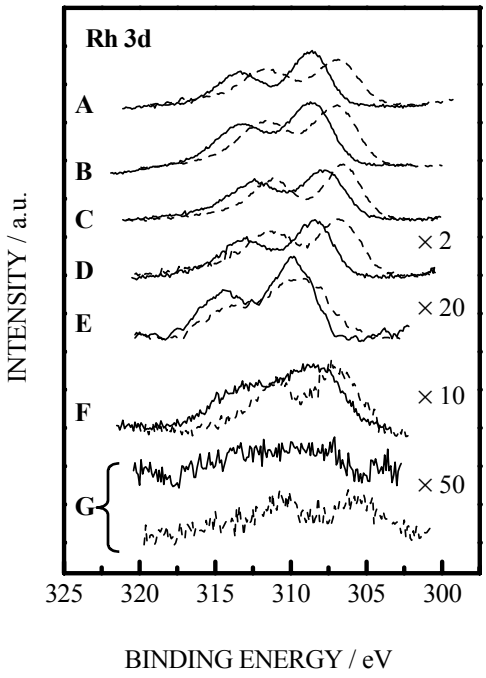

Fig. 39. Rh 3d XPS peaks measured both before (solid line) and after (dashed line) reduction of the samples *in situ* in 400 mbar of static H_2 at 300°C for 30 minutes. A) fresh; B) H_2/900°C/3h-aged; C) H_2/1000°C/3h-aged; D) H_2/1100°C/3h-aged; E) air/1000°C/3h-aged; F) engine-aged, and G) vehicle-aged catalysts.

In the fresh catalyst, all of Rh is initially oxidized to Rh_2O_3 as indicated by the binding energy value of the Rh $3d_{5/2}$ peak (308.8 eV) (Fierro *et al.* 1988, Weng-Sieh *et al.* 1997). The presence of the oxide phase is quite reasonable since the catalysts are calcined at 550°C in air. This Rh oxide phase is readily reducible, as indicated by the shift of the Rh $3d_{5/2}$ peak to 306.8 eV corresponding to metallic Rh (Weng-Sieh *et al.* 1997) after *in situ* reduction. When measuring the hydrogen-aged catalysts as received, rhodium has been oxidized to Rh_2O_3 (Fig. 39: B, C and D). The samples are transferred in air, which explains the observed presence of Rh_2O_3. However, this rhodium oxide phase is found to be in a reduced form in all cases (Fig. 39: B, C and D). (Lassi *et al.* 2002b)

The effect of ageing in air is rather different. After ageing in air at 1000°C for three hours (Fig. 39: E), the Rh $3d_{5/2}$ peak is shifted to higher binding energies at around 310 eV and the Rh oxide phase formed is no longer easily reducible. In the literature, there are two interpretations for this oxide phase formation. Firstly, Rh_2O_3 may diffuse into the γ-Al_2O_3 washcoat during the high temperature oxidative ageing and the strong interaction between rhodium and alumina results in the high Rh $3d_{5/2}$ binding energy of ~310 eV

(Yao *et al.* 1977, Wong & McCabe 1989, Beck & Carr 1993). Secondly, Weng-Sieh *et al.* (1997) have observed RhO_2 with HRTEM on alumina-supported catalysts after annealing in air at elevated temperatures. They have assigned the high binding energy of Rh $3d_{5/2}$ (~310 eV) to RhO_2. (Lassi *et al.* 2002b)

In the reductive ageing, the Rh 3d intensity remains rather unaffected in comparison to the effect of the oxidative ageing and the engine ageing. The reductive ageing at temperatures 900°C and 1000°C for 3 hours has almost no effect on the Rh 3d peak intensity, whereas ageing in hydrogen at 1100°C for 3 hours has decreased the Rh 3d intensity roughly to one half. Similar trends were also observed in BET surface areas (see Table 11), which are 69 m^2/g (fresh catalyst), 60 m^2/g (H_2/900°C/3h-aged catalyst), 49 m^2/g (H_2/1000°C/3h-aged catalyst) and 30 m^2/g (H_2/1100°C/3h-aged catalyst). Thus, the decrease in the Rh 3d intensity is likely to be caused both by the loss of the pore volume and by the sintering of the Rh particles in the washcoat. The decrease in the Rh 3d intensity in the air-aged catalyst can be accounted for the possible Rh_2O_3 diffusion to the washcoat, sintering of the Rh particles, structural changes in γ-Al_2O_3 support, such as the loss of the pore volume and phase transformation towards α-Al_2O_3 (Gitzen 1970). This may lead to occlusion of rhodium particles in the washcoat, which make them inaccessible to the gas molecules. BET and H_2-chemisorption results also reflect these phenomena. According to the BET measurements, the surface area of the air-aged catalyst (air/1000°C/3h: 25 m^2/g) is also clearly smaller than that of the hydrogen-aged catalyst (H_2/1000°C/3h: 49 m^2/g). Accordingly, the noble metal dispersion decreases clearly from 28% (fresh catalyst) below 1% (catalysts aged at a temperature of 900°C and above), as reported previously in section 5.2. (Lassi *et al.* 2002b)

The effect of engine ageing on Rh 3d can be seen in Fig. 39**,** spectra F. The intensity of the Rh 3d peaks has decreased remarkably in comparison to the fresh catalyst, but not as drastically as in the air ageing. Rhodium has also remained in the reduced form. These observations can be rationalised by the fact that the atmosphere during the engine ageing has been either stoichiometric or reductive (rich) and the total engine ageing time has been 40 hours. The reductive ageing atmosphere prevents the reaction between Rh and alumina support and thus Rh remains in the reduced form. The intensity of the Rh 3d peak was observed to begin to decrease during the 3 hours hydrogen ageing treatments. In the engine ageing, the time is much longer (40 hours) and thus the decrease in the Rh 3d peak intensity is also larger. In the vehicle-aged catalyst, the Rh 3d peak is barely visible (Fig. 39, spectra G). However, the shape of the Rh 3d peak resembles that of the engine-aged catalyst and Rh has also remained in the reducible form during the vehicle ageing. (Lassi *et al.* 2002b)

In Fig. 40, Rh 3d spectra measured after a longer ageing time (24 hours) are shown. The spectra of fresh, engine-aged and vehicle-aged catalysts are also shown as a reference. Due to a longer ageing time, the changes in the peak intensities are stronger in comparison to the spectra measured after 3 hours of ageing treatments. The effect of the ageing on the chemical state of Rh is very similar to the shorter ageing treatments. (Lassi *et al.* 2002b)

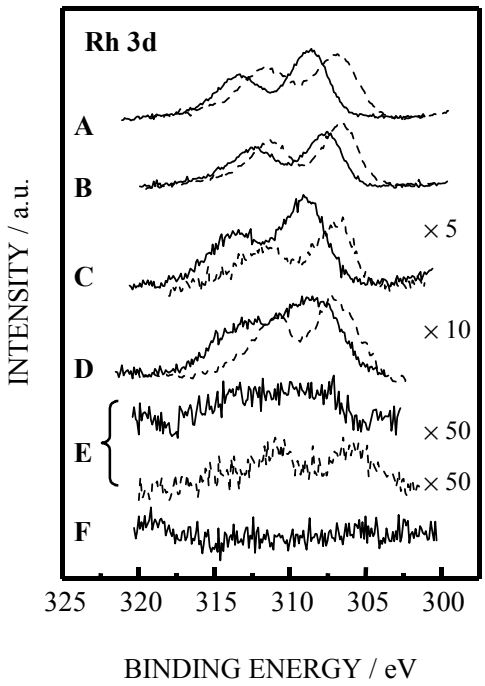

Fig. 40. Rh 3d XPS peaks measured both before (solid line) and after (dashed line) reduction of the samples *in situ* in 400 mbar of static H_2 at 300°C for 30 minutes. A) fresh; B) H_2/900°C/24h-aged; C) H_2/1000°C/24h-aged; D) engine-aged; E) vehicle-aged, and F) air/1000°C/24h-aged catalysts.

Active metals, palladium and rhodium, were added into the different washcoats, as was explained in section 4.1. According to XPS results, in the fresh sample no Pd 3d peaks were observed on the catalyst's surface (Fig. 41, A). Furthermore, in the air-aged catalysts, no Pd is present on the surface, but after the high temperature ageing in the reductive atmosphere, palladium is found to be also present on the surface of the catalyst (Fig. 41, C-F). Clearly, as the temperature of the reductive ageing is increased, the amount of Pd on the surface increases. There are two possible interpretations for this observation. Firstly, the surface of the washcoat may have eroded in the reductive ageing revealing the Pd particles present in the lower parts of the washcoat. Secondly, in the presence of H_2 at a high temperature, palladium may become mobile and may be transported from the washcoat to the surface. After ageing in air at 1000°C for three hours, there is no Pd on the catalyst surface (Fig. 41, B). The loss of Pd may be partially due to its volatilization into the gas phase. The vapour pressure of PdO is thus likely to be much lower than that of metallic Pd. Consequently, one role of hydrogen in the high temperature-induced transport of Pd is to keep the Pd particles in metallic form. The possible deactivation by the vaporization of palladium will be discussed later in this thesis. Some other mechanisms may also contribute to the high mobility of Pd at a high temperature and will be discussed in section 5.8. Furthermore, according to the results of XPS measurements, both the engine-aged catalyst and the vehicle-aged catalyst contain a

small amount of sulfur and the vehicle-aged catalyst also contains some calcium, as can be seen in Fig. 41 D (Lassi *et al.* 2002b). This is consistent with the poison analysis, which will be considered later in section 5.7.

As a summary for this section, the ageing-induced effects are clearly seen: the intensity of Rh 3d peaks decreased as a function of ageing temperature. According to XPS results, the loss of catalytic activity was associated with the sintering of rhodium metal particles in the washcoat. Sintering of Rh particles is more pronounced in the oxidative ageing atmosphere, which explains the lower catalytic activities and surface areas in this case. Furthermore, XPS measurements gave evidence of the possible volatilization of Pd as a result of ageing at elevated temperatures.

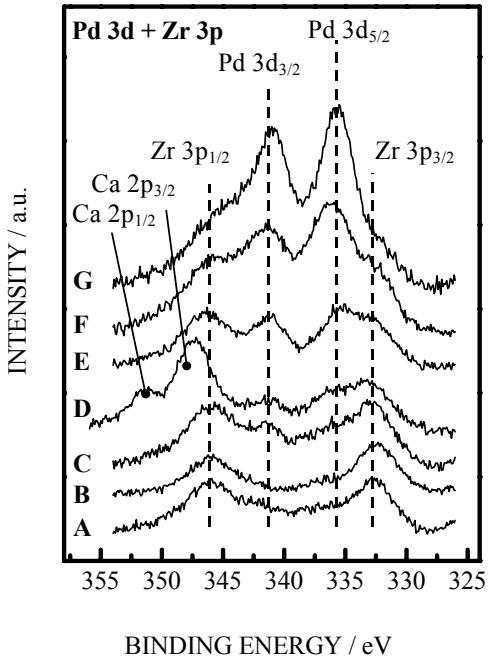

Fig. 41. Pd 3d XPS peaks together with the partially overlapping Zr 3p peaks measured from the catalyst's surface. A) fresh; B) air/1000°C/3h-aged; C) H_2/900°C/3h-aged; D) vehicle-aged; E) engine-aged; F) H_2/1000°C/3h-aged, and G) H_2/1100°C/3h-aged catalysts.

5.6 Loss of catalytic activity

Catalytic activities were determined after thermal, hydrothermal, engine bench and vehicle ageings in lean and rich conditions. The simple model reaction, the reduction of

NO by CO, was used to compare the catalysts after the ageings. Catalyst light-off temperature (T_{50}-value) is defined as the temperature at which 50% conversions of CO and/or NO is achieved. The light-off temperatures of CO and NO as a function of ageing temperature after oxidative and reductive ageings are presented in Figures 42 and 43, in lean and rich conditions, respectively. The conversions at 400°C have been determined in order to discover the final (maximum) conversions of NO and CO. These catalysts reach their maximum conversion by 400°C. The conversion curves (as presented in Figures 44 and 45) of the catalysts give evidence to this.

A)

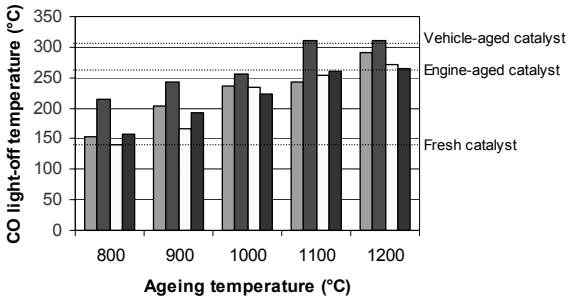

B)

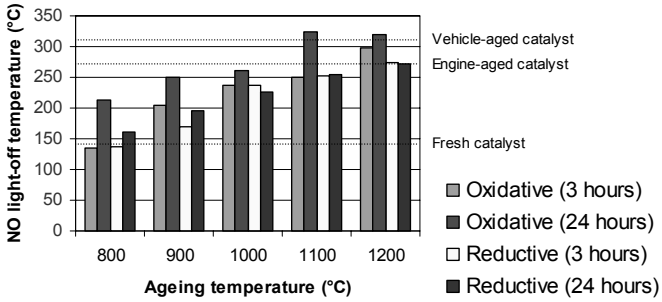

Fig. 42. Catalytic activities in lean conditions: determined as the light-off temperatures of A) CO and B) NO after 3 and 24 hours of oxidative and reductive ageings.

A)

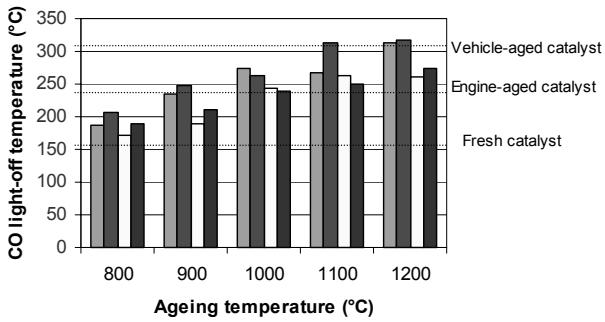

B)

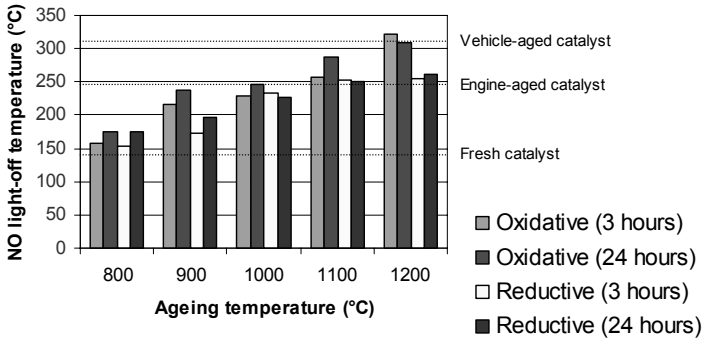

Fig. 43. Catalytic activities in rich conditions: determined as the light-off temperatures of A) CO and B) NO after 3 and 24 hours of oxidative and reductive ageings.

The light-off temperatures (T_{50} values) of CO and NO increased as a function of ageing temperature after the oxidative and reductive ageings (Figures 42 and 43). The activity of a catalyst remained clearly higher if ageing was carried out in the reductive atmospheres. After the inert ageing, similar behaviour in the catalytic activity was observed as in the reductive ageing atmosphere, as can be seen in Table 16, where the comparison of the light-off temperatures is presented after reductive, oxidative and inert ageings. As indicated, differences in the light-off temperatures were not found between reductive and inert ageings. Instead, after the oxidative ageing, higher light-off temperatures of CO and NO are systematically observed and so are lower catalytic activities. This is consistent with the BET results as presented in section 5.1, where the surface areas prevailed higher after reductive and inert ageings than after oxidative ageings. Therefore, the loss of catalytic activity can be associated with the loss of specific surface area. However, the evolution of catalytic activity cannot be explained exclusively in the terms of specific surface areas and textural properties of a catalyst. It is known that not only washcoat properties but also the changes in the active surface phases after the thermal ageings affect the catalytic activity. (González-Velasco *et al.* 2000c)

Table 16. Comparison of CO light-off temperatures (°C) after 3 hours of reductive, oxidative and inert ageings, in lean reaction conditions.

Ageing temperature (°C)	Reductive	Inert	Oxidative
800	140	142	154
900	167	n.d.	204
950	221	224	228
1000	234	238	239
1100	253	n.d.	248
1200	272	274	291

n.d. = not determined

Catalytic activity depends on the nature of ageing atmosphere and temperature, as substantiated above. The ageing time is also an essential factor for deactivation although, on the basis of this study, it is clearly of secondary importance compared to ageing atmosphere and high ageing temperature. As can be seen in Figures 42 and 43, the fresh catalyst showed the highest activity in lean and rich conditions, as expected. Thermal ageings in the oxidative or reductive ageing atmospheres in the temperature range of 800°–1200°C do not cause a significant performance decrease for the catalysts. All the aged catalysts maintained a high activity up to the ageing temperature of 800°C, and were active in decreasing the emissions of NO and CO. Even after the ageings at 1200°C, high catalytic activities remained. Considering the results presented earlier in Tables 10 and 11, this means that textural modifications induced by ageings do not greatly affect catalytic activity at normal operation temperatures. The comparison of the end conversions of the fresh and aged catalysts at 400°C showed that ageing atmosphere does not significantly affect these conversions. All the aged catalysts were active and converted well NO and CO after the ageings, and gave high conversions of CO and NO (determined at temperature of 400°C) in lean and rich reaction conditions. The conversions were above 80% for all the aged catalysts. The only exception was the oxidative ageing at the ageing temperature of 1200°C, where the conversions of CO at 400°C were 74% and 80% in rich and lean conditions, respectively. Furthermore, no significant differences were found in the formation of N_2 or the unwanted by-product (N_2O), *i.e.* in the selectivities of the aged catalysts or in the yields of N_2O as a function of ageing atmosphere. However, it has often been reported that a catalyst's selectivity is affected by ageing (Burch *et al.* 1996, Botas *et al.* 2001, González-Velasco *et al.* 2001). This inconsistency compared to the results presented in this thesis is probably due to a simple model reaction, reduction of NO by CO, which is used in the activity measurements. For that reason, selectivities to N_2 and N_2O and yields of N_2O are not further considered in this thesis.

In the activity testing of catalyst systems of metallic pre- and main converters (Härkönen *et al.* 2001), all the catalysts reached Euro IV emission limits after the engine bench and vehicle ageings. The pre-catalyst (from which the catalyst aged for 100 000 kilometres is considered detailed in this thesis) was mostly responsible for the system light-off, whereas the role of the main catalyst was to assist the pre-catalyst after the light-off occurred, and especially to achieve the high end conversion levels of CO, NO and total hydrocarbons needed for the Euro IV emission limits.

As indicated, the effect of ageing on catalytic activity is rather different in the reductive ageing compared to the oxidative ageing atmosphere. After the reductive ageing at low ageing temperatures of 800°–900°C with short ageing times, catalytic activities remained as high as in the case of the fresh catalyst (see Figures 42 and 43). This is also consistent with XPS results, where peak intensities remained almost unaffected after the reductive ageings at temperatures of 800°–1000°C. The H_2/800°C/3h-aged catalyst showed an even higher activity than the fresh catalyst. This may be due to an increased OSC after reduction, as explained by González-Velasco *et al.* (2001). Therefore, the effect of the reductive ageing on the catalyst's properties (on specific surface areas, pore sizes and particle sizes) is rather small compared to that of the oxidative ageing atmosphere. After the reductive ageings, the Rh oxide phase is also more easily reducible, and the phase transition towards the low-surface area α-Al_2O_3 responsible for the surface area decrease is prevented, as discussed earlier in section 5.5 concerning XPS measurements.

The effect of ageing time on deactivation has also been considered. Higher activities remained after three hours of ageing compared to 24 hours of ageing both in the reductive and oxidative atmospheres. These differences can clearly be observed at low ageing temperatures (below 950°C) in the reductive atmosphere. At higher ageing temperatures, the role of ageing atmosphere and temperature increased and the ageing time was not as critical a variable any more. This is consistent with BET and XPS results, where higher surface areas and peak intensities, in that order, were observed after 3 hours of ageing. However, ageing time does not induce observable changes in the chemical states of Rh and Pd, nor changes in the phase transitions observed by XRD, as reported in sections 5.5 and 5.4, respectively. Therefore, it can be stated that ageing time, again, is of secondary importance compared to ageing atmosphere and temperature. Table 17 presents a comparison between the light-off temperatures of CO after 3, 24 and 42 hours of ageing in the reductive ageing atmosphere. When comparing the results presented in Table 17 to the corresponding BET surface areas as presented in Fig. 21, the activity loss as a function of ageing time was similar to the surface area loss in the reductive ageing atmosphere.

Table 17. Comparison of CO light-off temperatures (°C) after 3, 24 and 42 hours of ageing in the reductive ageing atmosphere.

Ageing temperature (°C)	3 h	24 h	42 h
900	167	192	190
1000	234	223	244
1100	253	261	280

Figure 44 shows the conversion *vs.* temperature curves obtained for CO after reductive and oxidative ageings at ageing temperatures of 800°C, 1000°C and 1200°C. As can be seen, differences were observed in the catalytic activities (light-off values of CO) after oxidative and reductive ageings with the same ageing temperatures and times. After the oxidative ageing, the significant loss of catalytic activity was observed at ageing temperatures higher than 1000°C. This temperature region was also significant after the reductive ageing, but the activity of the catalyst remained higher with the same ageing temperatures and times. This is consistent with BET measurements, where higher surface

areas were observed after reductive ageings. After the oxidative ageings, catalysts also showed low thermal stabilities, as reported earlier. The differences in catalytic activity and thermal stability of a catalyst between these two ageing atmospheres can be explained by the changes in the chemical states of precious metals, in particular Rh, as explained above.

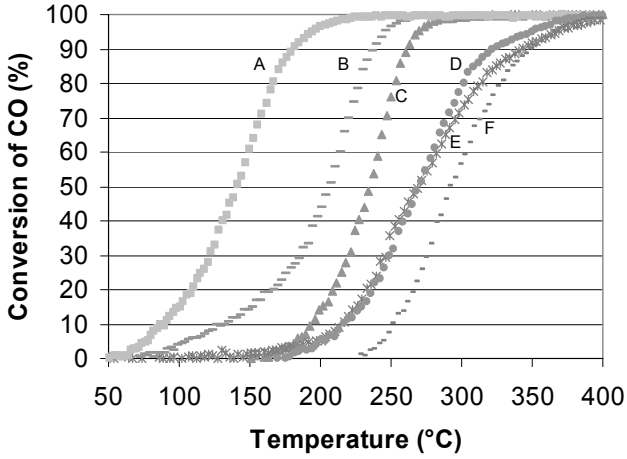

Fig. 44. Comparison of the light-off curves of CO after the reductive and oxidative ageings: A) H_2/800°C/3h-aged; B) air/800°C/3h-aged; C) H_2/1000°C/3h-aged; D) H_2/1200°C/3h-aged; E) air/1000°C/3h-aged, and F) air/1200°C/3h-aged; lean reaction conditions.

The presence of water in the ageing procedure has been reported to have an accelerating effect on the sintering of active metals, as described earlier. In this thesis, the hydrothermal ageings were carried out in the presence of 10 vol-% H_2O in the reductive and oxidative gas mixtures (corresponding to the composition of dry ageing gas mixtures). The temperatures required for 50% conversion of CO and NO after hydrothermal ageings are given in Table 18. In Table 19, comparison between dry and wet ageing atmospheres is presented, as an example, after three hours of ageing at an ageing temperature of 1200°C.

Table 18. CO and NO light-off temperatures (T_{50} values) after hydrothermal ageings in the oxidative and reductive ageing atmospheres. Ageing time was 3 hours.

Ageing temperature (°C)	Hydrothermal oxidative ageing atmosphere				Hydrothermal reductive ageing atmosphere			
	CO Light-off temperature, T_{50} (°C)		NO Light-off temperature, T_{50} (°C)		CO Light-off temperature, T_{50} (°C)		NO Light-off temperature, T_{50} (°C)	
	Lean	Rich	Lean	Rich	Lean	Rich	Lean	Rich
800	165	201	150	157	147	181	126	154
900	210	225	214	215	193	215	190	200
1000	271	290	278	273	221	235	214	221
1100	260	275	267	265	220	233	216	223
1200	305	334	305	309	253	274	253	261

* T_{50} indicates temperature at which 50% conversion was achieved for CO and NO

As presented in Table 18, the light-off temperatures of CO and NO increased as a function of ageing temperature after hydrothermal ageings in the reductive and oxidative ageing atmospheres, as expected. It was observed that the light-off temperatures (T_{50}-values) remained clearly lower if the hydrothermal ageing was carried out in the reductive gas atmosphere. Therefore, hydrothermal ageing in the presence of an oxidative gas atmosphere showed the lowest activities for the removal of CO and NO. This did not correlate well with the BET or chemisorption results presented earlier, where similar behaviour was observed after hydrothermal ageings in the reductive and oxidative atmospheres. Therefore, it was concluded that the loss in catalytic activity is associated with the surface area loss, and also with the ageing-induced changes in the chemical states of active metals and the oxides in the bulk washcoat.

Table 19. The comparison of dry and wet ageing atmospheres in lean and rich reaction conditions after 3 hours of ageing at 1200 °C.

Ageing atmosphere		Lean		Rich	
		CO T_{50} (°C)*	NO T_{50} (°C)*	CO T_{50} (°C)*	NO T_{50} (°C)*
Oxidative	Air	291	298	322	312
Hydrothermal oxidative	10 vol-% H_2O-air	305	305	334	309
Reductive	5% H_2	272	275	261	255
Hydrothermal reductive	10 vol-% H_2O-5% H_2	253	253	274	261

* T_{50} is a light-off temperature of CO and/or NO

As shown in Table 19, the lowest activities (determined as light-off temperatures of CO and NO) were observed after hydrothermal ageing in the oxidative gas phase. This was observed at all ageing temperatures in the temperature range of 800°–1200°C. Therefore, it can be concluded that water vapour has an accelerating effect on deactivation, at least

in the oxidative gas atmosphere, which is consistent with the earlier observations by Ihara *et al.* (1987), Carol *et al.* (1989) and Beck *et al.* (1997a). Furthermore, on the basis of activity measurements, it can be concluded that oxidative ageing treatments are clearly more demanding on the catalyst than the reductive ones. After reductive ageings, it is rather difficult to distinguish the role of water vapour. On the basis of results presented in Table 19, it seems that catalytic activities remained higher after hydrothermal reductive ageings at 1200°C in lean conditions, but the situation is quite the reverse in rich conditions. When comparing dry and wet reductive ageing atmospheres at other ageing temperatures, it was observed that there were only small differences in the catalytic activities between these two ageing atmospheres. Therefore, it can be stated that, in this study, catalytic activities remained highest after reductive ageings, and the lowest activities were observed after the hydrothermal oxidative ageing. The catalytic activities after oxidative ageing were between these two limits. Catalytic activities after inert ageings were close to those observed in the reductive ageing atmosphere, as previously reported. Furthermore, the presence of water vapour has an accelerating effect on deactivation, and it is clearly pronounced in the oxidative gas phase.

In Fig. 45, the light-off curves of CO after hydrothermal and thermal ageings for H_2/800°C/3h-aged (A); H_2O-air/800°C/3h-aged (B); air/1000°C/3h-aged (C); H_2O-H_2/1000°C/3h-aged (D); H_2/1000°C/3h-aged (E); H_2/1200°C/3h-aged (F); H_2O-air/1000°C/3h-aged (G); air/1000°C/3h-aged (H), and H_2O-air/1200°C/3h-aged (I) catalysts are presented. As indicated in Fig. 45, the presence of water vapour in the ageing cycle accelerates the activity loss compared to the dry ageing atmosphere. Hydrothermal ageing in the oxidative atmosphere showed the lowest activities with the same ageing temperatures and times, whereas the highest activities were observed after the reductive ageings. Similarly, the specific surface areas and active metal areas were lower after hydrothermal ageings compared to the dry ageing atmosphere. This supports the earlier assumption that sintering of bulk oxides and active metals is accelerated in the presence of water vapour.

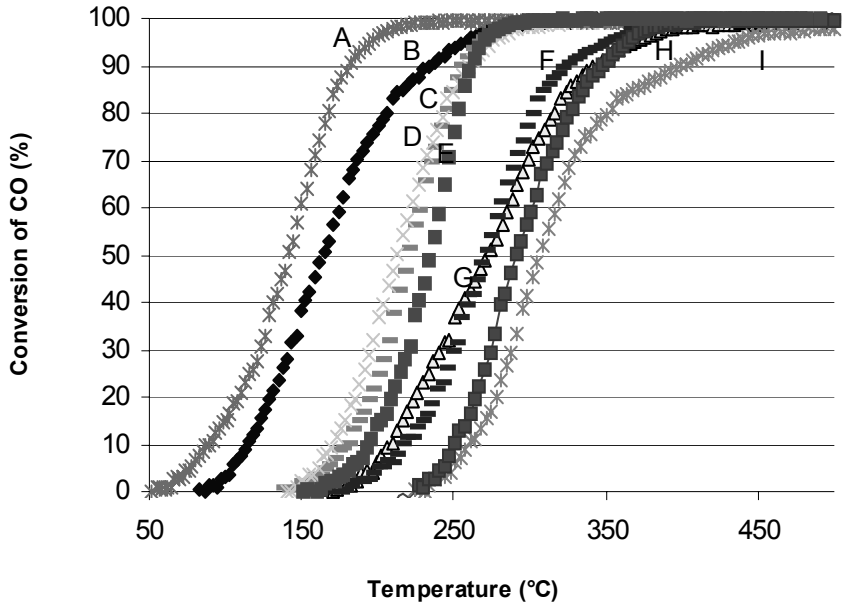

Fig. 45. Light-off curves of CO after hydrothermal and thermal ageings for A) H_2/800°C/3h-aged; B) H_2O-air/800°C/3h-aged; C) air/1000°C/3h-aged; D) H_2O-H_2/1000°C/3h-aged; E) H_2/1000°C/3h-aged; F) H_2/1200°C/3h-aged; G) H_2O-air/1000°C/3h-aged; H) air/1200°C/3h-aged, and I) H_2O-air/1200°C/3h-aged catalysts.

Thermal deactivation of the catalysts is likely to be caused by the collapse of surface area, the sintering of the Rh particles in the washcoat and the phase transitions observed in the bulk material as reported in earlier sections. High temperature ageing is known to favour the sintering of active metals and washcoat materials (Perrichon *et al.* 1995, Fornasiero *et al.* 1996). The lower catalytic activities after the oxidative ageings are thought to be the result of the formation of an inactive rhodium oxide that cannot be easily reduced. Precious metal particles may also be encapsulated in the sintered washcoat as a result of high temperature ageing that is observed as a decrease in the catalytic activity. These encapsulated metal particles cannot participate in catalysis since they are inaccessible to gas phase molecules (Graham *et al.* 1999), as will be further considered in section 5.8.

In Fig. 46, the light-off curves of CO for the fresh catalyst (A); H_2/800°C/3h-aged (B); H_2/1000°C/3h-aged (C); engine-aged (D); H_2/1200°C/3h-aged (E); air/1200°C/3h- aged (F), and vehicle-aged (G) catalysts are presented. On the basis of our studies, engine and vehicle ageings correlate to laboratory scale ageing in the reductive ageing atmosphere, as explained above. The engine-aged catalyst includes only small amounts of poisons (Zn, S, and P) originating from the fuel and lubrication oil, as will be reported in section 5.7, the presence of poisons in the engine-aged catalyst do not cause any significant activity loss. Thus, the engine-aged catalyst can be regarded as thermally deactivated and a deactivation correlation between the engine-aged catalyst and laboratory scale-aged catalysts can be presented.

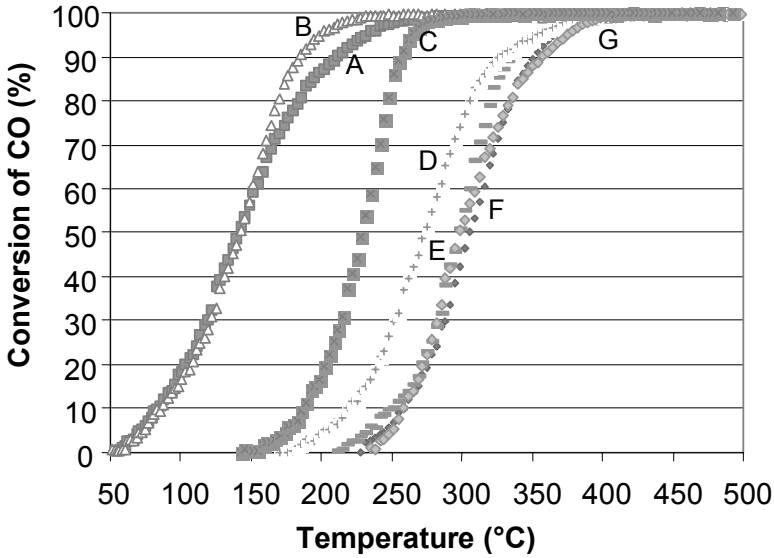

Fig. 46. Light-off curves of CO for A) the fresh catalyst; B) H_2/800°C/3h-aged; C) H_2/1000°C/3h-aged; D) engine-aged; E) H_2-H_2O/1200°C/3h-aged; F) air/1200°C/3h-aged, and G) vehicle-aged catalysts; lean reaction conditions.

In the activity measurements, the vehicle-aged catalyst showed the lowest catalytic activities in lean and rich reaction conditions (see Fig. 46). Furthermore, as will be considered in section 5.7, the front zone of the vehicle-aged catalyst clearly showed higher light-off temperatures (lower activities) compared to the rear zone of the catalyst. This was verified in the activity tests by changing the flow direction in the catalyst. Therefore, thermal deactivation does not only exclusively explain the low activity of the vehicle-aged catalyst, but deactivation is also linked to the accumulation of the poisons on the catalyst's surface. After the vehicle ageing, poisoning was remarkable in the front zone of the catalyst, where a high amount of poisons were observed. Therefore, poisoning is one of the relevant deactivation mechanisms of a vehicle-aged catalyst, and it is considered in detail in section 5.7.

Furthermore, the effect of ageing procedure on the oxygen storage capacity (OSC) was also evaluated. Oxygen storage capacities of the fresh, engine-aged and vehicle-aged catalysts and some of the aged catalysts were measured at adsorption temperatures of 450°C, 600°C and 750°C. Oxygen storage capacity values can be determined as total OSC, which represents the maximum amount of transferable oxygen at a given temperature (Trovarelli 1996), or as dynamic OSC. Based on dynamic OSC results (Härkönen *et al.* 2001), the OSC response increased systematically as a function of adsorption temperature, as expected, but decreased as a function of ageing temperature. Several studies support this observation (Vidal *et al.* 1999, Bedrane *et al.* 2002a, Fally *et al.* 2000, Hickey *et al.* 2001, Vidal *et al.* 2001). In this thesis, the lowest OSC values were determined for the vehicle-aged catalyst, which is consistent with the results of the

activity measurements. During the ageing procedure, the OSC materials (in particular Ce-containing compounds) in the catalyst underwent solid-solid phase transitions, as shown earlier in section 5.4. The observed decrease in OSC response of a vehicle-aged catalyst is caused both by thermal deactivation and poisoning. According to Bedrane *et al.* (2002b), OSC on ceria-based catalysts varies only slightly with adsorption temperature, whereas OSC on ceria-zirconia supported catalysts increases widely with temperature. This is associated with oxygen diffusion in the bulk. (Muraki & Zhang 2000)

In brief, ageings induced the loss of catalytic activity, which is related to the loss in surface area and also to the ageing-induced changes in the active surface phases. It was observed that the role of ageing atmosphere (reductive or oxidative) and the presence of water vapour during the ageing treatment was relevant. Decrease in catalytic activities was observed in the oxidative, reductive and inert atmospheres as a function of ageing temperature. The activity of a catalyst remained better if ageing was carried out in the reductive or inert ageing atmospheres. The effect of ageing time on the catalytic activity, on the other hand, was minimal and observed only slightly at low ageing temperatures. Furthermore, all the catalysts retained high catalytic activities after the ageings, which was observed as high-end conversions of CO and NO. The activity measurements were consistent with the results obtained by using other characterization techniques.

5.7 Poisoning

In the catalytic purification of exhaust gases, even a slow poisoning or traces of poisons may cause significant deactivation of the catalyst. The presence of poisons in the exhaust gas feed can originate either from the fuel and/or the engine's lubrication oils. Other possible sources of poisons may also be the engine's mechanical wear or the ambient air that is mixed with the fuel for combustion. Indeed, ambient air may contain higher levels of pollutants than purified exhaust gases (Twigg 2001), at least in contaminated urban areas. However, this source of pollution can be excluded in this study since the motor oil and fuel constituents are mostly responsible for the poisoning, as will be shown in this section.

In this thesis, aged catalysts were mostly thermally deactivated. Poisoning was observed only in the case of the engine-aged and vehicle-aged catalysts. The poison distribution is typically observed on the catalyst's surface in the axial direction, but in the radial direction to a smaller extent, depending on the flow distribution in the catalytic converter (Angelidis & Sklavounos 1995, Angove & Cant 2000a). In order to evaluate the importance of poisoning as a deactivation phenomenon, engine-aged and vehicle-aged catalysts were cut into small pieces in the axial (front and rear) and radial (outer and interior) direction, as previously described in Fig. 15, and the distribution of inorganic contaminants (poisons) was determined.

Table 20 provides the results of the elemental analyses of contaminants for fresh, engine-aged and vehicle-aged catalysts. In addition, the corresponding BET surface areas, catalytic activities of the removal of CO and NO, and oxygen storage capacities (measured at adsorption temperature of 750°C) are presented in Table 21. As indicated,

the engine-aged catalyst was poisoned by phosphorus (P), sulfur (S) and zinc (Zn). According to the SEM-EDS analysis, the amount of accumulated poisons in the engine-aged catalyst was small and no contaminated overlayer was observed as was shown in Fig. 13. Therefore, poisoning hardly affected the catalytic activity or the specific surface areas of the engine-aged catalyst (see Table 21). Instead, the vehicle-aged catalyst was clearly poisoned and this was also observed at significantly lower catalytic activities, as shown earlier (see Fig. 45). For example, the P content in the engine-aged catalyst was only 1/20 compared to the P content in the vehicle-aged catalyst.

Table 20. Contaminant levels of the fresh, engine-aged and vehicle-aged catalysts in axial and radial directions.

Catalyst		Contaminant levels (wt-%)			
		P	S	Zn	Ca
Fresh		<0.1	<0.1	<0.1	<0.1
Engine-aged	Front outer	0.2	0.2	0.2	<0.1
	Front interior	0.2	0.2	0.2	<0.1
	Rear outer	0.2	0.2	0.1	<0.1
	Rear interior	0.1	0.2	0.1	<0.1
Vehicle-aged	Front outer	3.5	<0.1	1.6	2.3
	Front interior	3.5	<0.1	1.5	2.5
	Rear outer	0.2	<0.1	1.2	0.3
	Rear interior	0.2	0.1	1.1	0.4

Table 21. The effect of poisoning of engine-aged and vehicle-aged catalysts on the BET surface area, oxygen storage capacities (measured at adsorption temperature of 750°C) and catalytic activities for the removal of CO and NO (in lean conditions).

Catalyst		BET surface area (m^2/g)	CO Light-off temperature, T_{50} (°C)	NO Light-off temperature, T_{50} (°C)	OSC (ml/g washcoat)
Fresh		69	140	130	5.1
Engine-aged	Front	22	272	273	4.5
	Rear	22	265	270	n.d.
Vehicle-aged	Front	8	320	322	2.0
	Rear	16	305	309	n.d.

n.d. = not determined

As can be seen in Table 20, the major contaminants in the vehicle-aged catalyst were phosphorus (P), calcium (Ca) and zinc (Zn). Instead, the amount of sulfur (S) was small in all parts of the vehicle-aged catalyst compared to the engine-aged catalyst. This is probably due to the different fuel used in the engine bench ageing, because sulfur originates mainly from the fuel, whereas P, Zn and Ca are contaminants of the lubrication oils. Therefore, the contaminants from the lubricants predominate since the sulfur concentration in the fuel is low and it has been continuously reduced over the past few decades.

As indicated in Table 20, the catalyst's deactivation after the vehicle ageing was clearly a position-dependent phenomenon. The front zone of the vehicle-aged catalyst

(first 2 cm from the inlet) was the most highly poisoned zone. The only exception was sulfur, which was also found in the rear part of the catalyst in small concentrations. Furthermore, while higher accumulation of poisons is observed in the inlet zone of the catalyst, the radial poison distribution is uniform. This is consistent with the studies of Angelidis & Sklavounos (1995). Poisoning was also associated with the collapse of surface area, as can be concluded on the basis of Table 21, and with the loss of catalytic activity. It was also observed that the adsorption of P and Ca was almost irreversible, whereas adsorption of Zn and, in particular, of S was reversible.

The results reported here are consistent with the results of Beck & Sommers (1995) over the vehicle-aged Pd monoliths. They concluded that the impact of sulfur on catalytic activity is irreversible at temperatures below 650°C. Instead, at higher temperatures the impact of sulfur on catalytic activity is minimal because the adsorption of sulfur is reversible. Therefore, at low temperatures the original activity of the catalyst can be at least partly restored, e.g. by acetic acid leaching (Angelidis & Papadakis 1997). Furthermore, the decrease in the light-off performance was non-linear with sulfur concentration. It has also been reported that the effect of sulfur on catalytic activity is more evident under reductive (rich) conditions than under oxidative (lean) conditions. This is due to the fact that under rich conditions, sulfur is present as H_2S, which strongly poisons the catalytic metal surfaces. (Rabinowitz *et al.* 2001)

In our study on the deactivation of vehicle-aged and engine-aged metallic pre- and main converters (Härkönen *et al.* 2001), the pre-converters were more highly poisoned compared to the main converters. The front areas of the converter contained the highest amounts of poisons (P, Zn and Ca) originating from the lubrication oil additives. In contrast, the amount of sulfur in the pre-converters was small. This is due to reversible sulfur poisoning at elevated temperatures, as explained in the previous paragraph. In the main catalysts, the amounts of Ca and Zn were significantly higher than that of P in the front zone, but the amount of these poisons decreased in the axial direction. In the rear zone of the main catalysts, the Zn content was only 20% compared to the front zone. There were no observable differences in the amounts of S and P in the rear and front zones of the main catalysts.

The role of poisoning as a position-dependent deactivation phenomenon was also observed in the activity measurements by changing the direction of the gas flow in the catalyst. The changed flow direction confirmed that the front zone of the vehicle-aged catalyst showed more poisoning (see Table 21). This was observed as an increase in the light-off temperatures and as a decrease in the end conversions of CO, NO and hydrocarbons (Härkönen *et al.* 2001). It can now be said that the causes of deactivation of the vehicle-aged catalyst are primarily thermal ageing and poisoning. Thermal deactivation is dominant at first, but after a few tens of thousands of kilometres of driving (an estimation in this case is approximately 70 000 kilometres), the role of poisoning as a relevant deactivation mechanism will become more relevant (Härkönen *et al.* 2001). The influence of the vehicle's active life is obvious since the surface concentrations of contaminants increased considerably with the rise in consumption of lubrication oil showing a cumulative effect (Angelidis & Sklavounos 1995). Poisoning also explains why the lowest activities were observed in the case of the vehicle-aged catalyst, as mentioned earlier in section 5.6. On the basis of the activity results, it can be concluded that poisoning contributes to approximately one fifth (20%) of the total deactivation in

the case of the vehicle-aged catalyst. The rest is caused by the other reasons of deactivation as reported earlier.

Poisoning of the vehicle-aged catalyst was clearly observed visually, as can be seen in Fig. 47, where the photographs of the vehicle-aged pre-catalyst are shown on different scales. According to the optical microscope, the inlet of the vehicle-aged catalyst had a brown coating on the surface of the topmost washcoat that flaked off quite easily. The chemical analysis of the overlayer material, which was scraped from the inlet region of the vehicle-aged catalyst, showed that the contaminated overlayer contained mainly phosphorus, calcium, oxygen and zinc. According to the chemical analysis, the contaminated overlayer contained mainly $Ca_3(PO_4)_2$.

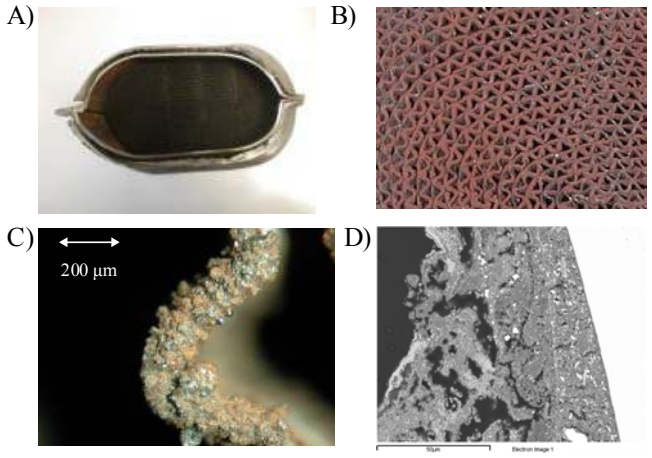

Fig. 47. Visual analysis of the vehicle-aged catalyst (this thesis): A) metallic pre-converter, B) enhanced view of the metallic monolith, C) poisoned channel walls of the monolith, and D) a back-scattered electron image taken at the inlet of the vehicle-aged catalyst. The figures A, B and C are adapted from Härkönen *et al.* (2001).

Figure 48 presents the elemental analysis data from the inlet region of the vehicle-aged catalyst, including a back-scattered electron image and elemental distribution maps (X-ray maps) obtained by EDS. Moving from right to left in the Fig. 48A, the following layers were observed: the metallic foil, the washcoat and the contaminated overlayer. As can be seen in Fig. 48, the surface of the top overlayer of the vehicle-aged catalyst was the poisoned layer. According to the elemental distribution maps (presented in Figures 48 B to F), the poisons were observed as an overlayer on the surface of the vehicle-aged catalyst. The thickness of the poisoned overlayer was approximately 20 micrometres, but according to the SEM analysis, it even had a thickness of 50 micrometres in some areas on the catalyst's surface. Therefore, it can be stated that the poisons were unevenly distributed on the catalyst's surface.

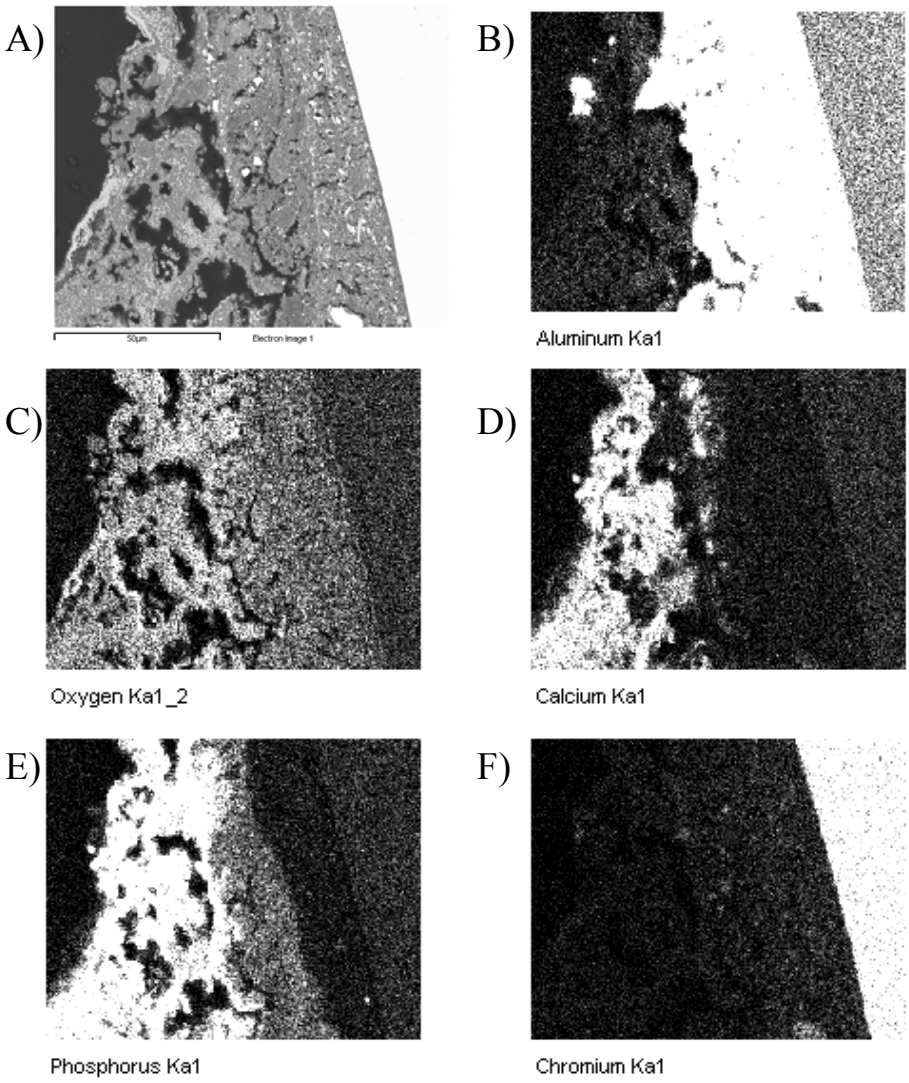

Fig. 48. Elemental analysis (X-ray maps) data taken at the inlet of the vehicle-aged catalyst (magnification 1000x); A) back-scattered electron image showing the metal foil, washcoat and contaminant overlayer; EDS elemental maps of B) Al, C) O, D) Ca, E) P, and F) Cr.

The elemental distribution maps in Fig. 48 show the penetration of phosphorus, and to a lesser extent, penetration of calcium into the upper areas of the washcoat. Based on this visual observation, an assumption of the possible interaction of poisons with the washcoat compounds in the upper parts of the washcoat was made, but no evidence of the formation of cerium (III) phosphates ($CePO_4$ and/or $Ce(PO_3)_3$) and aluminium phosphate ($AlPO_4$) was observed by other characterizations, such as by X-ray diffraction studies.

Furthermore, the lower parts of the washcoat were not contaminated, as observed in Figures 48D and 48E. The elemental poison distribution observed in the SEM-EDS analysis was close to that presented in Table 20. The only exception was Zn, which was not observed in the SEM-EDS analysis.

In Fig. 49, a SEM image (top view) of the poisoned overlayer of the vehicle-aged catalyst (inlet) indicated the porous structure. Poisoning of the vehicle-aged catalyst was also observed by chemical analysis and XPS, as mentioned above. The poisoned overlayer, in particular in the front zone of the catalyst, decreased the catalytic activity, as reported earlier. Furthermore, the lower BET surface areas were observed in the front zone of the vehicle-aged catalyst. This may indicate that the poisoned overlayer of the catalyst blocks the pores to some extent.

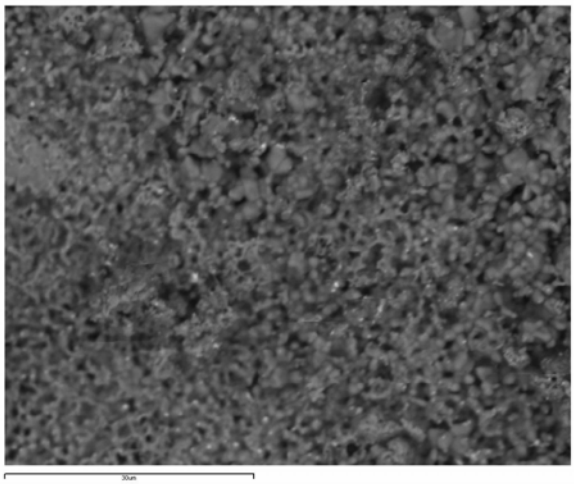

Fig. 49. A top view of a SEM back-scattering image (scale: 30 μm) taken at the inlet of the vehicle-aged catalyst.

It is also possible that the accumulated contaminants in the vehicle-aged catalyst act rather as impurities than as poisons. Such as phosphorus, which has been noted in many earlier studies (Williamson *et al.* 1985, Brett *et al.* 1989), and has no direct interaction with the active metals, but acts as a cumulative fouling mechanism. This affects the catalytic activity by blocking the pores and, therefore, the gas molecules do not reach the catalytically active sites in the catalyst. This also diminishes the mass transfer inside the converter. However, as observed in a SEM-EDS analysis, the contaminants were mainly accumulated on the washcoat surface of the vehicle-aged catalyst and the accumulation inside the washcoat was considerably lower.

In brief, poisoning was a relevant deactivation mechanism of the vehicle-aged catalyst. The vehicle-aged catalyst was poisoned in the axial direction by phosphorus, calcium, and zinc. In particular, the front zone of the catalyst was the most highly poisoned. According to the chemical analysis, the contaminat overlayer on the catalyst's surface

contained phosphates, particularly $Ca_3(PO_4)_2$. Furthermore, the penetration of P and Ca into the upper areas of the washcoat was observed in the SEM-EDS analysis.

5.8 Volatilization and encapsulation of metal particles

The most important and relevant ageing-induced changes in the catalyst are presented in sections 5.1 to 5.7. Additionally, the deactivation of the Pd/Rh catalysts may be due to some other reasons, e.g. the encapsulation of metal particles in the sintered washcoat, or the volatilization of active metals at high ageing temperatures, which will be discussed in this section. The effect of these two as possible deactivation mechanisms is, however, of secondary importance compared to the ageing-induced collapse in surface area, to the sintering of active metals and to ageing-induced solid-solid phase transitions in the catalyst's bulk washcoat.

According to the thermodynamics, when heating the catalyst above a critical temperature, the vapour pressure of metals or metal oxides rises so that significant amounts of material can be transported either to react with the substrate, or into the gas phase where they are lost in the effluent gas streams. This property of volatilization limits the use of active metals as catalysts, and potentially represents the limiting trade-off between high activity and a long, active lifetime independent of the design and structure of the catalyst. (McCarty *et al.* 1999)

First, the volatilization of active metals as a possible deactivation mechanism is considered. Active metals, palladium and rhodium, were added onto the different washcoats, as stated previously. In the fresh catalyst, palladium was not observed on the catalyst's surface, as shown by XPS measurements. However, after high temperature ageings, palladium is found to be present on the catalyst's surface, and as the ageing temperature increased, the amount of palladium on the surface of the catalyst increased. This is clearly observed in the XPS and XRD measurements. Furthermore, according to the XPS results, the amount of Pd on the surface of the catalyst increased in the reductive gas atmosphere as the ageing temperature increased (see Fig. 41). However, based on XRD results, this kind of conclusion could not be drawn. (Lassi *et al.* 2002b, Lassi *et al.* 2002c)

There are two possible interpretations for the observation of Pd on the surface of the catalyst after the ageings. First, the surface of the catalyst may be eroded during the ageing, revealing the Pd metal particles present in the lower areas of the washcoat. However, this does not explain why palladium is concentrated on the catalyst's surface after the reductive ageing, but not after the oxidative ageing. Second, at high ageing temperatures, palladium may become mobile and may be transported to the surface through the washcoat and volatilized into the surrounding gas phase. Therefore, it may be possible that the total amount of palladium in the catalyst diminishes during ageing (Lassi *et al.* 2002b). The transport of Pd to the surface over a distance of couple of tens of microns is quite likely to take place at least partially *via* the gas phase. The vapour pressure of Pd at 1000°C is $\sim 10^{-6}$ Torr and at 1100°C $\sim 10^{-5}$ Torr (Margrave 1967), whereas the vapour pressure of Rh is several orders of magnitude lower. Furthermore, as

indicated earlier in Chapter 3 (Figures 9A and 9B), according to thermodynamic equilibrium calculations, Pd is more volatile than Rh in a 5 vol-% O_2/N_2 atmosphere. In addition, the vapour pressure of metallic palladium is higher than that of PdO, whereas in the case of Rh the behaviour is the reverse. This explains why the amount of Rh remained unchanged during the ageing treatments. On the other hand, it is reasonable to assume that at high ageing temperatures, Pd may be lost *via* volatilization into the gas phase, as will be discussed in the following paragraphs. (Lassi *et al.* 2002b)

One role of the wet analysis (see section 4.3.8) was to provide information on the significance of the volatilization of active metals as a possible deactivation mechanism. According to the ICP-AES results, the Rh content in the washcoat of the fresh catalyst was close to rhodium loading. After the thermal and hydrothermal ageings in the temperature range of 800°–1200°C, equal amounts of rhodium within the measurement accuracy were observed in the catalyst, indicating that Rh has not been volatilized during the ageing treatments. Similarly, the Rh content in the washcoat after engine and vehicle ageings was close to that of the fresh catalyst. Therefore, it can be said that Rh metal particles are sintered in the washcoat, as shown earlier, but Rh is not lost as a result of its volatilization into the gas phase. This is also consistent with the results of other characterization methods where no Rh loss was observed as a result of ageing.

The effect of ageing on Pd metal particles is rather different. The wet analysis confirmed, namely, that the amount of palladium in the aged catalysts differed from that of the fresh catalyst. It can, therefore, be assumed that high temperature ageing-induced changes in the washcoat decreased the amount of palladium in the catalyst. According to the ICP-AES analysis, the amount of Pd in the washcoat of the fresh catalyst was close to palladium loading. The Pd content in the aged catalysts was smaller than that of the fresh catalyst, but no systematically increased loss in Pd content was observed as a function of ageing temperature. The loss of Pd after the ageings was at a maximum of 15%. The only exception was the air/1200°C/3h-aged catalyst in which the loss of Pd was significantly larger compared to other aged catalysts. It was also rather difficult to discover differences in the Pd content of the catalysts between the reductive and oxidative ageings as a function of ageing temperature and therefore, no support for the earlier XPS observations is obtained. Furthermore, after engine bench and vehicle ageings, no significant Pd loss was observed. Therefore, it can be concluded that Pd is most likely lost *via* volatilization into the gas phase as a result of ageing under extreme conditions, as is also expected by thermodynamics, but under the vehicle operating conditions, this is not a significant mechanism of deactivation. It is also rather difficult to draw any reliable conclusions if volatilization of palladium is more pronounced in the reductive ageing atmosphere (as assumed earlier based on XPS results) or not. Therefore, further studies of volatilization; for example, with simplified model catalysts, are needed, and the analytical methods used to determine Pd content in the complex matrix should also be improved.

The vapour phase transport of Pd was also recently discussed by Graham *et al.* (1999), where they considered the role of vapour phase transport within the pore structure of the ceria-zirconia being significant relative to transport *via* surface diffusion. High temperature ageing of ceria-zirconia-supported Pd may result in deep encapsulation of sintered Pd metal particles, affecting the catalytic activity. This phenomenon is also observed on Rh catalysts but not on Pt catalysts. The encapsulated particles cannot participate in catalysis since they are inaccessible to gas-phase molecules. The

encapsulation and incorporation of metal particles in the sintered washcoat after the ageings were also studied by SEM-EDS. Ageing-induced encapsulation of metal particles was observed in a SEM image as an increase in the metal particle size. After the ageing treatments, metal particles are relatively large and probably even more susceptible to encapsulation because of their limited mobility. In a SEM-EDS analysis, palladium was also observed clearly to be concentrated to ceria-zirconia mixed oxide (e.g. in the fresh catalyst) and, therefore, this was considered as a preparation-induced phenomenon rather than as an ageing-induced phenomenon.

In order to understand the microstructural evolution of catalysts upon ageing, especially the incorporation and encapsulation of Rh and Pd metal particles, as presented by Graham *et al.* (1999) and Weng-Sieh *et al*. (1997), more sophisticated characterization methods would be needed. For instance, transmission electron microscopy (TEM) would provide detailed information on metal particle size and shape of active metals after the ageings. However, in this thesis it was not utilized as a characterization tool because the use of TEM technique requires a specific sample preparation. Usually, TEM samples are prepared by scraping the washcoat of the catalyst and crushing the sample to a very fine and thin layer in order to allow the electron beams to penetrate through the sample. This sample preparation destroys the macrostructure of the catalyst and, therefore, in the author's opinion, does not give a representative view of ageing-induced changes in the catalyst. Currently, methods for TEM sample preparation, which do not destroy the macrostructure of the catalyst, are under development. (Polvinen 2002)

5.9 Other aspects on deactivation

In the literature, there are some other aspects on the deactivation of Pd/Rh monoliths, which should also be considered. Some of these aspects were also evaluated in the course of this study and they will be briefly discussed in this section.

At high ageing temperatures, metal-metal or metal-washcoat interactions may become more apparent and can have an effect on the catalytic activity (Bartley *et al.* 1993). The presence of two active metals in the washcoat may lead to the formation of an alloy, as reported by Pitchon *et al.* (1997) and Hu *et al.* (1998). However, the formation of Pd-Rh alloys was not observed in this study after high temperature ageings by the characterization techniques applied. This is due to the preparation of the catalyst by adding the active Pd and Rh metals onto the separate washcoats. Therefore, the interaction of Pd and Rh metals is an unlikely mechanism of deactivation. Instead, the ageing-induced metal-washcoat interactions, in particular the interaction of Rh with alumina to form inactive Rh-aluminates in the washcoat (see section 5.5) is quite likely to occur, but no clear evidence of it was obtained in this work.

Visual observations after the ageings showed that no mechanical damages were seen in the catalysts, but deactivation was visually observed as different colour contrasts in the aged catalysts. In the front area of the vehicle-aged catalyst, blockages were formed as a result of poisoning. The SEM-EDS method was used as an electron optical method for microstructural analyses. In the SEM images, as shown in Figures 50A and 50B, the gray

scale was determined based on the atomic numbers. The heavier the element is, the lighter is the area in the image. According to the SEM back-scattering images, the structure of catalysts was rather heterogeneous, as can be seen in Figures 50A and 50B, and the washcoat was added on the both sides of the metal foil. The washcoat, with a layer thickness of 50 to 60 micrometers, was evenly distributed on the surface of the metal foil. However, in the case of corrugated metal foil, the accumulation of washcoat material was observed at the bottom of the corrugation valleys.

A) B)

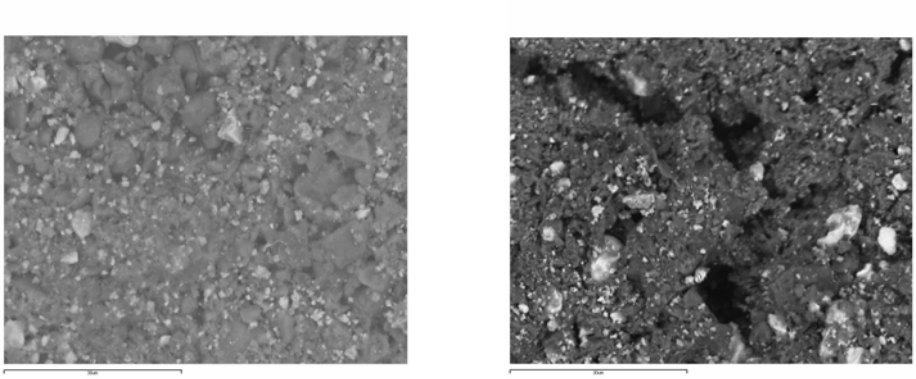

Fig. 50. SEM back-scattering images (scale: 30 μm) of A) fresh and B) air-aged (1200°C) catalysts.

Poisoning and the ageing-induced changes in the chemical states of bulk oxides and active metals have been considered in this thesis. In addition to the washcoat and its properties, it is also relevant to study the role of the metallic substrate, the Fe-Cr-Al foil, in thermal treatments. This is important since the metal foil has to be highly inactive under high temperature ageing conditions. Another significant requirement is also the corrosion tolerance because exhaust gases contain water vapour and other impurities.

In this thesis, the Fe-Cr-Al foil was used as a blank sample and some of the studied ageings were also performed on the foil. Furthermore, the fresh and aged metal foils were characterized similarly to the aged catalysts. This should be noted since the metallic foil compounds (Fe and Cr) may also act as catalyst poisons. It is known that the metallic foil may be oxidized, especially under oxidative conditions at high temperatures, and the formed Fe and/or Cr oxides might incorporate into the washcoat phases. According to the SEM analysis, the metal foil was mainly composed of Fe and Cr, having a few wt-% of Al and also some traces of Ni. As well, small quantities of Fe and Cr in the bottom of the washcoat were observed after the 24 hours of oxidative ageing at 1200°C. At lower ageing temperatures as well as after the reductive ageings, the presence of these metals (and their oxides) was not observed in the lower parts of the washcoat beyond the EDS sensitivity. The oxides of Fe and Cr were detected as being unevenly distributed as a thin layer on the bottom areas of the washcoat. Consequently, at lower ageing temperatures, and after the reductive and inert ageings, this oxidation phenomenon is not present. Instead, after hydrothermal ageings, the oxidation of metal foil was also observed at high ageing temperatures (at 1200°C). This is reasonable due to the presence of oxygen. It can

now be said that the oxidation of metal foil is not a significant phenomenon of the ageing conditions studied in this thesis and, therefore, its role has been disregarded. Furthermore, similar observations of the oxidation of metal foil were made in the case of uncoated metal foil, but at lower temperatures, at around 1000°–1100°C. Therefore, the washcoat clearly prevents the oxidation of the metal foil.

Poisoning by carbonaceous species (coke formation) is often referred to as a significant deactivation mechanism among the combustion catalysts (Marécot *et al.* 1998, Bartholomew 2001). However, the high-temperature three-way catalysts, as examined in this thesis, work under temperatures where the possible carbon deposits originating from exhaust gases (CO and hydrocarbons) are oxidized. Furthermore, no evidence of coke formation is observed in characterizations of engine-aged and vehicle-aged pre-catalysts. Thus, it is reasonable to conclude that deactivation by coke formation is not an essential deactivation mechanism under the extreme operating conditions studied.

6 Deactivation correlations

This Chapter will give the integration of the results as well as the evaluation of the deactivation correlation between laboratory scale and engine bench/vehicle ageings. The role of ageing temperature, atmosphere and time are considered in particular.

6.1 Integration of results

Based on the results presented in this thesis, the deactivation of Pd/Rh monoliths was caused by several mechanisms. The aged catalysts were clearly deactivated, which was observed in the activity measurements as significantly lower activities (higher light-off temperatures of CO and NO) compared to the fresh catalyst. However, all the aged catalysts were still active in the removal of major pollutants, which was observed as high final conversions (conversion values determined at 400°C), which were, in general, over 80% for CO and NO. Furthermore, the engine-aged and vehicle-aged catalyst systems reached the Euro IV emission level limits and, therefore, converted NO_X, HC and CO well in a European test driving cycle, as reported in Härkönen *et al.* (2001).

In Fig. 51, a short summary of ageing-induced phenomena, as found in this thesis, is presented. The main reasons for the deactivation of aged catalysts were the sintering of active metal particles in the washcoat and the collapse in the surface area and pore structure of the catalyst. The results of H_2 chemisorption gave information on the ageing-induced loss in the active metal surface area, which led to the increased metal particle size. The loss of metal surface area was associated with the sintering of active metals in the washcoat, in particular the Rh metal particles in the washcoat which were sintered at a high ageing temperature, and which was verified by XPS measurements. NO-TPD results showed the ageing-induced loss in the amount of active surface sites of the catalysts, which was consistent with chemisorption results. Furthermore, based on XPS and XRD results, evidence of the possible active metal loss *via* volatilization into the gas phase was obtained. In particular, this was one mechanism of deactivation for Pd metal particles which became mobile as the ageing temperature increased, diffused through the washcoat

onto the surface and volatilized into the surrounding gas phase under extreme ageing conditions.

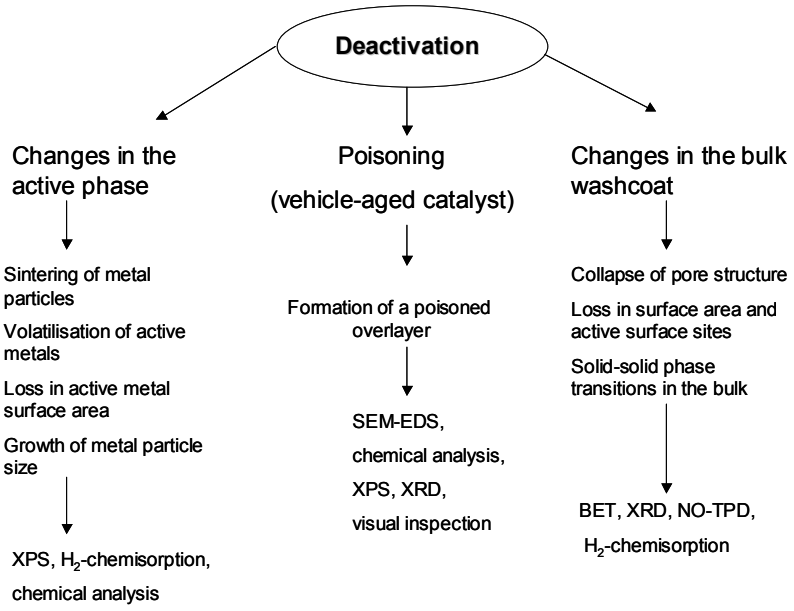

Fig. 51. Ageing-induced structural and chemical changes in the catalyst.

Ageing also induced structural and chemical changes in the bulk washcoat, as seen in Fig. 51. These changes included the collapse in pore structure and the loss in surface area, the increased pore size and the crystal growth, the sintering of the oxides in the washcoat, and the ageing-induced solid-solid phase transformations in the bulk washcoat. These phenomena were not separate reasons for deactivation, but closely associated with each other. The collapse in the pore structure and the loss in surface area were associated with the sintering of the high surface area metal oxides (γ-Al_2O_3, CeO_2) in the bulk washcoat. It should also be noted that these pure oxides formed a new crystalline phase, $CeAlO_3$, as a result of ageing. The formation of $CeAlO_3$ was more pronounced after the reductive and inert ageings and it prevented the phase transformation from γ-Al_2O_3 to low-surface area α-Al_2O_3. This also explained why the surface areas remained higher after the reductive and inert ageings compared to the oxidative ageing. Furthermore, $Ce_XZr_{1-X}O_2$ mixed oxides underwent the ageing induced decomposition, which led to the formation of new mixed oxides with the molar compositions 30 mol-%< Ce < 70 mol-%. In addition to ageing-induced changes in the active phase and bulk material, the vehicle-aged catalyst was also deactivated by poisoning. The accumulation of poisons was observed in a SEM-EDS analysis as a thin, contaminated overlayer, which was mostly composed of calcium, phosphorus and oxygen. All the deactivation phenomena led to a loss in the catalytic activity, as mentioned earlier.

Ageing has induced several changes in the catalyst, and this has been shown in this thesis. These changes were critical to the catalyst's performance, since the changes are typically irreversible and the original activity of the catalyst is not restored after the ageings. As indicated, the reasons of deactivation of Pd/Rh monoliths found in this thesis were commonly known. Therefore, any new insight of deactivation in this respect is not provided. Instead, a new insight of deactivation correlation can be presented in this thesis. Although the ageing-induced phenomena in the catalyst are quite evident, it is rather difficult to clearly discriminate between the impact of some separate deactivation mechanisms.

Ageing temperature, atmosphere and time were all important variables in the deactivation of the catalysts. Deactivation is always a function of time, but in this study the role of ageing atmosphere and high ageing temperature was clearly pronounced compared to ageing time. Ageing temperature was an important variable since high ageing temperatures favour the sintering of active metals and washcoat materials that can be regarded as significant deactivation mechanisms in this case. Temperature also affected the catalytic activity and the ageing-induced structural changes observed in the bulk washcoat. Catalysts treated at high ageing temperatures were more deactivated than those aged at lower ageing temperatures, as expected. This was observed in the activity measurements, where the light-off temperatures increased systematically as a function of ageing temperature.

Based on NO-TPD results, ageing temperature had an effect on the desorption of NO. Thermal ageing at temperatures T>800°C at least partly destroyed the higher temperature desorption peak of NO. This peak originated from NO-active metal and NO-Al_2O_3 interactions and so this supports the ageing-induced sintering of active metals in the washcoat. Ageing temperature also affected the crystalline structure of catalysts. In the reductive and oxidative atmospheres, the crystal growth started after ageings at around 900°C. Ageing temperature was an important factor on the catalyst's activity and stability. The increase in CO and NO light-off temperatures (decrease in catalytic activity) was proportional to ageing temperature. The activities of catalysts decreased as a function of ageing temperature. This was related to the loss of the active metal area.

In addition to ageing temperature, gas phase composition also affected the catalytic activity and structural properties. Ageings decreased the catalyst specific surface areas and pore volumes which correlated well with the changes observed by other characterization methods. According to BET results, ageing in the reductive atmosphere was not so strong compared to ageing in air. Thus pore sizes were clearly larger in the oxidative atmosphere. Furthermore, in the presence of water vapour, sintering phenomena were accelerated. Catalytic activities also remained high if ageing was carried out in the reductive or inert atmospheres, rather than in the presence of the oxidative gas phase. Ageing atmosphere either accelerated or inhibited phase transitions in the bulk material, as observed by XRD measurements, and it had an influence on the chemical states of active metals, as shown by XPS.

6.2 Deactivation correlations

The most notable results presented in this thesis are based on the evaluation of the effects of ageing atmosphere, temperature and time. Several surface characterizations were utilised and the results were integrated, as reported in previous sections, to present and evaluate the deactivation correlations between laboratory scale ageing and engine bench/vehicle ageings.

Deactivation of the engine-aged and vehicle-aged catalysts was a combination of several deactivation mechanisms. As indicated in Chapter 5, thermally-induced deactivation was dominant in both cases. According to the characterization results, the engine-aged catalyst can be considered as thermally deactivated because the accumulation of poisons on the catalyst surface was only minimal, as observed by several characterizations. On the other hand, the vehicle-aged catalyst had also been clearly deactivated by poisoning. Therefore, it is impossible to present a precise deactivation correlation between laboratory scale ageing and vehicle ageing exclusively on the basis of this study, where only the thermally aged catalysts were used as reference catalysts. However, in this case, deactivation correlations between laboratory scale ageing and vehicle ageing can also be found, if the role of poisoning is excluded and only the effects of ageing temperature, atmosphere and time are taken into account.

As indicated in this work, the engine-aged catalyst corresponds closely to the laboratory scale ageing in the reductive ageing atmosphere in the presence of water vapour. The results of all the characterizations support this thesis. First, ageings induced changes in the chemical states of Rh, as substantiated by XPS, and are similar to those observed after the reductive ageing. Second, in the NO-TPD measurements, close-to-similar desorption behaviour of NO and other desorption products was observed. Furthermore, the ageing-induced solid-solid phase transformations, such as the formation of $CeAlO_3$ and $LaAlO_3$, were also observed after high temperature ageing in the reductive atmosphere, and these XRD diffractograms were very much alike to those observed after the engine bench ageing. According to the NO-TPD measurements, H_2O-H_2/1100°C-aged and H_2O-H_2/1200°C-aged catalysts showed similar desorption behaviour of NO than the engine-aged catalyst. Furthermore, the BET value of the engine-aged catalyst (22 m^2/g) corresponded well to the BET value of H_2O-H_2/1100°C-aged catalyst. Finally, according to the activity measurements, the catalytic activity of the engine-aged catalyst was close to the activity of H_2O-H_2/1200°C-aged catalyst.

In the case of vehicle ageing, the deactivation correlations were not self-evident because the ageing phenomenon on the vehicle-aged catalyst was a combination of thermal and chemical deactivation, and only the effects of the former were studied extensively in this thesis. In the vehicle ageing, thermal deactivation was dominant at first, but as a result of increased driving kilometres, the role of poisoning increased, which is notable for the catalyst's system efficiency. In the SEM-EDS analysis, the poisoned overlayer was observed on the catalyst's surface after 100 000 kilometres of driving. Especially, as shown by the chemical analysis, the front zones of the vehicle-aged catalyst were poisoned by phosphorus, zinc and calcium deposits. The poisoning of the vehicle-aged catalyst was observed as lower activities compared to thermally aged catalysts. According to the characterization results, the vehicle-aged catalyst corresponds

to catalysts thermally aged in the reductive gas phase (10 vol-% H_2O, 5 vol-% H_2 and N_2 balance), if the role of poisoning is excluded. In effect, the only clear differences between the engine-aged and vehicle-aged catalysts were in the amounts of accumulated poisons and, therefore, lower activities and BET surface areas were observed in the latter case.

In this thesis, deactivation correlations are presented based on the effects of ageing temperature, atmosphere and time. These correlations gave evidence that laboratory scale ageings in air do not correspond to ageing in an engine-bench, nor the ageing on-road. Therefore, based on the results, it can be stated that there is a need for further development of laboratory scale ageing cycles, which are typically based on air ageing.

6.3 Evaluation and utilization of the results

In this section, the author will discuss the evaluation of the present study, its reliability and the possible omissions if so noted. As well, the evaluation of the applicability of characterization techniques considered in this thesis is also presented. As reported earlier, the characterization techniques used in this study were selected mainly based on their availability and suitability and the informative aspects of the method. Based on the experience acquired during the course of this work, it can be said that characterization methods applied in this thesis were suitable tools for catalyst thermal deactivation studies. As indicated, correlations between the results obtained by characterization methods were found. This enabled the interpretation of data and gave valuable information on the mechanisms of deactivation. Furthermore, characterization methods were well controlled, the repeatability was high and clear differences between the fresh and aged catalysts were observed. However, this required both the development of the measurement method as well as the sample pre-treatment work behind each of the characterization methods, since most of them were unsuitable for this study without the methodology development in the early phase of this work. In summary, it can be stated that the deactivation phenomena of three-way catalysts cannot be understood on the basis of some separate results of different catalyst characterization techniques. Several properties, such as catalyst chemistry, operating conditions and catalyst history affect a catalyst's performance. A broader view of the deactivation phenomena is obtained by combining several surface characterization techniques.

The results presented in this thesis are mainly based on laboratory scale ageings because ageings on-road are expensive and slow, as mentioned earlier, and so are not useful for rather fast testing of the catalyst's performance. Therefore, there are some limitations in the utilization of the results of this work. Primarily, the industrially manufactured catalysts have a very complex structure, as indicated. There are several ageing-induced phenomena present in the catalyst and many compounds may interact with each other. Thus, the investigation of the effect of some separate variable –ageing atmosphere, temperature and time– on the physical and chemical changes in the catalyst is complex. Additionally, it is rather difficult to evaluate the contribution of separate deactivation mechanisms, e.g. the role of sintering of active metals, phase transformations in the bulk or volatilization of metals, and so, to draw straightforward

conclusions. On the other hand, it should be kept in mind that the deactivation correlation should be found in real catalysts and, therefore, it is meaningful to use catalysts which have close to a commercial structure, as was done in this thesis.

The results of this thesis can be utilized and applied in the research and development stage of the catalyst's manufacturing. In parallel with and as a close continuation of this work, but outside the scope of this thesis, Kemira Metalkat Oy is currently modifying the laboratory scale ageing procedure. In this development work of the laboratory scale ageing procedure, the results presented in this thesis can be utilized and the effects of ageing temperature, atmosphere and time are taken into account.

6.4 Requirements for further research

The results of this thesis have shown that there is a clear need for a further development of laboratory scale ageing cycle which corresponds to the ageing-induced changes in the catalyst either after the engine bench ageing, or under vehicle operation. The results of this thesis can be utilized in this development work which, in the author's opinion, requires the testing of a number of different catalyst compositions in order to guarantee the reliability of the ageing cycle and more realistic models of deactivation. This development and testing work has been initiated in parallel with this thesis, but outside the scope of it, as mentioned above.

In the course of this study, several characterization techniques were used to examine ageing-induced changes in the catalyst, and as shown in this work deactivation of a TWC cannot be understood on the basis of some separate characterization technique. Many properties affect the catalyst's performance and the integration of the results of several characterization techniques are required for the fundamental understanding of the deactivation phenomena of the three-way catalysts. In the future, it would be informative to utilize TEM (Transmission Electron Microscopy) to study ageing-induced changes in the active metals. TEM would provide detailed information e.g. on metal particle size and shape of active metals after the ageings, and thus some additional information on the deactivation mechanisms of Pd/Rh monoliths. On the other hand, it would give few new insights into the deactivation correlation between laboratory scale ageings and engine bench/vehicle ageings.

Furthermore, the use of Diffuse Reflectance Fourier Transform Infrared Spectroscopy (DRIFT) would increase the information on the adsorption of NO on catalytically active sites on the surface (Keiski *et al.* 1995), and so assist the interpretation of the NO-TPD spectra. In this respect, characterizations were carried out with simplified model catalysts, which helped with the interpretation of the origin of desorption peaks of NO. The additional information obtained from the DRIFT technique would increase the understanding of deactivation phenomena at the molecular level, but it provides little or no new information concerning the deactivation correlations.

7 Summary and conclusions

Throughout the course of this work and the writing of this thesis, three principal goals have been dominant. These were, and still are: (1) The knowledge of the deactivation mechanisms of Pd/Rh monoliths under different ageing conditions, (2) The deactivation correlation between laboratory scale ageing and engine bench and vehicle ageings, and (3) The utilization and the evaluation of the results of the first two main goals and the critical evaluation of ageing cycles. The attainment of these goals enables, at least partly, the development of a new laboratory scale ageing cycle, which corresponds to the ageing-induced changes in the catalyst during vehicle operation.

As presented in this thesis, the deactivation of Pd/Rh monoliths after the ageings is caused by several mechanisms, such as the sintering of active metals, the collapse in pore structure and the solid-solid phase transformations in the bulk washcoat. As a result of high temperature ageing, Rh particles in the washcoat were sintered and the active metal surface area of catalysts was collapsed. The surface area of catalysts decreased and pore sizes increased as a result of ageing. These phenomena were clearly enhanced in the oxidative gas phase as well as in the presence of water vapour. High temperature ageings also induced solid-solid phase transformations in the bulk washcoat, which were observed as a formation of $CeAlO_3$ and $LaAlO_3$ in the washcoat. The solid-solid phase transformations prevented the formation of low surface area α-Al_2O_3, which was mostly responsible for the surface area loss. This explained why the specific surface areas of catalysts remained higher in the presence of hydrogen. Furthermore, ageings induced the decomposition of Ce- and Zr- rich $Ce_XZr_{1-X}O_2$ mixed oxides, which led to a formation of new mixed oxides with molar compositions of 30 wt-% < Ce < 70 wt-%. After the vehicle ageing, the front zone of the catalyst was also poisoned, but poisoning in this case contributed only to one fifth of the total deactivation, as shown in the activity measurements.

In this thesis, an approach has been introduced for the deactivation correlation between the laboratory scale ageings and the engine and vehicle ageings. As indicated, the laboratory scale ageing in the reductive ageing atmosphere corresponds best to the engine bench and vehicle ageings. This is reasonable since the engine ageing cycle consists of both stoichiometric and rich air-to-fuel ratios. During vehicle operation, the gas phase composition fluctuates between lean and rich conditions. A deactivation

correlation after oxidative (air) ageing, as commonly used in a catalyst's laboratory scale testing, is also possible to discover on the basis of the activity tests and BET measurements. However, this correlation does not correspond to the ageing-induced chemical and physical changes in the catalyst that were observed after engine bench and vehicle ageings. Therefore, the commonly-used laboratory scale ageing in air is not a sufficiently reliable ageing procedure in the evaluation of the deactivation of Pd/Rh monoliths, as substantiated in this thesis.

The conclusions that can be drawn from the results of the current work can be presented as the following theses in support of the empirical evidence:

1. The deactivation of a Pd/Rh monolith is a combination of several ageing phenomena.
2. Temperature, gas phase composition and exposure time are essential variables in the deactivation of a Pd/Rh three-way catalyst.
3. The accelerated laboratory scale ageing in air does not correspond to ageing-induced changes in the catalyst under vehicle operation.
4. A deactivation correlation between the laboratory scale ageing and the engine bench ageing can be presented as a function of ageing temperature and atmosphere and time. When considering the deactivation correlation between the laboratory scale ageing and the vehicle ageing, poisoning has a notable role, which should also be taken into account.

In addition to the scientific contribution, the results of the current work can be utilized in the further development of the laboratory scale ageing cycles, which correspond to real ageing conditions in an engine bench or during vehicle operation. This further enables fast testing procedures in the research and development stage of catalyst's manufacturing and it would also assist in making significant cost reductions in catalyst testing.

References

Acke F (1998) Mechanistic aspects on the heterogeneous reduction of nitric oxide: Roles of substrate, reductive agent and oxygen. Doctoral Thesis. Göteborg University, Department of Inorganic Chemistry.

Ahola J & Lassi U (2001) Katalyytin deaktivoituminen ja sen havainnointi pakokaasujen puhdistuksessa. TEKES, Promotor moottoritekniikan tutkmiusohjelma, 171-183.

Ahola J, Lassi U & Kangas J (2002) Catalyst deactivation and diagnostics. TEKES, Promotor moottoritekniikan tutkmiusohjelma, 37-54.

Altman EI & Gorte RJ (1988) A temperature-programmed desorption study of NO on Rh particles supported on α-Al_2O_3 {0001}. Journal of Catalysis 113: 185-192.

Angelidis TN & Sklavounos SA (1995) A SEM-EDS study of new and used automotive catalysts. Applied Catalysis A: General 133: 121-132.

Angelidis TN & Papadakis VG (1997) Partial regeneration of an aged commercial automotive catalyst. Applied Catalysis B: Environmental 12: 193-206.

Angove DE & Cant NW (2000a) Position dependent phenomena during deactivation of three-way catalytic converters on vehicles. Catalysis Today 63: 371-378.

Angove DE, Cant NW, French DH & Kinealy K (2000b) The effect of temperature on a ceria-alumina-baria cordierite monolith combination under oxidizing and reducing conditions. Applied Catalysis A: General 194-195: 27-34.

Anon (1988) Q.T.M.D. User manual. Carlo Erba Instruments, Milan, Italy. 78 p.

Anon (1992) Coulter Omnisorp 100/360 Series Reference Manual. Coulter Electronics Limited, Luton, England. 159 p.

Armor JN (1992) Environmental catalysis. Applied Catalysis B: Environmental 1: 221-256.

Atkins PW (1995) Physical Chemistry. Oxford University Press, Oxford.

Barbier J & Duprez D (1994) Steam effects in three-way catalysis. Applied Catalysis B: Environmental 4: 105-140.

Bartholomew CH (1984) Chemical Engineering 12: 97.

Bartholomew CH (2001) Mechanisms of catalyst deactivation. Applied Catalysis A: General 212: 17-60.

Bartholomew CH (1997) Sintering and redispersion of supported metals: perspectives from the literature of the past decade. In: Bartholomew CH & Fuentes GA (eds.) Catalyst deactivation 1997, Elsevier, Amsterdam, Studies in Surface Science and Catalysis Vol. 111.

Bartholomew CH & Fuentes GA (eds.) (1997) Catalyst deactivation 1997, Elsevier, Amsterdam, Studies in Surface Science and Catalysis Vol. 111.

Bartley GJJ, Shady PJ, D'Aniello MJ, Chandler GR, Brisley RJ & Webster DE (1993) Advanced three-way catalyst formulations for high temperature applications. SAE Technical Paper Series 930076: 1-13.

Bhattacharya AK, Pyke DR, Walker GS & Werrett CR (1997) The surface reactivity of different aluminas as revealed by their XPS C1s spectra. Applied Surface Science 108: 465-470.
Beck DD & Carr CJ (1993) Effects of high-temperature aging on the dispersion of Rh/Al_2O_3. Journal of Catalysis 144(1): 296-310.
Beck DD, Krueger MH, Monroe DR, Upton DJ, Lendway JM & Smith DR (1992) Improvement of laboratory tests for evaluating three-way catalyst activity. SAE Technical Paper Series 920099: 1-12.
Beck DD & Sommers JW (1995) Impact of sulfur on the performance of vehicle-aged palladium monoliths. Applied Catalysis B: Environmental 6(2): 185-200.
Beck DD, Sommers JW & DiMaggio CL (1997a) Axial characterization of catalytic activity in close-coupled lightoff and underfloor catalytic converters. Applied Catalysis B: Environmental 11: 257-272.
Beck DD, Sommers JW & DiMaggio CL (1997b) Axial characterization of oxygen storage capacity in close-coupled lightoff and underfloor catalytic converters and impact of sulfur. Applied Catalysis B: Environmental 11: 273-290.
Becker ER & Watson RJ (1998) Future trends in automotive emission control. SAE Technical Paper Series 980413: 11-17.
Bedrane S, Descorme C & Duprez D (2002a) Towards the comprehension of oxygen storage processes on model three-way catalysts. Catalysis Today 73: 233-238.
Bedrane S, Descorme C & Duprez D (2002b) Investigation of the oxygen storage process on ceria and ceria-zirconia supported catalysts. Catalysis Today 75: 401-405.
Bernal S, Calvino JJ, Cifredo GA, Gatica JM, Perez Omil JA & Pintado JM (1993) Hydrogen chemisorption on ceria: influence of the oxide surface area and degree of reduction. J. Chem. Soc. Faraday Trans. 89: 3499-3505.
Bernal S, Calvino JJ, Cauqui MA, Gatica JM, Larese C, Perez Omil JA & Pintado JM (1999) Some recent results on metal/support interaction effects in NM/CeO_2 (NM: noble metal) catalysts. Catalysis Today 50: 175-206.
Bird RB, Stewart WE & Lightfoot EN (1960) Transport phenomena. John Wiley & Sons, Inc., New York.
Bogdanchikova NE, Fuentes S, Avalos-Borja M, Farías MH, Boronin A & Díaz G (1998) Structural properties of Pd catalysts supported on Al_2O_3-La_2O_3 prepared by sol-gel method. Applied Catalysis B: Environmental 17: 221-231.
Borg HJ, Reijerse JFC, van Santen RA & Niemantsverdriet JW (1994) The dissociation kinetics of NO on Rh(111) as studied by temperature programmed static secondary ion mass spectrometry and desorption. J. Chem. Phys. 101(11): 10052-10063.
Bosteels D & Searles RA (2002) Exhaust emission catalyst technology: New challenges and opportunities in Europe. Platinum Metals Rev. 46 (1): 27-36.
Botas JA, Gutiérrez-Ortiz MA, González-Marcos MP, González-Marcos JA & González-Velasco JR (2001) Kinetic considerations of three-way catalysis in automobile exhaust converters. Applied Catalysis B: Environmental 32: 243-256.
Bozo C, Guilhaume N, Garbowski E & Primet M (2000) Combustion of methane on CeO_2-ZrO_2 based catalysts. Catalysis Today 59: 33-45.
Bozo C, Gaillard F & Guilhaume N (2001) Characterisation of ceria-zirconia solid solutions after hydrothermal ageings. Applied Catalysis A: General 220: 69-77.
Brett PS, Neville AL, Preston WH and Williamson J (1989) An investigation into lubricant related poisoning of automotive three-way catalysts and lambda sensors. SAE Technical Paper Series 890490: 1-12.
Bunluesin T, Gorte RJ & Graham GW (1997) CO oxidation for the characterization of reducibility in oxygen storage components of three-way automotive catalysts. Applied Catalysis B: Environmental 14: 105-115.
Bunluesin T, Gorte RJ & Graham GW (1998) Studies of the water-gas-shift reaction on ceria-supported Pt, Pd, and Rh: implications for oxygen-storage properties. Applied Catalysis B: Environmental 15: 107-114.
Burch R, Loader PK & Cruise NA (1996) An investigation of the deactivation of Rh/alumina catalysts under strong oxidising conditions. Applied Catalysis A: General 147(2): 375-394.

Butt JB & Petersen EE (1988) Activation, deactivation and poisoning of catalysts. Academic Press, Inc., New York.
Carol LA, Newman NE & Mann GS (1989) High temperature deactivation of three-way catalyst. SAE Technical Paper Series 892040.
Chin AA & Bell AT (1983) Kinetics of NO decomposition on silica-supported rhodium. Journal of Physical Chemistry 87: 3700-3706.
Ciuparu D, Bensalem A & Pfefferle L (2000) Pd-Ce interactions and adsorption properties of palladium: CO and NO TPD studies over Pd-Ce/Al_2O_3 catalysts. Applied Catalysis B: Environmental 16: 241-255.
Colón G, Pijolat M, Valdivieso F, Vidal H, Kašpar J, Finoccjio E, Daturi M, Binet C, Lavalley JC, Baker RT & Bernal S (1998) Surface and structure characterization of $Ce_XZr_{1-x}O_2$ CEZIRENCAT mixed oxides as potential three-way catalyst promoters. J. Chem. Soc., Faraday Trans., 94: 3717-3726.
Colón G, Valdivieso F, Pijolat M, Baker RT, Calvino JJ & Bernal S (1999) Textural and phase stability of $Ce_XZr_{1-x}O_2$ mixed oxides under high temperature oxidising conditions. Catalysis Today 50: 271-284.
Cotton FA & Wilkinson G (1988) Advanced inorganic chemistry. Wiley-Interscience, New York, p. 880.
Cuif J-P, Blanchard G, Touret O, Seigneurin A, Marczi M & Quéméré E (1997) (Ce, Zr)O_2 solid solutions for three-way catalysts. SAE Technical Paper Series 970463: 1-13.
Cuif J-P, Deutsc S, Marczi M, Jen H-W, Graham GW, Chung W & McCabe RW (1998) High temperature stability of ceria-zirconia supported Pd model catalysts. SAE Technical Paper Series 980668.
Culley SA, McDonnell TF, Ball DJ, Kirby CW & Hawes SW (1996) The impact of passenger car motor oil phosphorus levels on automotive emissions control systems. SAE Technical Paper Series 961898: 13-21.
Cybulski A & Moulijn JA (1994) Monoliths in heterogeneous catalysis. Catal. Rev. –Sci. Eng. 36(2): 179-270.
Datye AK, Bravo J, Nelson TR, Atanasova P, Lyubovsky M & Pfefferle L (2000) Catalyst microstructure and methane oxidation reactivity during the Pd↔PdO transformation on alumina supports. Applied Catalysis A: General 198: 179-196.
Di Monte R, Fornasiero P, Kašpar J, Rumori P, Gubitosa G & Graziani M (2000) Pd/$Ce_{0.6}Zr_{0.4}O_2$/Al_2O_3 as advanced materials for three-way catalysts part 1. Catalyst characterisation, thermal stability and catalytic activity in the reduction of NO by CO. Applied Catalysis B: Environmental 24: 157-167.
Directive 98/69/EC. Emission standards: European Union. Cars and light trucks. http://www.dieselnet.com/standards/eu/ld.html (20.8.2002).
Directive 98/70/EC. Emission standards: European Union. Cars and light trucks. http://www.dieselnet.com/standards/eu/ld.html (20.8.2002).
Falconer JL & Schwarz JA (1983) Temperature-programmed desorption and reaction: Applications to supported catalysts. Catal. Rev.-Sci. Eng. 25(2): 141-227.
Fally F, Perrichon V, Vidal H, Kašpar J, Blanco G, Pintado JM, Bernal S, Colón G, Daturi M & Lavalley JC (2000) Modification of the oxygen storage capacity of CeO_2-ZrO_2 mixed oxides after redox cycling aging. Catalysis Today 59: 373-386.
Farrauto RJ & Heck RM (1999) Catalytic converters: state of the art and perspectives. Catalysis Today 51: 351-360.
Farrauto RJ & Heck RM (2000) Environmental catalysis into the 21th century. Catalysis Today 55: 179-187.
Farrauto RJ, Hobson MC, Kennelly T & Waterman EM (1992) Catalytic chemistry of supported palladium for combustion of methane. Applied Catalysis A: General 81: 227-237.
Farrauto RJ, Lampert JK, Hobson MC & Waterman EM (1995) Thermal decomposition and reformation of PdO catalysts; support effects. Applied Catalysis B: Environmental 6: 263-270.
Fernández-García M, Martínez-Arias A, Iglesias-Juez A, Hungría AB, Anderson Ja, Conesa Jc & Soria J (2001) New strategies for the improvement of automobile catalysts. International Journal of Molecular Sciences 2: 251-262.

Ferrandon M, Ferrand B, Björnbom E, Klingstedt F, Kalantar Neyestaki A, Karhu H & Väyrynen J (2001) Copper Oxide–Platinum/Alumina Catalysts for Volatile Organic Compound and Carbon Monoxide Oxidation: Synergetic Effect of Cerium and Lanthanum. Journal of Catalysis 202: 354-366.

Fierro JLG, Palacios JM & Tomas F (1988) An analytical SEM and XPS study of platinum-rhodium gauzes used in high pressure ammonia burners. Surface and Interface Analysis 13: 25-32.

Flynn PC, Wanke SE & Turner PE (1975) The limitation of the transmission electronic microscopy for characterisation of supported metal catalysts. Journal of Catalysis 33(2): 233-249.

Fornasiero P, Di Monte R , Ranga Rao G, Kašpar J, Meriani, S, Trovarelli, A & Graziani M (1995) Rh-loaded CeO_2-ZrO_2 solid solutions as highly efficient oxygen exchangers: dependence of the reduction behavior and the oxygen storage capacity on the structural properties. Journal of Catalysis 151: 168-177.

Fornasiero P, Balducci G, Di Monte R, Kašpar J, Sergo V, Gubitosa G, Ferrero A & Graziani M (1996) Modification of the redox behaviour of CeO_2 induced by structural doping with ZrO_2. Journal of Catalysis 164: 173-183.

Fornasiero P, Kašpar J, Sergo V & Graziani M (1997) Redox behaviour of high surface area Rh-loaded $Ce_{0.5}Zr_{0.5}O_2$ mixed oxide. Journal of Catalysis 167:576-580.

Fornasiero P, Kašpar J, Sergo V & Graziani M (1999) Redox behaviour of high-surface-area Rh-, Pt-, and Pd-loaded $Ce_{0.5}Zr_{0.5}O_2$ mixed oxides. Journal of Catalysis 182: 56-69.

Forzatti P & Lietti L (1999) Catalyst deactivation. Catalysis Today 52: 165-181.

Froment GF (2001) Modeling of catalyst deactivation. Applied Catalysis A: General 212: 117-128.

Froment GF & Bischoff KB (1990) Chemical Reactor Analysis and Design, John Wiley & Sons., New York.

Fuentes GA & Gamas ED (1991) In: Bartholomew CH & Butt JB (eds.) Catalyst deactivation 1991, Elsevier, Amsterdam, Studies in Surface Science and Catalysis.

Fuentes GA & Salinas-Rodriguez E (1997) Asymptotic behavior during sintering of supported catalysts. In: Bartholomew CH & Fuentes GA (eds.) Catalyst deactivation 1997, Elsevier, Amsterdam, Studies in Surface Science and Catalysis Vol. 111.

Fuentes S, Bogdanchikova N, Avalos-Borja M, Boronin A, Farías MH, Díaz G, Cortes AG & Barrera A (2000) Structural and catalytic properties of Pd/Al_2O_3-La_2O_3 catalysts. Catalysis Today 55: 301-309.

Funabiki M & Yamada T (1988) A study on three-way conversion catalyst. Thermal deactivation and improvement. SAE Technical Paper Series 881684.

Gasser RPH (1985) An introduction to chemisorption and catalysis by metals. Clarendon Press, Oxford.

Gitzen WH (1970) Alumina as a ceramic material, American Ceramics Society, Columbus.

González-Velasco JR, Entrena J, González-Marcos JA, Gutiérrez-Ortiz JI & Gutiérrez-Ortiz MA (1994) Preparation, activity and durability of promoted platinum catalyst for automotive exhaust control. Applied Catalysis B: Environmental 3: 191-204.

González-Velasco JR, Gutiérrez-Ortiz MA, Marc J-L, Botas AJ, González-Marcos, MP & Blanchard G (1999) Contribution of cerium/zirconium mixed oxides to the activity of a new generation of TWC. Applied Catalysis B: Environmental 22: 167-178.

González-Velasco JR, Gutiérrez-Ortiz MA, Marc J-L, Botas AJ, González-Marcos, MP & Blanchard G (2000a) Effects of redox thermal treatments and feedstream composition on the activity of Ce/Zr mixed oxides for TWC applications. Applied Catalysis B: Environmental 25: 19-29.

González-Velasco JR, Gutiérrez-Ortiz MA, Marc J-L, Botas AJ, González-Marcos, MP & Blanchard G (2000b) Catalytic activity study of ceria-zirconia mixed oxides submitted to different aging treatments under simulated exhaust gases. Ind. Eng. Chem. Res. 39: 272-276.

González-Velasco JR, Botas AJ, Ferret R, González-Marcos MP, Marc J-L & Gutiérrez-Ortiz MA (2000c) Thermal aging of Pd/Pt/Rh automotive catalysts under a cycled oxidizing/reducing environment. Catalysis Today 59: 395-402.

González-Velasco JR, Gutiérrez-Ortiz MA, Marc J-L, González-Marcos MP & Blanchard G (2001) Selectivity of high surface area $Ce_{0.68}Zr_{0.32}O_2$ for the new generation of TWC under environments with different redox character. Applied Catalysis B: Environmental 33: 303-314.

Graham GW, Jen HW, Chun W & McCabe RW (1999) High-temperature-aging-induced encapsulation of metal particles by support materials: Comparative results for Pt, Pd, and Rh on cerium-zirconium mixed oxides. Journal of Catalysis 182: 228-233.

Graham GW, Jen HW, McCabe RW, Straccia AM & Haack LP (2000) Characterization of model automotive exhaust catalysts: Pd on Zr-rich ceria-zirconia supports. Catalysis Letters 67: 99-105.

Gunter PLJ, Niemantsverdriet JW, Ribeiro FH & Somorjai GA (1997) Surface science approach to modelling supported catalysts. Catal. Rev.-Sci. Eng. 39(1-2): 77-168.

Haneda M, Mizushima T, Kakuta N, Ueno A, Sato Y, Matsuura S, Kasahara K & Sato M (1993) Structural characterization and catalytic behavior of Al_2O_3-supported cerium oxides. Bull. Chem. Soc. Jpn. 66: 1279-1288.

Hannington NA (1991) A comparative performance study of vehicle, static engine and synthetically aged autocatalysts using CVS, static engine and synthetic gas RIG testing methods. Catalysis Today 11: 151-160.

Hayes RE & Kolaczkowski ST (1997) Introduction to Catalytic Combustion. Gordon and Breach Science Publishers, Amsterdam.

Heck R & Farrauto R (1996) Automotive catalysts. Automotive Engineering 104(2): 93-96.

Heck RM & Farrauto RJ (1997) The automobile catalyst: Its present and future family tree. Cattech 2: 117-124.

Heck RM & Farrauto RJ (2001) Automobile exhaust catalysts. Applied Catalysis A: General 221: 443-457.

Herz RK (1981) Dynamic behavior of automotive catalysts: 1. Catalyst oxidation and reduction. Ind. Eng. Chem. Prod. Res. Dev. 20: 451-457.

Hickey N, Fornasiero P, Kaspar J, Gatica JM & Bernal S (2001) Effects of the nature of the reducing agent on the transient redox behavior of $NM/Ce_{0.68}Zr_{0.32}O_2$ (NM = Pt, Pd, and Rh). Journal of Catalysis 200: 181-193.

Holmgren A (1998) Catalysts for car exhaust: Oxygen storage in platinum/ceria and mass transfer in monoliths. Doctoral Thesis, Chalmers University of Technology, Göteborg, Sweden.

Hu Z, Allen FM, Wan CZ, Heck RM, Steger JJ, Lakis RE & Lyman CE (1998) Performance and structure of Pt-Rh three-way catalysts: Mechanism for Pt/Rh synergism. Journal of Catalysis 174: 13-21.

Huang S-J, Walters AB & Vannice MA (2000) TPD, TPR and DRIFTS studies of adsorption and reduction of NO on La_2O_3 dispersed on Al_2O_3. Applied Catalysis B: Environmental 26: 101-118.

Härkönen MA, Aitta E, Lahti A, Luoma M & Maunula T (1991) Thermal behaviour of metallic TWC: Evaluation of the structural and performance properties. SAE Technical Paper Series 910846: 1-13.

Härkönen M, Kallinen K, Vakkilainen A, Louhelainen M & Lassi U (2001) Performance and Deactivation Correlations of Metallic Front- and Main-Converters for Euro 4 Limits, Paper presented in: Materials Aspects in Automotive Catalytic Converters (MACC2001) Conference, Munich, Germany.

Ihara K, Ohkubo K & Niura Y (1987) Thermal effect on three-way catalyst deactivation and improvement. SAE Technical Paper Series 871192: 192.1-192.8.

Inoue K, Kurahashi T, Negishi T, Akiyama K, Arimura K & Tasaka K (1992) Effects of phosphorus and ash contents of engine oils on deactivation of monolithic three-way catalysts and oxygen sensors. SAE Technical Paper Series 920654: 1-9.

Jen H-W, Graham GW, Chun W, McCabe RW, Cuif J-P, Deutsch SE & Touret O (1999) Characterization of model automotive exhaust catalysts: Pd on ceria and ceria-zirconia supports. Catalysis Today 50: 309-328.

Jobson E, Laurell M, Hoegberg E, Bernler H, Lundgren S, Wirmark G & Smedler G (1993) Deterioration of three-way automotive catalysts. Part I – Steady state and transient emission of aged catalyst. SAE Technical Paper Series 930937.

Johnson MFL (1990) Surface area stability of aluminas. Journal of Catalysis 123: 245-259.
Joy GC, Molinaro FS & Homeier Eh (1985) Influence of phosphorus on three-component control catalysts: Catalyst durability and characterization studies. SAE Technical Paper Series 852099: 53-64.
Kašpar J, Fornasiero P & Graziani M (1999) Use of CeO_2 –based oxides in the three-way catalysis. Catalysis Today 50: 285-298.
Keiski RL, Härkönen M, Lahti A, Maunula T, Savimäki A & Slotte T (1995) An infrared study of CO and NO adsorption on Pt, Rh, Pd 3-way catalysts. In: Catalysis and Automotive Pollution Control III (A. Frennet & JM Bastin eds.), Elsevier Science B.V., Amsterdam, Studies in Surface Science and Catalysis Vol. 96, 85-96.
Kenevey K, Valdivieso F, Soustelle M & Pijolat M (2001) Thermal stability of Pd or Pt loaded $Ce_{0.68}Zr_{0.32}O_2$ and $Ce_{0.50}Zr_{0.50}O_2$ catalyst materials under oxidizing conditions. Applied Catalysis B: Environmental 29: 93-101.
Kijlstra WS, Brands DS, Poels EK & Bliek A (1997) Mechanism of the selective catalytic reduction of NO by NH_3 over MnO_X/Al_2O_3. Journal of Catalysis 171: 208-218.
Koltsakis GC & Stamatelos AM (1997) Catalytic automotive exhaust aftertreatment. Prog. Energy Combust. Sci. 23: 1-39.
Kubsh JE, Rieck JS & Spencer ND (1991) Cerium oxide stabilization: Physical property and three-way catalytic activity considerations. In: Catalysis and Automotive Pollution Control II (A. Crucq ed.), Elsevier Science B.V., Amsterdam, Studies in Surface Science and Catalysis Vol. 71, 617-628.
Kumar SV, Hochmuth JK & Heck RM (1994) A novel approach to studying the effect of various rapid aging cycles on the performance of a high tech palladium only three way catalyst. SAE Technical Paper Series 941997: 247-255.
Lassi U, Hietikko M., Ahola J, Kallinen, K, Härkönen, M & Keiski RL (2001) Evaluation of exhaust gas catalyst deactivation based on XRD analysis. In: Proceedings of 5th European Congress on Catalysis, Limerick, 2001.
Lassi U, Hietikko M, Keiski RL, Kallinen K, Härkönen M & Laitinen R (2002a) Thermal and hydrothermal deactivation of Pd/Rh exhaust gas catalysts. In: Proceedings of 10th Nordic Symposium on Catalysis, Helsingør, 2002.
Lassi U, Polvinen R, Suhonen S, Kallinen K, Savimäki A, Härkönen M, Valden M & Keiski RL (2002b) Effect of Ageing Atmosphere on the Deactivation of Pd/Rh Automotive Exhaust Gas Catalysts; Activity and XPS Studies, to be submitted for publication to *Applied Catalysis B: Environmental.* (manuscript)
Lassi U, Hietikko M, Kallinen K, Savimäki A, Härkönen M, Pursiainen J, Laitinen R & Keiski RL (2002c) Effect of the Ageing Atmosphere on Catalytic Activity and Textural Properties of Pd/Rh Exhaust Gas Catalysts Studied by XRD, revised for publication in *Applied Catalysis B: Environmental.*
Lassi U, Ahola J, Kallinen K, Härkönen M, Savimäki A & Keiski RL (2002d) NO-TPD Studies of the Effect of Thermal and Engine Ageings on Pd/Rh Exhaust Gas Catalysts. (manuscript)
Laurikko J (1994) Emissions performance of current TWC vehicles at low ambient temperature over FTP and ECE test cycles. SAE Technical Paper Series 940933: 273-287.
Laurikko J (1995) Ikä painaa-kolhut vaurioittavat. Katalysaattorin kestoikä ja siihen vaikuttavat tekijät. Suomen autolehti 1: 12-16.
Laurikko J (2001) Autojen pakokaasumittaukset edellyttävät monimutkaisen laitteiston. Ilmansuojelu 2: 28-33.
le Page JF (1987) Applied heterogeneous catalysis. Editions Tecnip., Paris.
Liu DR & Park J-S (1993) Electron microprobe characterization of phosphorus containing deposits on used automotive catalyst surfaces. Applied Catalysis B: Environmental 2: 49-70.
Lox ESJ & Engler BH (1997) Environmental Catalysis-Mobile Sources. In: Ertl G, Knözinger H & Weitkamp (eds) Handbook of Heterogeneous Catalysis, Vol. 4. Wiley-VCH, Weinheim, p. 1559-1695.
Malet P (1990) Thermal desorption methods. In: Fierro, J.L.G. (ed.) Spectroscopic characterisation of heterogeneous catalysts. Part B 57: Chemisorption of probe molecules. Elsevier, Amsterdam 1990, Elsevier. P. B333-B382.

Marécot P, Akhachane A, Micheaud C & Barbier J (1998) Deactivation by coking of supported palladium catalysts. Effect of time and temperature. Applied Catalysis A: General 169: 189-196.
Margrave J (ed) (1967) The characterization of high temperature vapors, John Wiley & Sons., New York.
Marin GB & Hoebink JHBJ (1997) Kinetic modeling of automotive exhaust catalysis. Cattech 2: 137-148.
McCarty JG, Gusman M, Lowe DM, Hildenbrand DL & Lau KN (1999) Stability of supported metal and supported metal oxide combustion catalysts. Catalysis Today 47: 5-17.
Monroe DR (1980) Phosphorus and lead poisoning of pelleted three-way catalysts. SAE Technical Paper Series 800859: 1-12.
Monteiro RS, Noronha FB, Dieguez LC & Schmal M (1995) Characterisation of Pd-CeO_2 interaction on alumina support. Applied Catalysis A: General 131: 89-106.
Moulijn JA, van Diepen AE & Kapteijn F (2001) Catalyst deactivation: is it predictable? What to do? Applied Catalysis A: General 212: 3-16.
Mowery DL, Graboski MS, Ohno TR & McCormick RL (1999) Deactivation of PdO-Al_2O_3 oxidation catalyst in lean-burn natural gas engine exhaust: aged catalyst characterization and studies of poisoning by H_2O and SO_2. Applied Catalysis B: Environmental 21: 157-169.
Muraki H & Zhang G (2000) Design of advanced automotive exhaust catalysts. Catalysis Today 63: 337-345.
Narula CK, Allison JE, Bauer DR & Gandhi HS (1996) Materials chemistry issues related to advanced materials applications in the automotive industry. Chem. Mater. 8: 984-1003.
Niemantsverdriet JW (2000) Spectroscopy in Catalysis. An Introduction. Wiley-VCH, Weinheim.
Oh SH & Eickel CC (1988) Effects of cerium addition on CO oxidation kinetics over alumina-supported rhodium catalysts. Journal of Catalysis 112: 543-555.
Oudet F, Vejux A & Courtine P (1989) Evolution during thermal treatment of pure and lanthanum-doped Pt/Al_2O_3 and Pt-Rh/Al_2O_3 automotive exhaust catalysts. Applied Catalysis 50: 79-86.
Ozawa M, Kimura M & Isogai A (1993) The application of Ce-Zr oxide solid solution to oxygen storage promoters in automotive catalysts. Journal of Alloys and Compounds 193: 73-75.
Ozawa M (1998) Role of cerium-zirconium mixed oxides as catalysts for car pollution: A short review. Journal of Alloys and Compounds 275-277: 886-890.
PDF-2 Powder Diffraction File Database, International Centre for Diffraction Data, 12 Campus Boulevard Newtown Square, PA 19073-3273 USA.
Perrichon V, Laachir A, Abouarnadasse S, Touret O & Blanchard G (1995) Thermal stability of a high surface area ceria under reducing atmosphere. Applied Catalysis A: General 129: 69-82.
Piras A, Trovarelli A & Dolcetti G (2000) Remarkable stabilization of transition alumina operated by ceria under reducing and redox conditions. Applied Catalysis B: Environmental 28: L77-L81.
Pitchon V, Garin F & Maire O (1997) Influence of the surrounding atmosphere upon the catalytic performances of three-way catalysts. Applied Catalysis A: General 149: 245-256.
Polvinen R (2002) Personal communications.
Pulkkinen (Lassi) U, Ahola J, Härkönen M & Keiski RL (2000) The effect of thermal and engine ageing on surface adsorption states on exhaust gas catalysts. In: Proceedings of 9th Nordic Symposium on Catalysis, Lidingö, 2000.
Pulkkinen (Lassi) U, Ahola J, Savimäki A, Härkönen M & Keiski RL (2001) Effect of ageing atmosphere on catalyst activity and surface properties of exhaust gas catalysts. In: Proceedings of 17th North American Catalysis Society Meeting, Toronto, 2001.
Rabinowitz HN, Tauster SJ & Heck RM (2001) The effects of sulfur & ceria on the activity of automotive Pd/Rh catalysts. Applied Catalysis A: General 212: 215-222.
Rahkamaa K, Pulkkinen (Lassi) U, Wärnå J, Zhou Y, Salmi T & Keiski RL (2000) Investigation of the catalytic reduction of NO_X on supported Rh catalyst with transient techniques. In: Proc. of 14th International Congress of Chemical and Process Engineering, Praha 2000.
Rahkamaa-Tolonen K (2001) Investigation of the catalytic NO_X reduction with transient techniques, isotopic exchange and FT-IR Spectroscopy. Doctoral Thesis, Åbo Akademi University, Turku.

Rahkamaa-Tolonen K, Salmi T, Murzin DY, Barreto Dillon L, Lassi U & Keiski RL (2002) Investigation of NO reduction by H_2 on Pd monolith with transient and isotopic exchange techniques. II. H_2/D_2 Exchange in the reduction of NO. Journal of Catalysis 210: 30-38.

Ribeiro FH, Chow M & Dalla Betta RA (1994) Kinetics of the complete oxidation of methane over supported palladium catalysts. Journal of Catalysis 146: 537-544.

Rokosz MJ, Chen AE, Lowe-Ma CK, Kucherov AV, Benson D, Paputa Beck MC & McCabe RW (2001) Characterization of phosphorus-poisoned automotive exhaust catalysts. Applied Catalysis B: Environmental 33: 205-215.

Root TW, Schmidt LD & Fisher GB (1983) Adsorption and reaction of nitric oxide and oxygen on Rh(111). Surface Science 134(1): 30-45.

Salvador F & Merchán MD (1998) Controlled-rate thermal desorption. Journal of Thermal Analysis and Calorimetry 51(2): 383-396.

van Santen RA, van Leeuwen PWNM, Moulijn JA & Averill BA (eds.) (1999) Catalysis: An Integrated Approach. Elsevier Science B.V., Amsterdam, Studies in Surface Science and Catalysis Vol. 123.

Sellmer C, Schmatloch V & Kruse N (1995) NO dissociation on rhodium. Catalysis Letters 35: 165-174.

Serwicka EM (2000) Surface area and porosity, X-ray diffraction and chemical analyses. Catalysis Today 56: 335-346.

Shelef M, Otto K & Otto NC (1978) Poisoning of automotive catalysts. Adv. Catal. 27: 311-365.

Shelef M & Graham GW (1994) Why rhodium in automotive three-way catalysts? Catal. Rev. – Sci. Eng. 36(3): 433-457.

Shelef M & McCabe RW (2000) Twenty-five years after introduction of automotive catalysts: What next? Catalysis Today 62: 35-50.

Shinjoh H, Muraki H & Fujitani Y (1991) Effect of severe thermal ageing on noble metal catalysts. In: Catalysis and Automotive Pollution Control II (A. Crucq ed.), Elsevier Science B.V., Amsterdam, Studies in Surface Science and Catalysis Vol. 71, 617-628.

Sideris M (1998) Methods for Monitoring and Diagnosing the Efficiency of Catalytic Converters, Elsevier Science B.V., Amsterdam, Studies in Surface Science and Catalysis Vol. 115.

Somorjai GA (1994) Introduction to Surface Chemistry and Catalysis, John Wiley & Sons, Inc., New York. 667 p.

Stakheev AY & Kustov LM (1999) Effects of support on the morphology and electronic properties of supported metal clusters: modern concepts and progress in 1990s. Applied Catalysis A: General 188: 3-35.

Suhonen S (2002) Ageing induced effects on noble metal oxides on exhaust catalysts studied by Photoelectron Spectroscopy. Doctoral thesis, Tampere University of Technology, Tampere.

Summers JC, Williamson WB & Scaparo JA (1990) The role durability and evaluation conditions on the performance of Pt/Rh and Pd/Rh automotive catalysts. SAE Technical Paper Series 900495.

Tas AC & Akinc M (1994) Phase relations in the system Ce_2O_3-Al_2O_3 in inert and reducing atmospheres. Journal of American Ceramic Society 77(11): 2961-2967.

Taylor KC (1993) Nitric oxide catalysis in automotive exhaust systems. Catal. Rev.-Sci. Eng. 35(4): 457-481.

Teixeira ACSC & Giudici R (1999) Deactivation of steam reforming catalysts by sintering: experiments and simulation. Chemical Engineering Science 54: 3609-3618.

Thomas JM & Thomas WJ (1997) Principles and Practice of Heterogeneous Catalysis, VCH, Weinheim.

Trovarelli A (1996) Catalytic properties of ceria and CeO_2-containing materials. Catal. Rev. Sci. Eng.38: 439-520.

Turpeinen E & Maunula T (1993) Termodynaamiset tasapainot katalyysireaktioissa. Kemira Oulu Research Centre, tutkimusselostus.

Twigg MV (ed.) (1989) Catalyst Handbook, Wolfe Publishing Ltd, London.

Twigg MV (2001) Critical topics in exhaust gas aftertreatment. Platinum Metals Rev. 45(4): 176-178.

Ueda F, Sugiyama S, Arimura K, Hamaguchi S & Akiyama K (1994) Engine oil additive effects on deactivation of monolithic three-way catalysts and oxygen sensors. SAE Technical Paper Series 940746: 197-206.

Usmen RK, McCabe RW, Graham GW, Weber WH, Peters CR & Gandhi HS (1992) Techniques for analysing thermal deactivation of automotive catalysts. SAE Technical Paper Series 922336: 147-157.

Wachs IE (1992) Characterisation of Catalytic Materials, Manning Publications Co., Greenwich.

Valden M, Keiski RL, Xiang N, Pere J, Aaltonen J, Pessa M, Maunula T, Savimäki A, Lahti A & Härkönen M (1996) Reactivity of Pd/Al_2O_3, Pd/La_2O_3-Al_2O_3 and $Pd/LaAlO_3$ catalysts for the reduction of No by CO: CO and NO adsorption. Journal of Catalysis 161: 614-625.

Vidal H, Bernal S, Kašpar J, Pijolat M, Perrichon V, Blanco G, Pintado JM, Baker RT, Colón G & Fally F (1999) Influence of high temperature treatments under net oxidizing and reducing conditions on the oxygen storage and buffering properties of a $Ce_{0.68}Zr_{0.32}O_2$ mixed oxide. Catalysis Today 54: 93-100.

Vidal H, Kašpar J, Pijolat M, Colón G, Bernal S, Cordón A, Perrichon V & Fally F (2000) Redox behavior of CeO_2-ZrO_2 mixed oxides I. Influence of redox treatments on high surface area catalysts. Applied Catalysis B: Environmental 27: 49-63.

Vidal H, Kašpar J, Pijolat M, Colón G, Bernal S, Cordón A, Perrichon V & Fally F (2001) Redox behavior of CeO_2-ZrO_2 mixed oxides II. Influence of redox treatments on low surface area catalysts. Applied Catalysis B: Environmental 30: 75-85.

Vlaic G, Monte RD, Fornasiero P, Fonda E, Kašpar J & Graziani M (1999) Redox property-local structure relationships in the Rh-loaded CeO_2-ZrO_2 mixed oxides. Journal of Catalysis 182: 378-389.

Wan C-Z (1991) Engelhard Corp. Catalyst composition containing segregated platinum and rhodium components. US patent 5.057.483.

Wanke Se & Flynn PC (1975) The sintering of supported metal catalysts. Catal. Rev. –Sci. Eng. 12: 93-135.

Weng-Sieh Z, Gronsky R & Bell AT (1997) Microstructural evolution of γ-alumina-supported Rh upon aging in air. Journal of Catalysis 170: 62-74.

Weng-Sieh Z, Gronsky R & Bell AT (1998) Effects of support interaction on the phase stability of Rh oxides formed during the aging of α-alumina supported Rh in air. Journal of Catalysis 174: 22-33.

Wickam DT, Banse BA & Koel BE (1991) Adsorption of nitrogen dioxide and nitric oxide on Pd(111). Surface Science 243(1-3): 83-95 .

Williamson WB, Gandhi HS, Heyde ME & Zawacki GA (1979a) Deactivation of three-way catalysts by fuel contaminants: lead, phosphorus and sulfur. SAE Technical Paper Series 790942: 1-9.

Williamson WB, Stepien HK, Watkins WLH & Gandhi HS (1979b) Poisoning of platinum-rhodium automotive three-way catalysts by lead and phosphorus. Environmental Science and Technology 13(9): 1109-1113.

Williamson WB, Perry J, Goss RL, Gandhi HS & Beason RE (1984) Catalyst deactivation due to glaze formation from oil-derived phosphorus and zinc. SAE Technical Paper Series 841406: 1-10.

Williamson WB, Perry J, Gandhi HS & Bomback JL (1985) Effects of oil phosphorus of monolithic three-way catalysts. Applied Catalysis 15: 277-292.

Wong C & McCabe RW (1989) Effects of high-temperature oxidation and reduction on the structure and activity of Rh/Al_2O_3 and Rh/SiO_2 catalysts. Journal of Catalysis 119: 47-64.

Yao HC, Japar S & Shelef M (1977) Surface interactions in the system Rh/Al_2O_3. Journal of Catalysis 50: 407-418.

Yao MH, Baird RJ, Kunz FW & Hoost TE (1997) An XRD and TEM investigation of the structure of alumina- supported ceria-zirconia. Journal of Catalysis 166: 67-74.

Yu T-C & Shaw H (1998) The effect of sulfur poisoning on methane oxidation over palladium supported on γ-alumina catalysts. Applied Catalysis B: Environmental 18: 105-114.